

**THIS IS THESIS RESULTS : NOTHING IN THIS SLIDE REPRESENTS  
PHENIX COLLABORATION'S OFFICIAL STATEMENT!!**

# **Event shape dependence of jet correlations at RHIC**

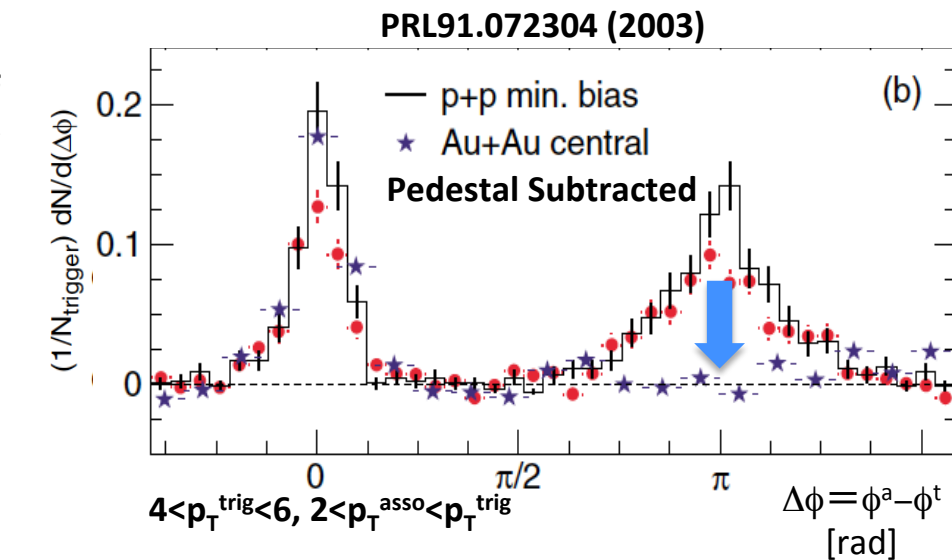
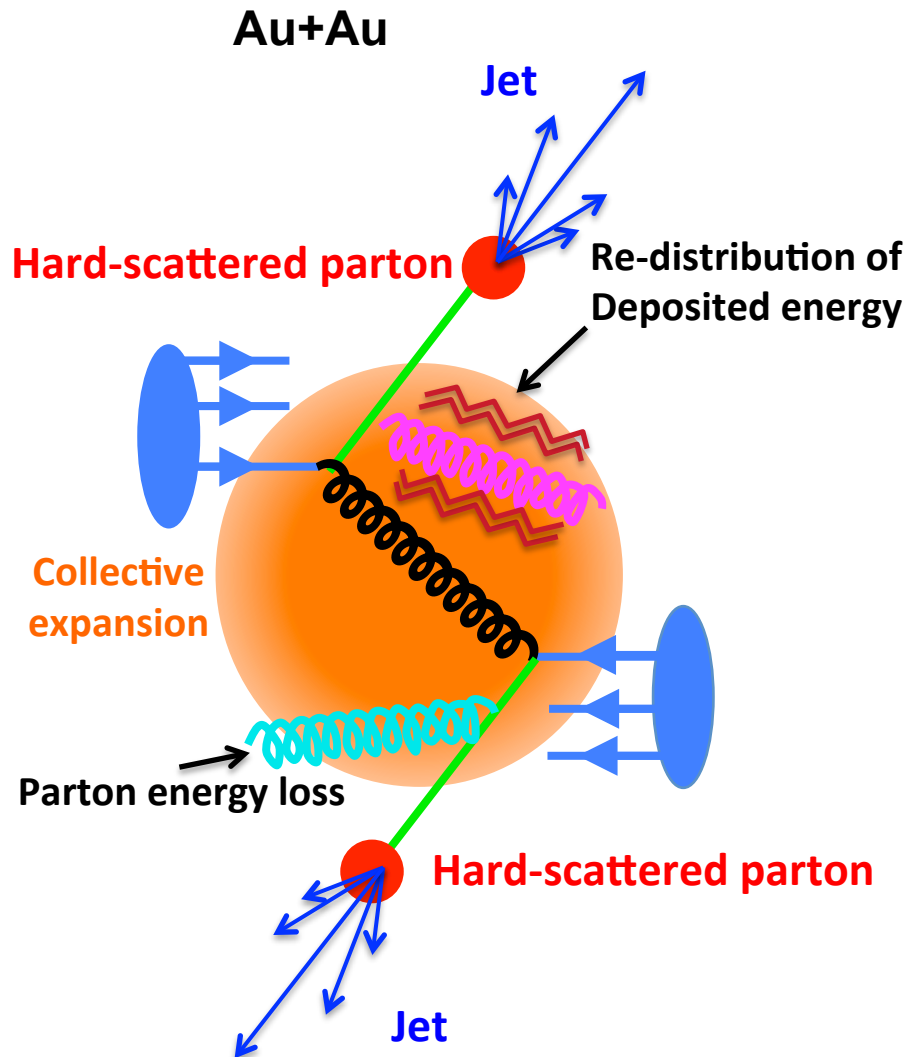
Takahito Todoroki

University of Tsukuba

2014/July/19

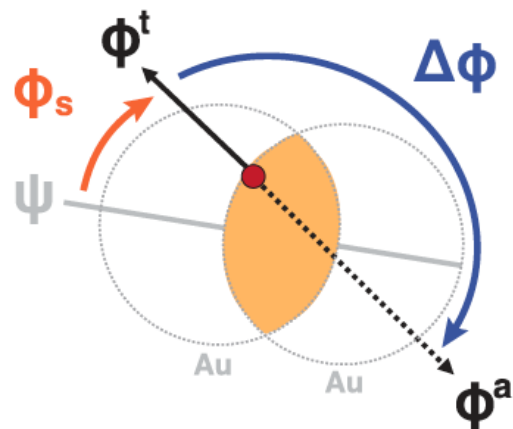
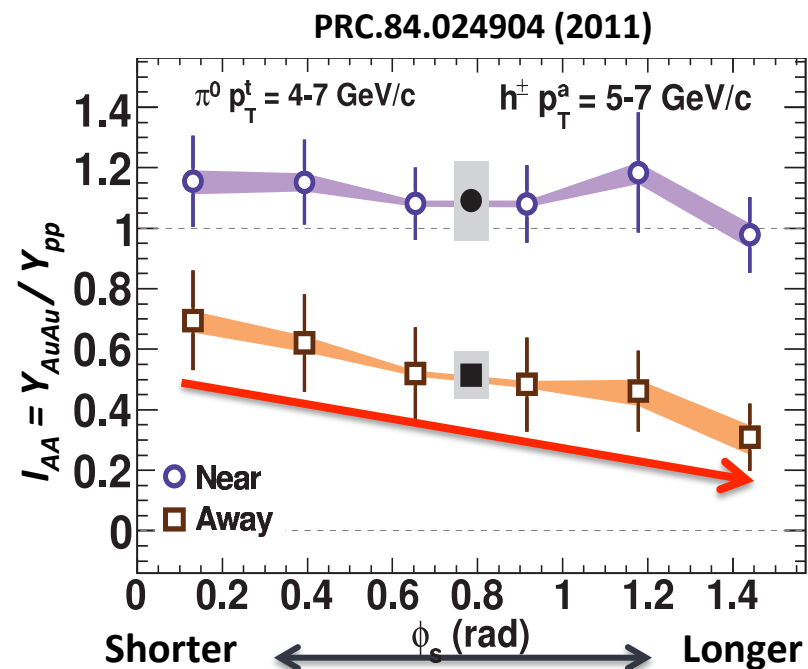
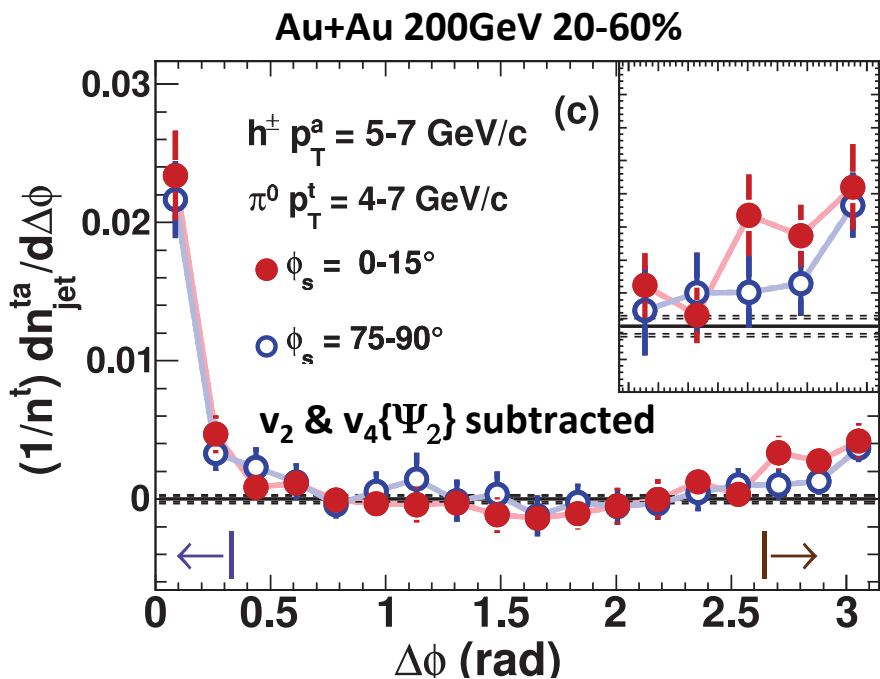
Heavy Ion Café @ University of Tokyo

# Jet-Quenching



❖ Suppression of away-side

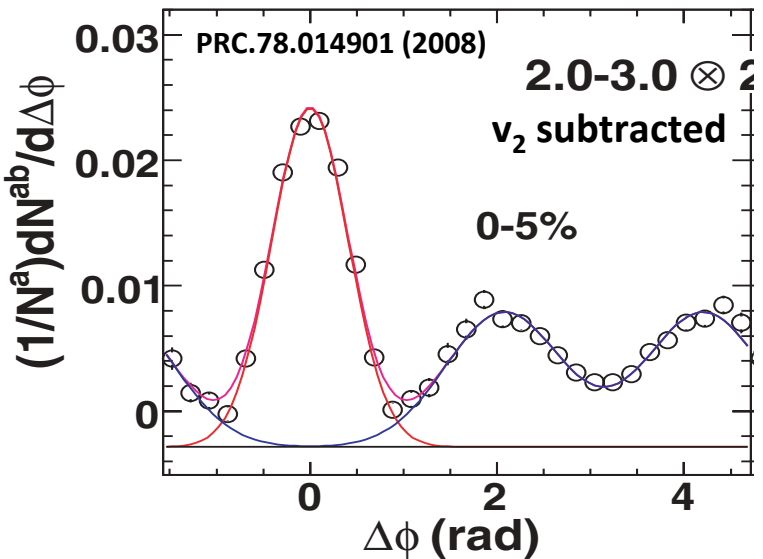
# $\Psi_2$ Dependence of Suppression in High $p_T$ correlations



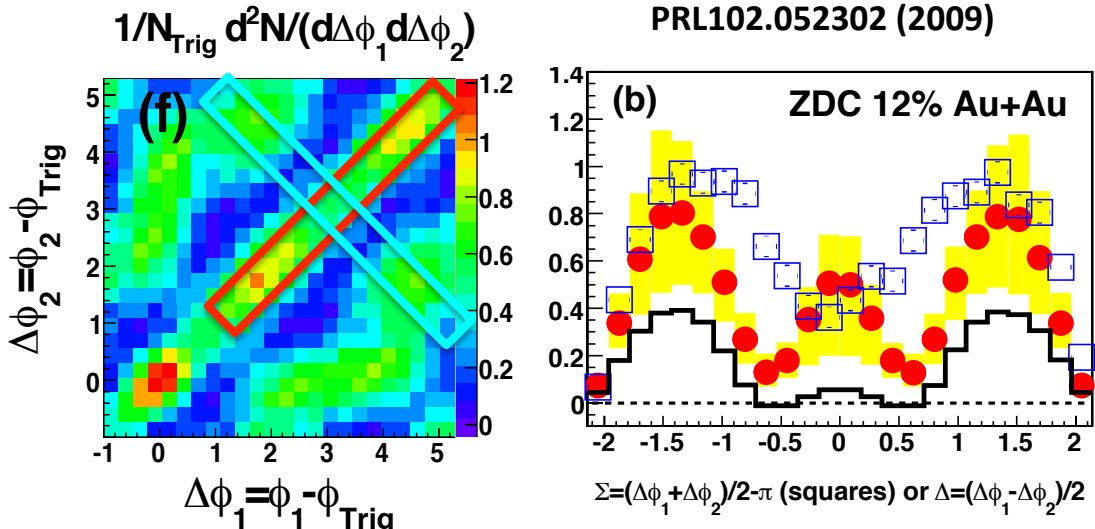
- ❖ Monotonic suppression with increase of path length, which can be taken as “parton energy loss”
- ❖ Where deposited energy goes?

# Conical Emission of Intermediate $p_T$ correlations

## Two-Particle Correlations



## Three-Particle Correlations



- ✧ Away-side double hump in two-particle correlations
- ✧ Conical Emission confirmed by three-particle correlations
- ✧ Seems parton-medium interactions



# Models for Double-Hump : 1

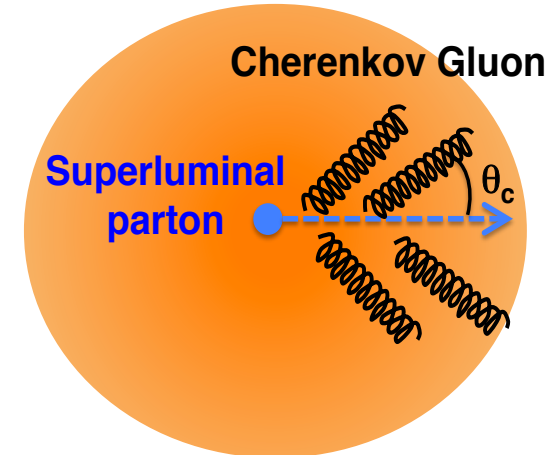
- ✧ Cherenkov gluon radiation by superluminal partons

$$\cos \theta_c = 1/n(p)$$

$n(p)$  : Index of refraction

$p$  : Gluon Momentum

PRL 96.172302 (2006)



- ✧ Shock-wave by supersonic partons

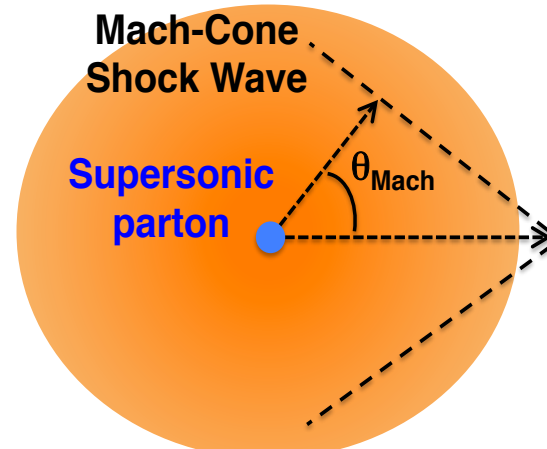
$$\cos \theta_{Mach} = c_s/v_{part}$$

$c_s$  : Speed of sound

$v_{part}$  : Speed of parton

Phys. Rev. C 73, 011901(R), (2006)

PRL 105.222301 (2010)



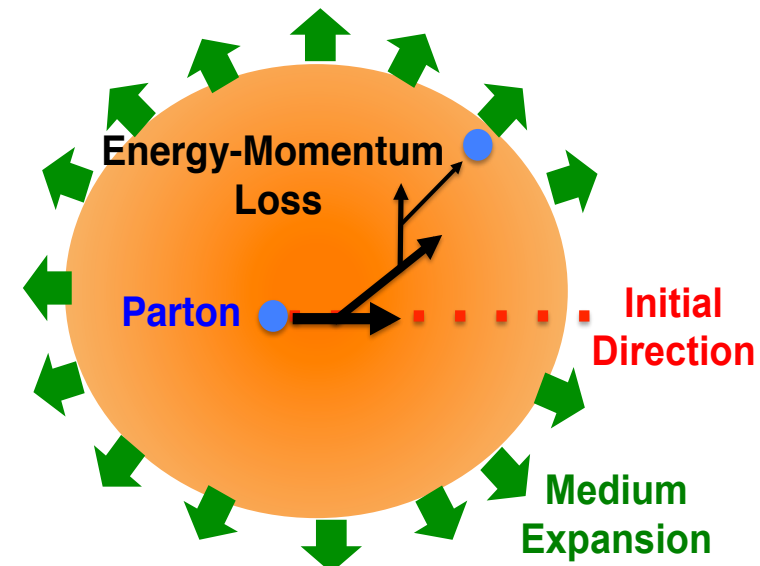
# Models for Double-Hump : 2

- ◇ Energy-momentum loss + expanding medium

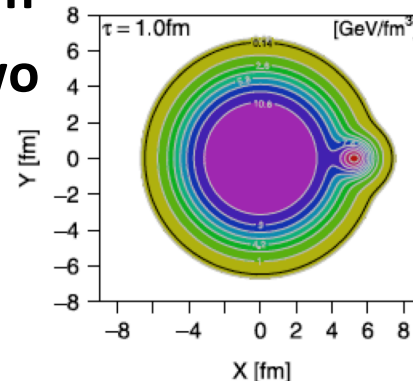
$$\partial_\mu T^{\mu\nu} = S^\nu$$

$$S^\nu(t, \vec{x}) = \frac{1}{(\sqrt{2\pi}\sigma)^3} \exp \left[ -\frac{[\vec{x} - \vec{x}_{jet}(t)]^2}{2\sigma^2} \right] \\ \times \left( \frac{dE}{dt}, \frac{dM}{dt}, 0, 0 \right) \left[ \frac{T(t, \vec{x})}{T_{max}} \right]^3$$

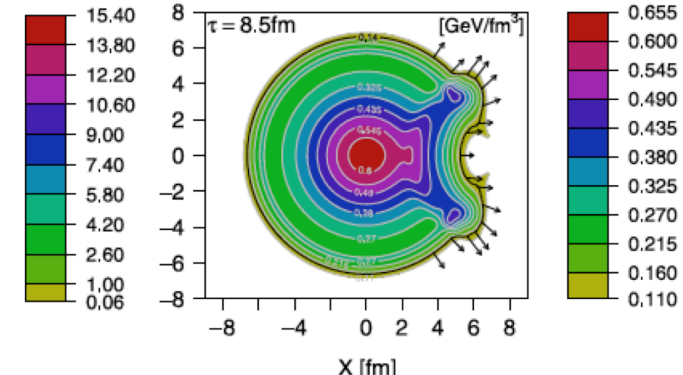
PRL 105.222301 (2010)



- ◇ Hot spot+ expanding medium
  - Split of the hot spot into two directions

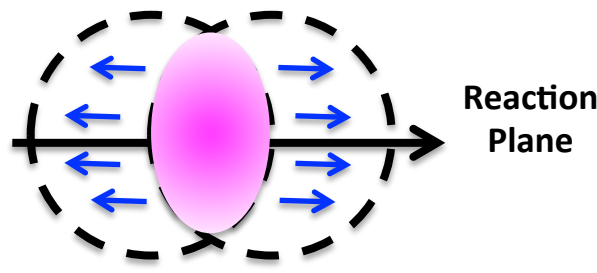


Phys. Let. B 712 (2012) 226-230



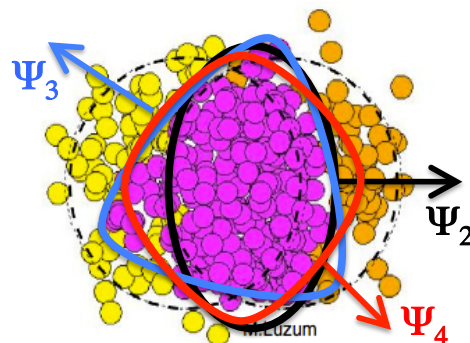
# Higher-Order Event-Planes & Flow-Harmonics

## Smooth participant density



Expansion to the short-axis direction by pressure gradient

## Fluctuating participant density



Expansion to the short-axis directions of event-planes by pressure gradient

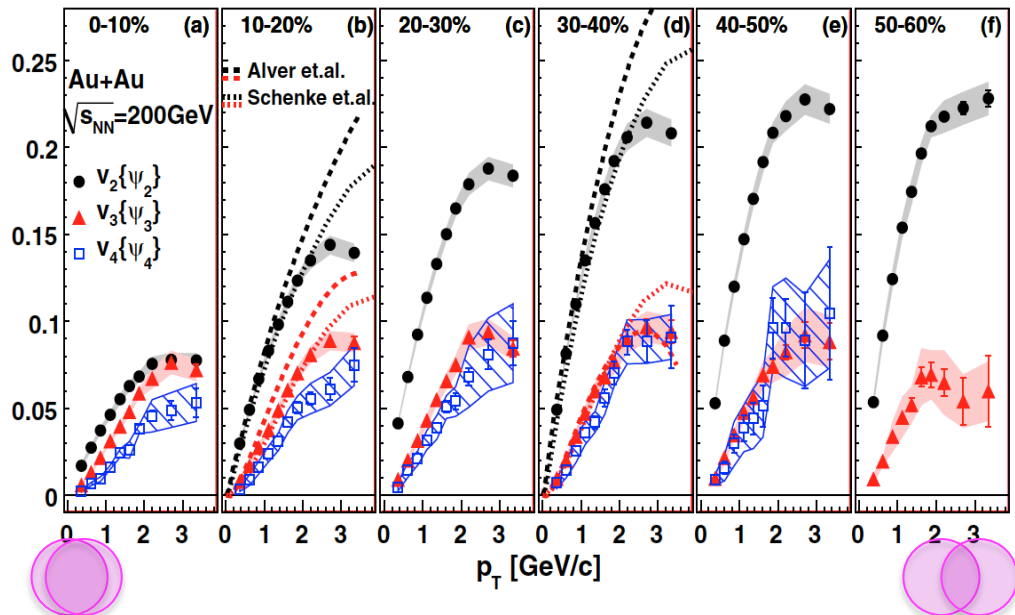
- ◊ Azimuthal distribution of emitted particles

$$\begin{aligned}\frac{dN}{d\phi} \propto & 1 + 2v_2 \cos 2(\phi - \Psi_2) \\ & + 2v_3 \cos 3(\phi - \Psi_3) \\ & + 2v_4 \cos 4(\phi - \Psi_4) \dots \\ v_n = & \langle \cos n(\phi - \Psi_n) \rangle\end{aligned}$$

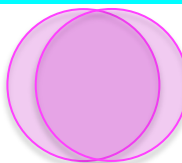
- $v_n$  : Higher-order flow harmonics  
 $\Psi_n$  : Higher-order event planes  
 $\phi$  : Azimuthal angle of emitted particles

# Higher-Order Flow Harmonics

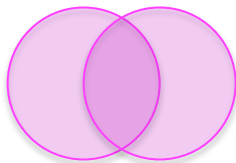
PRL107.252301 (2011)



Central Collisions



Peripheral Collisions



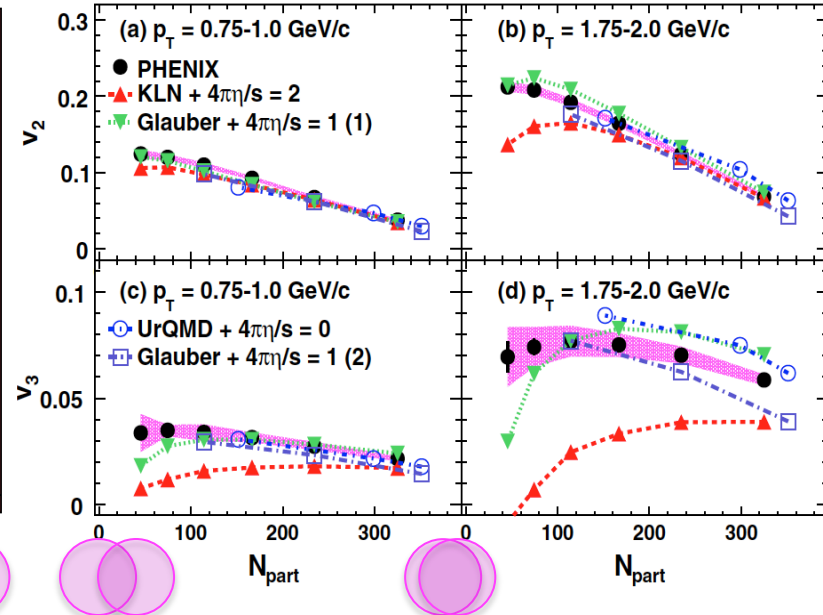
2014/7/19

$N_{\text{part}}$  : # of participant nucleons in a collision

Centrality  $\sim 0\%$

$N_{\text{part}} \sim 394$

Centrality  $\sim 100\%$   
 $N_{\text{part}} \sim 2$



HIC

- ✧ None-zero  $v_n(n>2)$  is observed
- ✧ Degeneracy of models disentangled
  - Initial Condition, shear viscosity of QGP, different expansion mechanism between  $v_2$  &  $v_3$
- ✧ Backgrounds in correlation functions

# Motivation of analysis

- ✧ Providing experimental results of two-particle correlations after  $v_n$  background subtractions
- ✧ Examine the path length dependence of  $\Psi_2$  dependent intermediate- $p_T$  correlations in order to search for deposited energy from high  $p_T$  partons
- ✧ Search for differences between  $\Psi_2$  &  $\Psi_3$  dependent correlations which may reflects **possible different** evolution processes between the 2nd- and 3rd-order geometry planes

# Analysis Flow-Chart

## Single-particle analysis

Event-Plane  
(Resolution)

Flow harmonics  $v_n$

Pure flow  
backgrounds

Tracking efficiency

## Two-particle analysis

Two-particle  
correlations

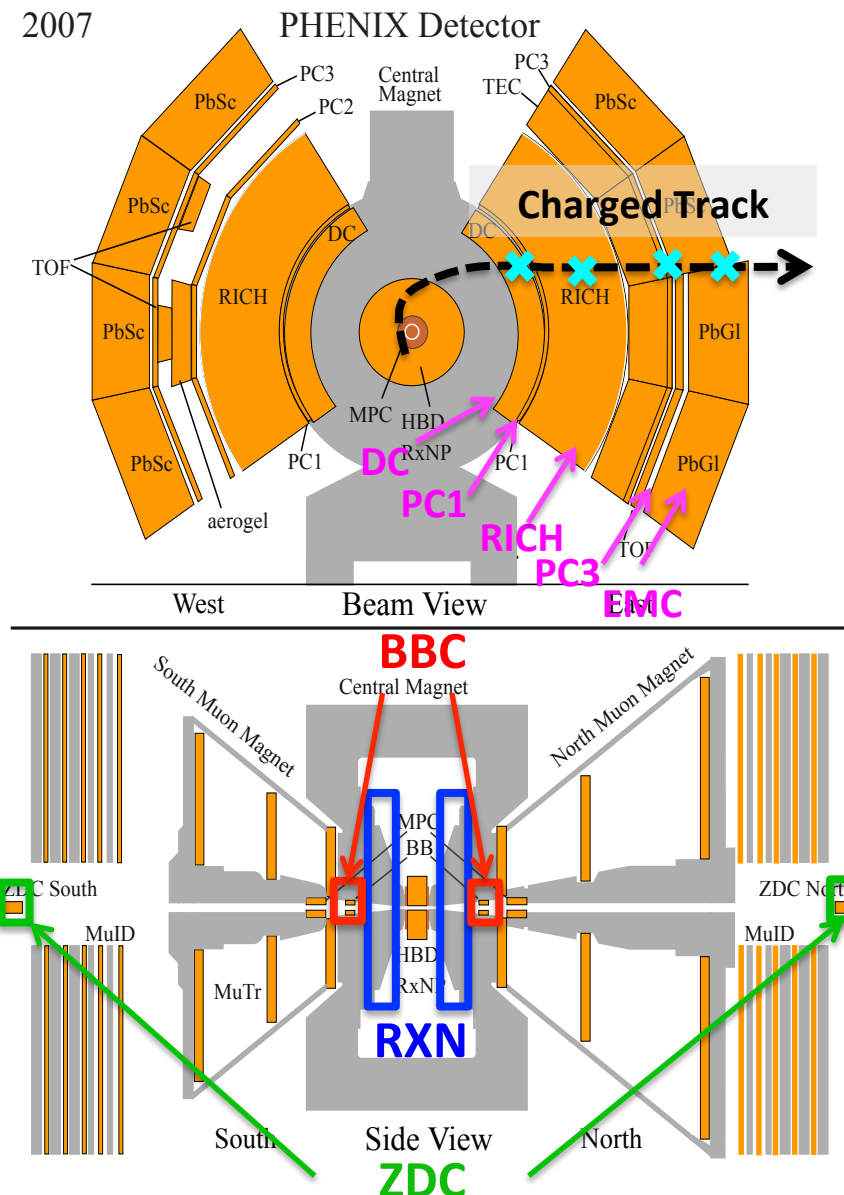
Flow subtracted  
correlations

Pair yield per a  
trigger

Unfolding of event-  
plane resolution

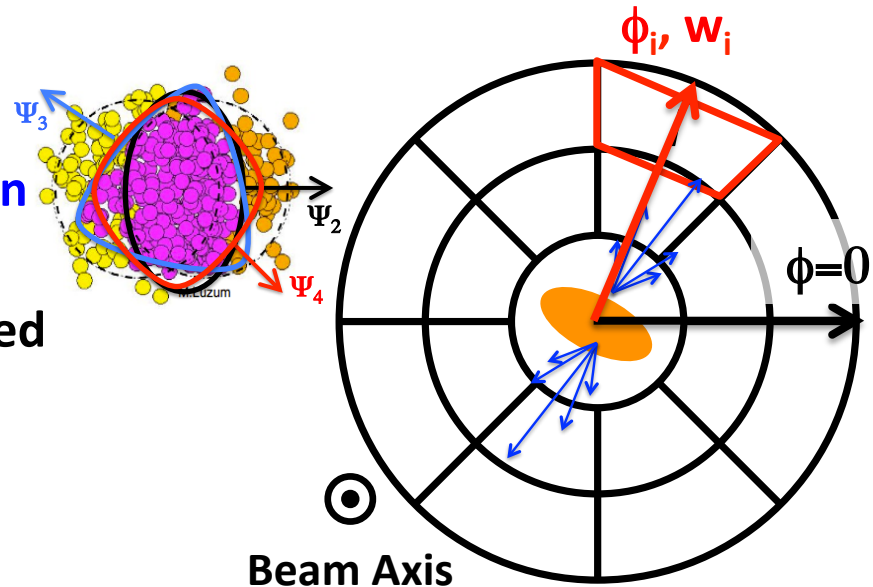
# PHENIX 2007 Experiment: Au+Au 200 GeV Collisions

- ❖ Minimum Bias trigger : 4.4 billion events
- ❖ Trigger, collision vertex, centrality
  - Zero-Degree-Calorimeter(ZDC)
  - Beam-Beam-Counter (BBC)
- ❖ Event-plane
  - BBC
  - Reaction-Plane-Detector(RxN)
- ❖ Central Arm,  $\Delta\phi=\pi$ ,  $|\eta|<0.35$ 
  - Drift Chamber (DC)
  - Pad Chambers(PC)
  - Electromagnetic Calorimeter(EMC)
    - Momentum, charged particle tracking
  - Ring Image Cherenkov Detector(RICH)
    - Electron rejection



# Event-Plane

- ❖ Expansion to the initial short-axis direction by pressure gradient
  - EP is a direction most particles are emitted after freeze-out
  - EP is determined by flow signal itself

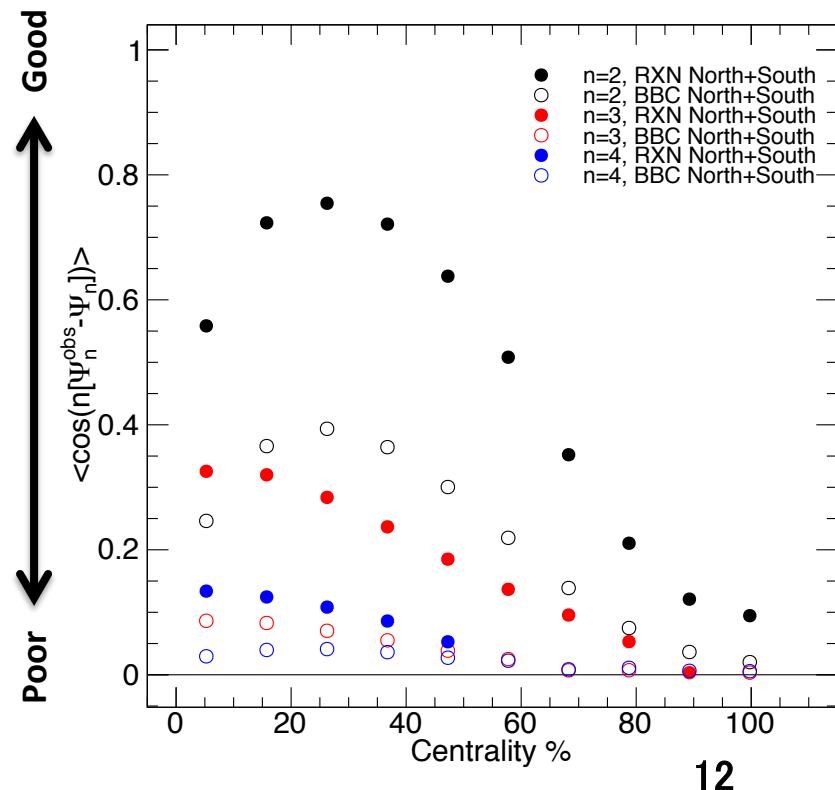


- ❖ EP is determined by RXN and BBC detectors
  - RXN ( $1 < |\eta| < 2.8$ ) : 24 segments x 2 sectors
  - BBC ( $3 < |\eta| < 3.9$ ) : 64 segments x 2 sectors

$$\Psi_n = \frac{1}{n} \tan^{-1} \left( \frac{\sum_i w_i \cos(n\phi_i)}{\sum_i w_i \sin(n\phi_i)} \right)$$

$\phi_i$  : Azimuthal angle of  $i^{\text{th}}$  segments

$w_i$  : Weight (Charge etc.) of  $i^{\text{th}}$  segments



# Rapidity Selections in Analysis

- ✧ Rapidity ranges of CNT, RXN, & BBC
  - 2PC at  $|\Delta\eta|<0.35$
  - Rapidity gap between particles & EP to avoid auto-correlations by jets



## ✧ Raw flow harmonics

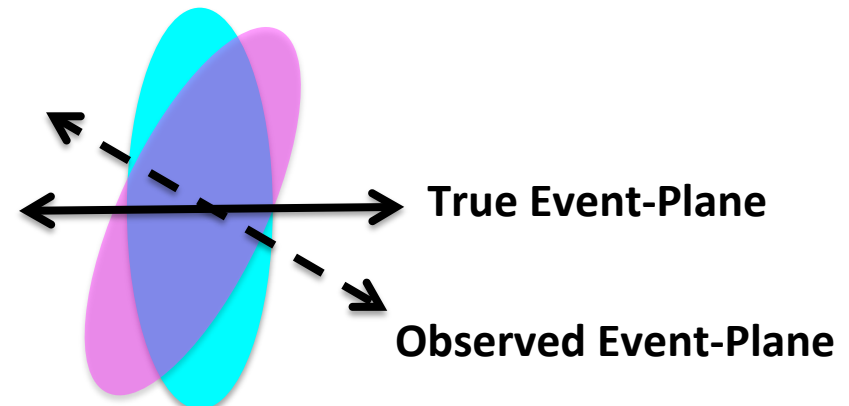
$$v_n^{raw} = \langle \cos n(\phi - \Psi_n^{obs}) \rangle$$

## ✧ Resolution correction

- Smearing due to limited resolution

$$v_n = \frac{\langle \cos n(\phi - \Psi_n^{obs}) \rangle}{\langle \cos n(\Psi_n - \Psi_n^{obs}) \rangle}$$

Event-Plane Resolution

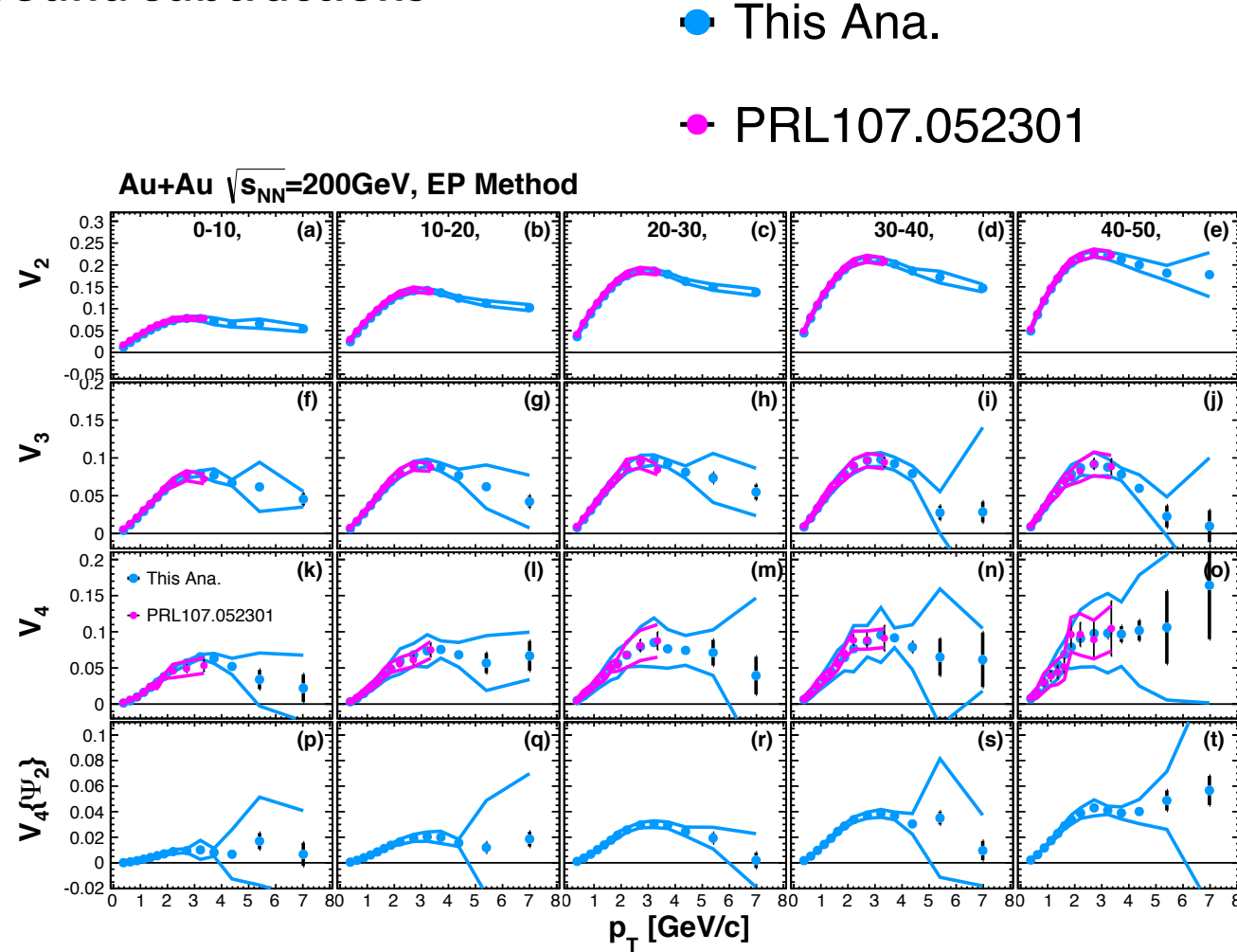


# $v_n$ Results

- ✧ Consistent results with previous PHENIX measurements
  - Used for background subtractions

Total systematics (%)  
at  $p_T=1-2 \text{ GeV}/c$

Centrality	0-10%	40-50%
$v_2$	4.3 %	2.7%
$v_3$	4.9%	12%
$v_4$	10%	34%
$v_4\{\Psi_4\}$	15%	6.5%



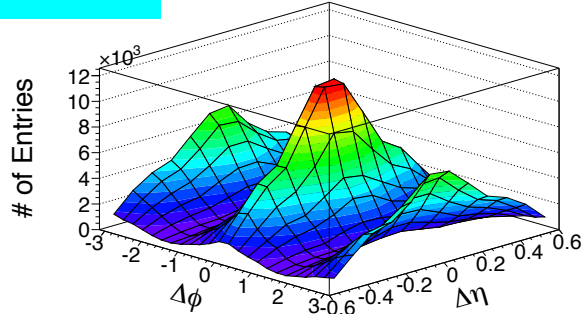
# Two-Particle Correlations

## Definition

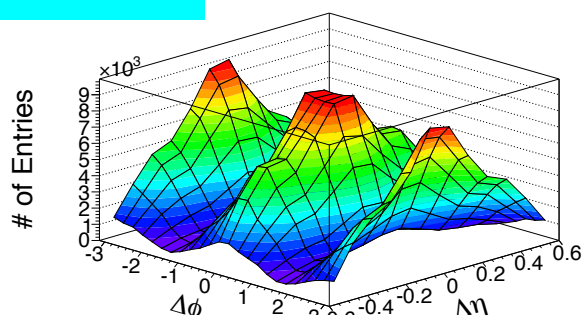
Ratio of two-particle probability over single-particle ones

$$C(\Delta\phi, \Delta\eta) = \frac{P(\phi^a, \phi^t | \eta^a, \eta^t)}{P(\phi^a | \eta^a)P(\phi^t | \eta^t)}$$

## Real Pair



## Mixed Pair



2014/7/19

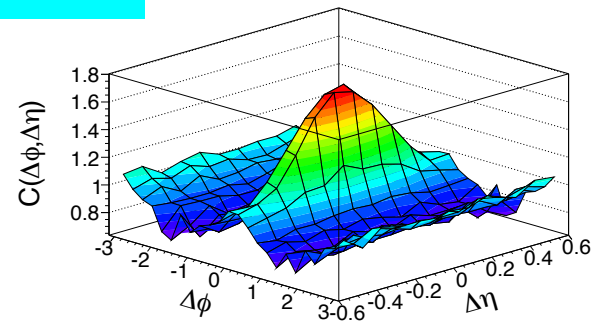
## Experimental Def.

Ratio of real pair distribution over mixed one

$$C(\Delta\phi, \Delta\eta) = \frac{N_{mix}^{ta}}{N_{real}^{ta}} \frac{d^2 N_{real}^{ta} / d\Delta\phi d\Delta\eta}{d^2 N_{mix}^{ta} / d\Delta\phi d\Delta\eta}$$
$$\Delta\phi = \phi^a - \phi^t, \Delta\eta = \eta^a - \eta^t$$

## Correlations = Real/Mixed

Event mixing also corrects acceptance effects by choosing similar events: centrality, collision points



## Pair Yield Per a Trigger

Dimension : Number of Particles

$$\frac{1}{N^t} \frac{d^2 N^{ta}}{d\Delta\phi d\Delta\eta} = \frac{1}{2\pi\varepsilon} \frac{N^{ta}}{N^t} C(\Delta\phi, \Delta\eta)$$

# Flow Subtraction & Pair Yield per a Trigger (PTY)

## ✧ Pure flow background

$$F(\Delta\phi) = 1 + \sum 2v_n^t v_n^a \cos(n\Delta\phi)$$

## ✧ Flow subtractions by ZYAM

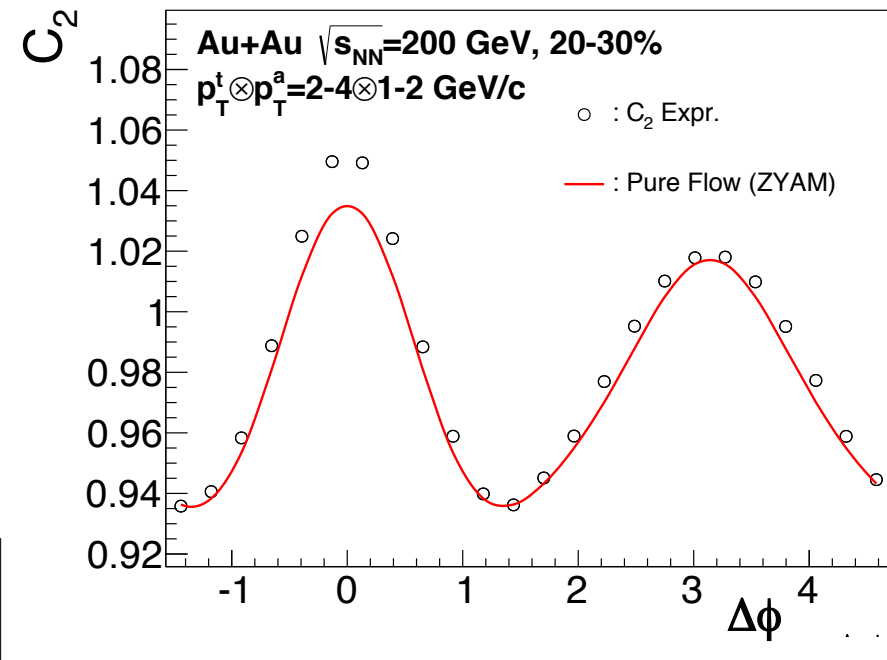
### – Zero Yield At Minimum Assumption

$$j(\Delta\phi) = C(\Delta\phi) - b_0 \left[ 1 + \sum_{n=1} 2v_n^t v_n^a \cos(n\Delta\phi) \right]$$

## ✧ Pair yield per a trigger (PTY)

### — Dimension : number of particles

$$\frac{1}{N^t} \frac{dN^{ta}}{d\Delta\phi} = \frac{1}{2\pi\varepsilon} \frac{N^{ta}}{N^t} j(\Delta\phi)$$

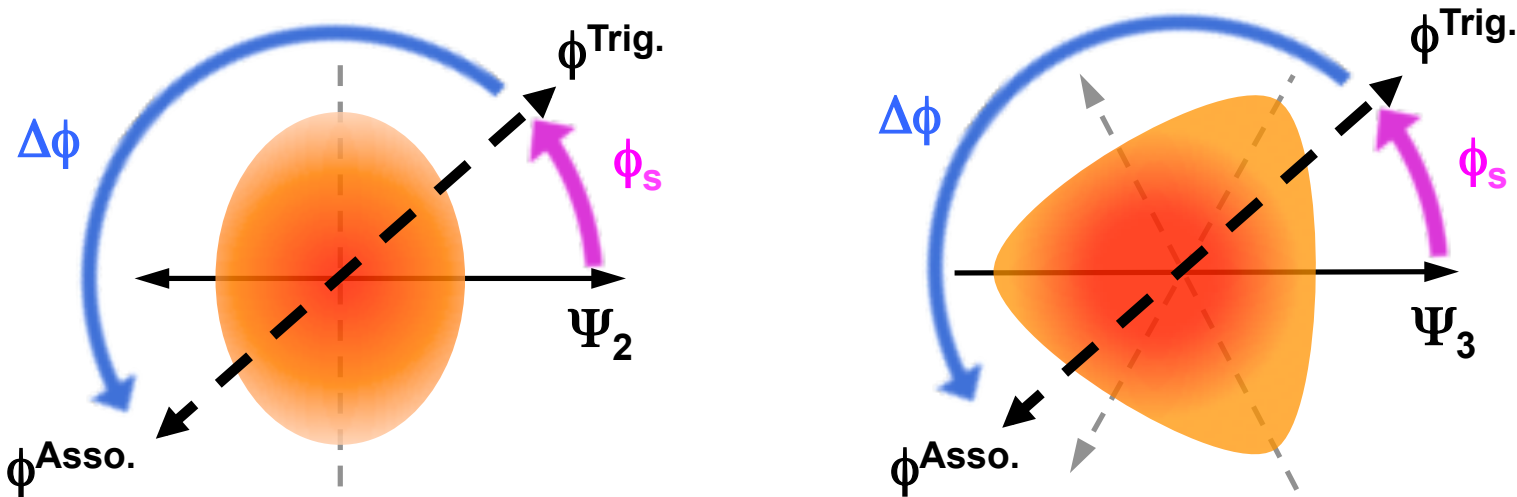


$\varepsilon$  : Tracking efficiency of associate particles

$N^t$  : Number of triggers

$N^{ta}$  : Number of pairs

# Trigger Selection with respect to Event-Plane

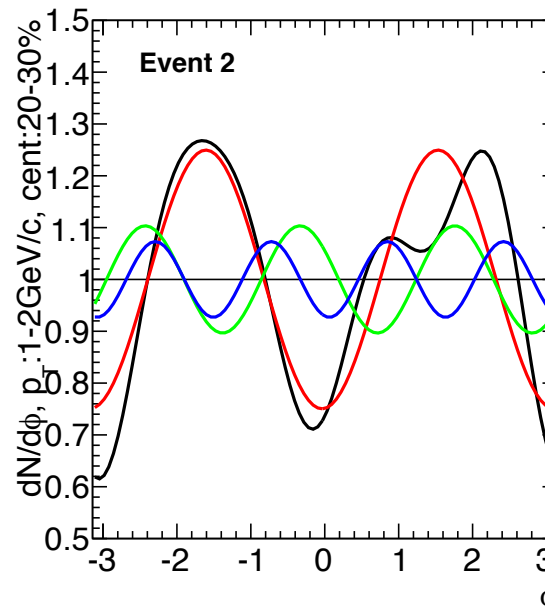
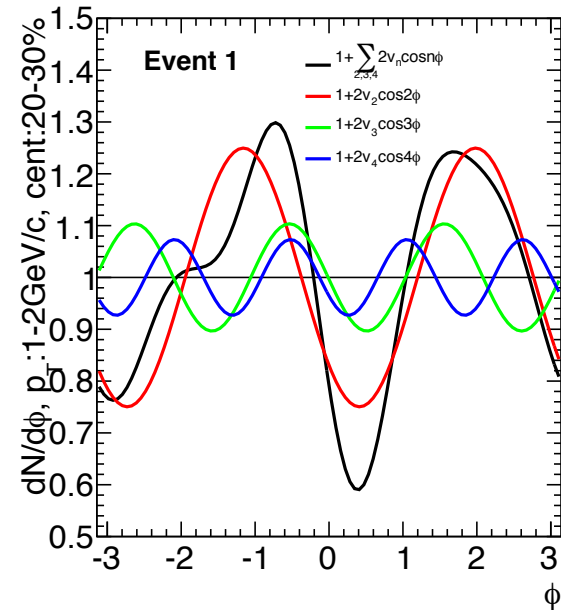


- ✧ Expansion to the short-axis direction by pressure gradient
  - EP : direction most particles are emitted after freeze-out
- ✧ Selecting trigger particles with respect to  $\Psi_2$  &  $\Psi_3$ 
  - 8 bins :  $\phi^{trig} - \Psi_n : [-\pi/n, \pi/n]$
- ✧ Control of path length of trigger and associate particles
- ✧ Three  $p_T$  combinations: 2-4x1-2, 2-4x2-4, 4-10x2-4 GeV/c

# Flow Backgrounds with respect to EP

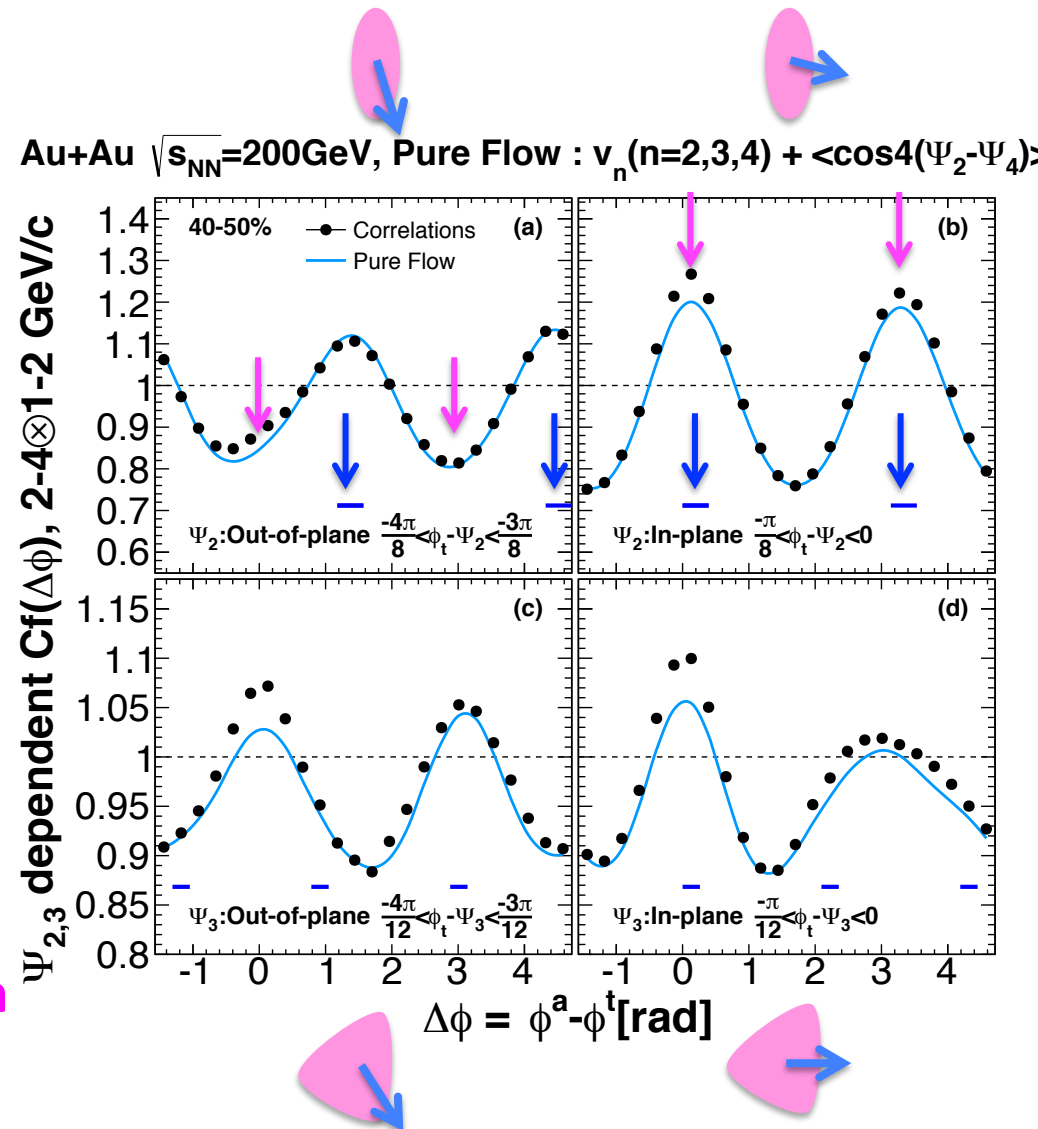
- ❖ A Monte Carlo simulation employed
- ❖ Azimuthal distribution using
  - Measured  $v_n$
  - Observed correlation between EP
    - $\langle 4(\Psi_2 - \Psi_4) \rangle = v_4\{\Psi_2\}/v_4\{\Psi_4\}$
    - $\langle 6(\Psi_2 - \Psi_3) \rangle = 0$
- ❖ Determine trigger particle relative to EP taking into account EP resolutions
- ❖ Calculate two-particle correlations

$$\frac{dN}{d\phi} \propto 1 + \sum_{n=2,3,4} 2v_n \cos n(\phi - \Psi_n)$$



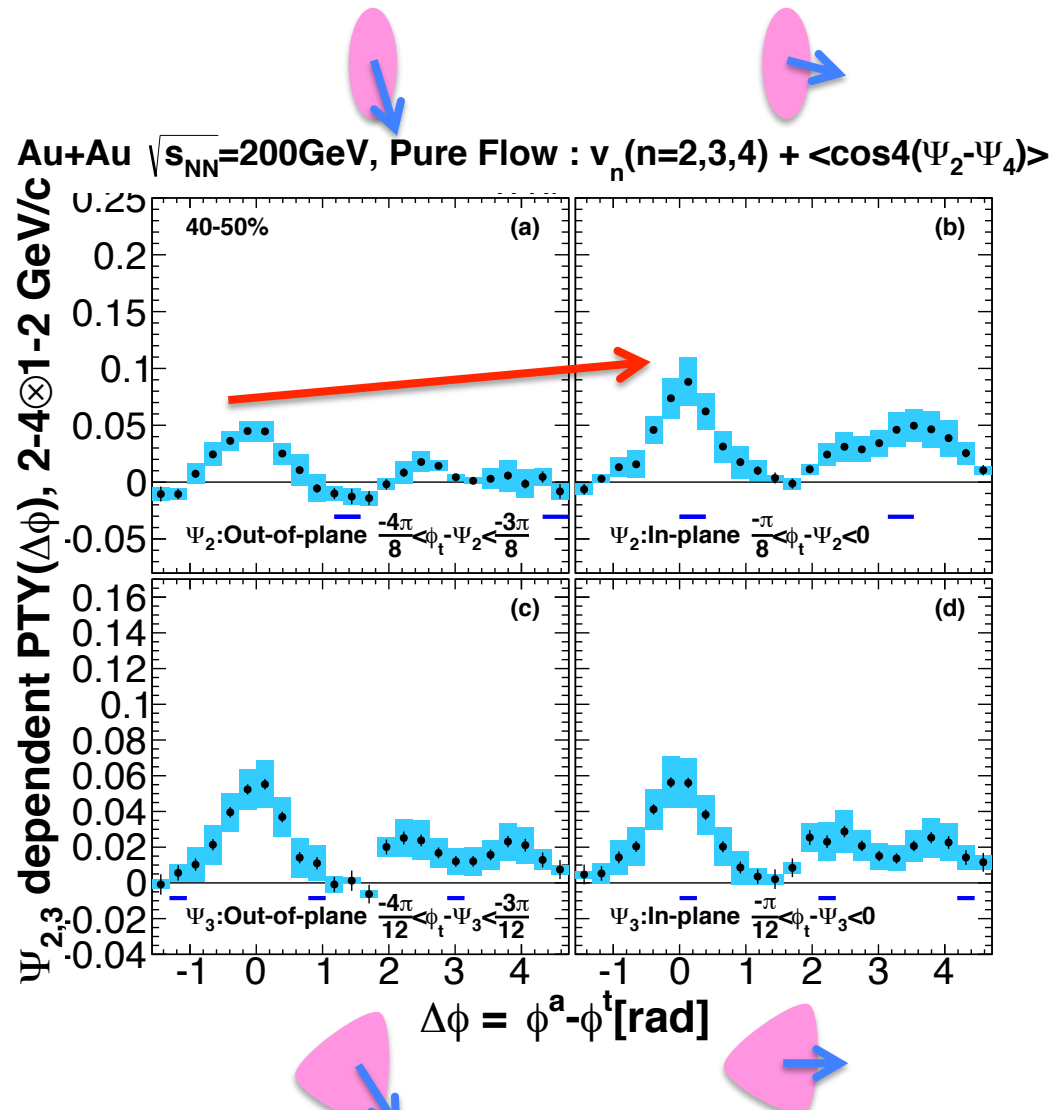
# Flow Backgrounds with respect to EP

- ❖ Good reconstruction of  $\Psi_2$ ,  $\Psi_3$  dependent correlations by MC simulation
    - Before PTY normalization
  - ❖ Except around  $\Delta\phi=0, \pi$  where contribution of jet exists
    - Correlations
    - Pure Flow
- : EP Direction**
- : Back-to-Back Direction**



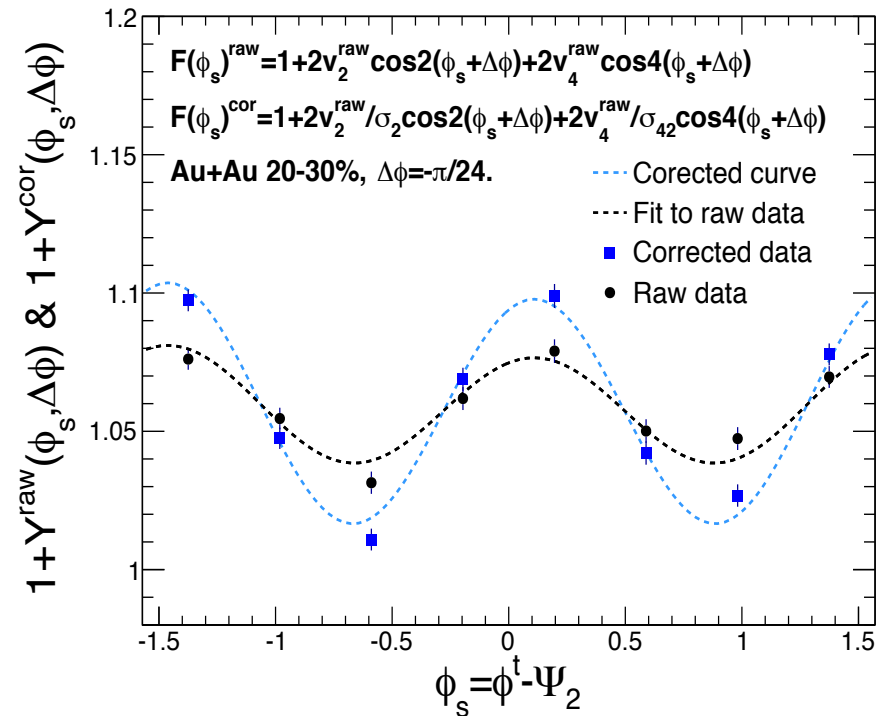
# Two-Particle Correlations with respect to EP

- ❖ Flow subtracted  $\Psi_2, \Psi_3$  dependent correlations
- ❖ Clear  $\Psi_2$  dependence
- ❖ No  $\Psi_3$  dependence?
- ❖ Smearing by neighboring trigger bins due to limited EP resolution
  - Needs unfolding !!



# Unfolding Methods of EP Resolution

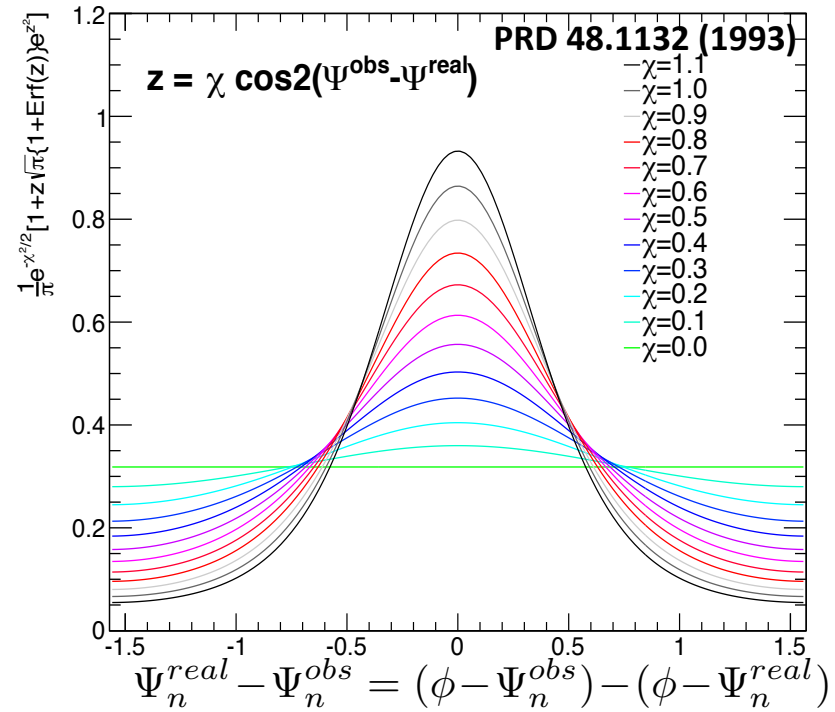
## Fitting Method



❖ Azimuthal anisotropy of correlation yield corrected by the event-plane resolution

Method by PRC.84.024904 (2011)

## Iteration Method

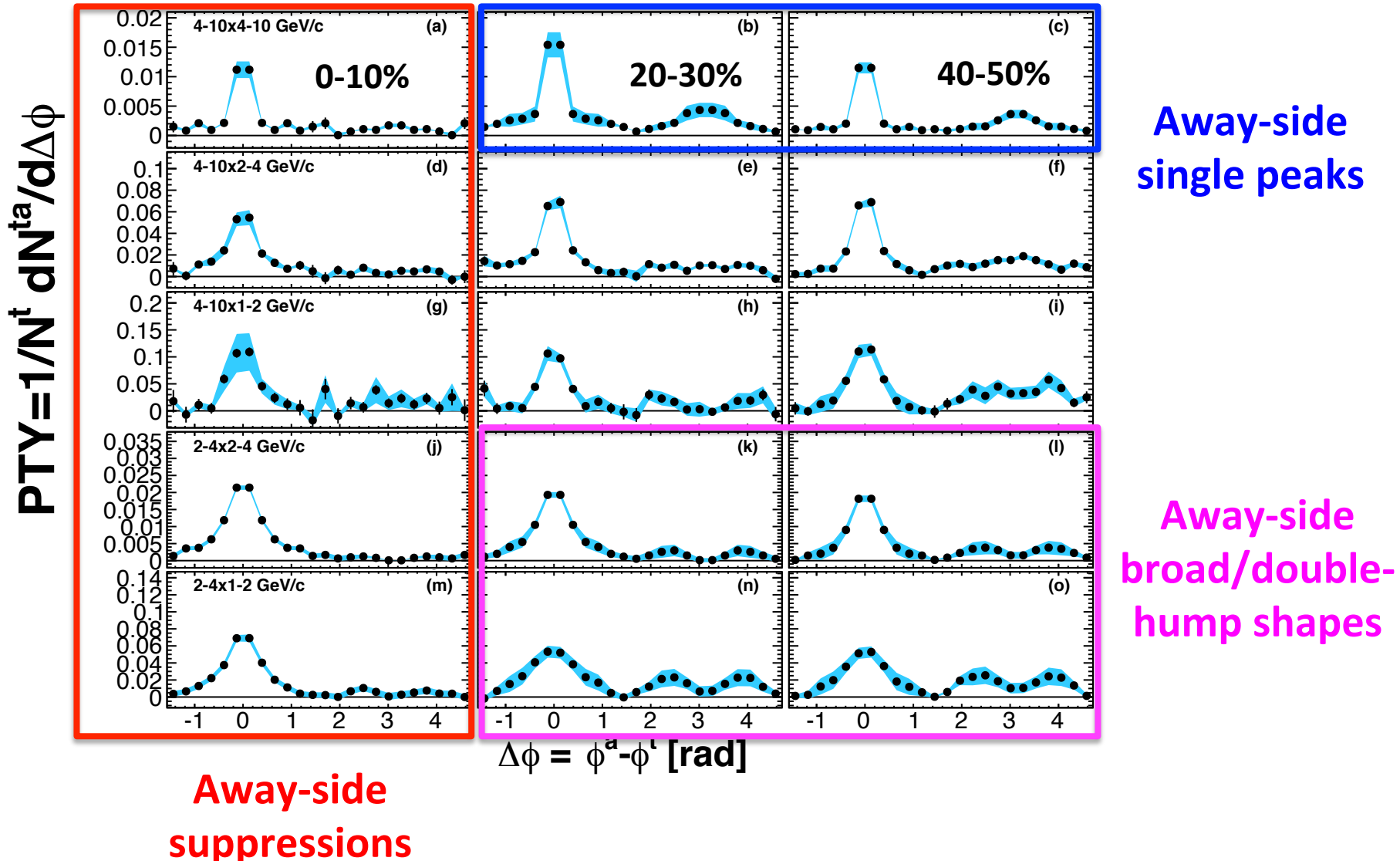


- ❖ Trigger smearing matrix “S”
- ❖ True & Observed Correlations “A” & “B”
  - Vector elements : Trigger bin
- ❖ Solve simultaneous equations via iteration

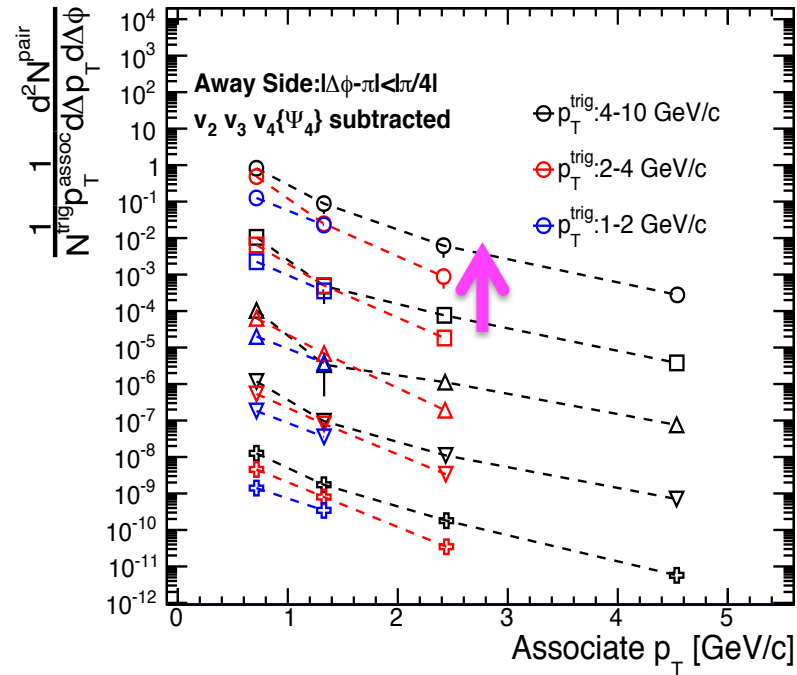
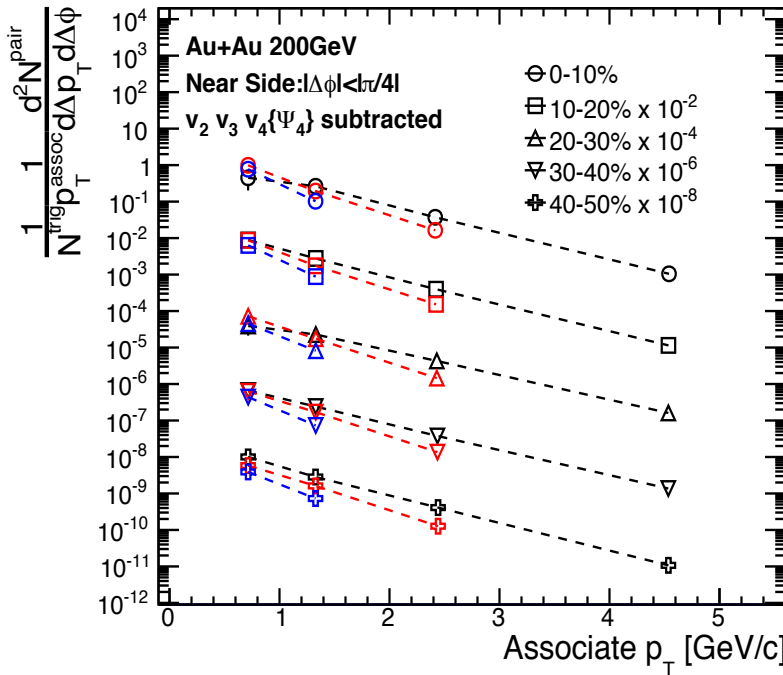
$$B = SA \quad \xrightarrow{\text{blue arrow}} \quad A = S^{-1}B$$

# $v_n$ ( $n=2,3,4$ ) subtracted correlations

Au+Au  $\sqrt{s_{NN}}=200$  GeV,  $v_n$  ( $n=2,3,4$ ) subtracted

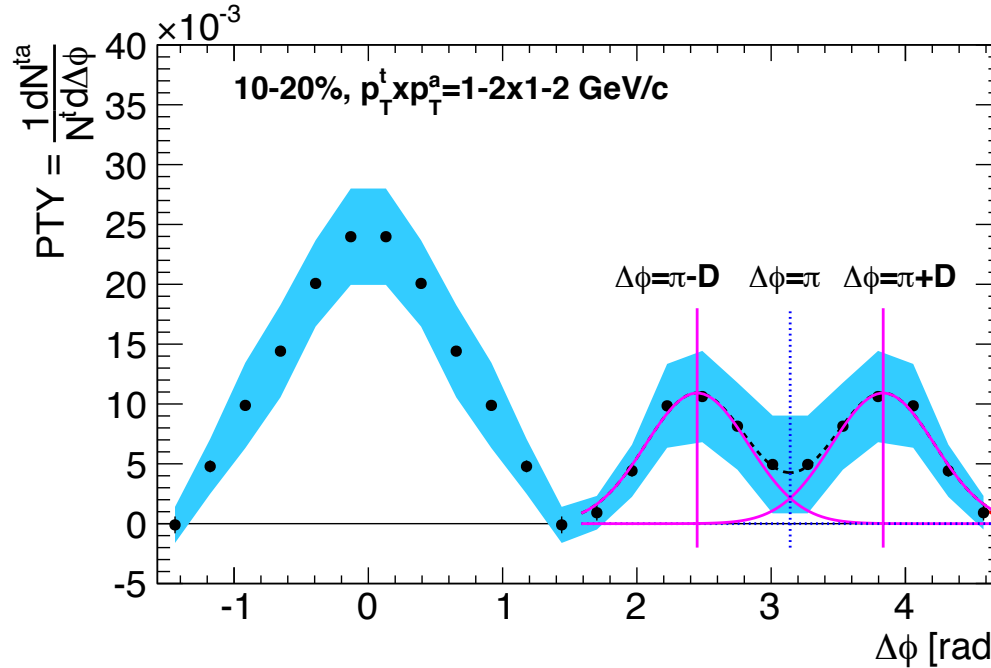


# $p_T$ spectra of Per Trigger Yields



- ✧ Hardness increases with trigger and associate  $p_T$
- ✧ Existence of high  $p_T$  particles enhances low  $p_T$  particles

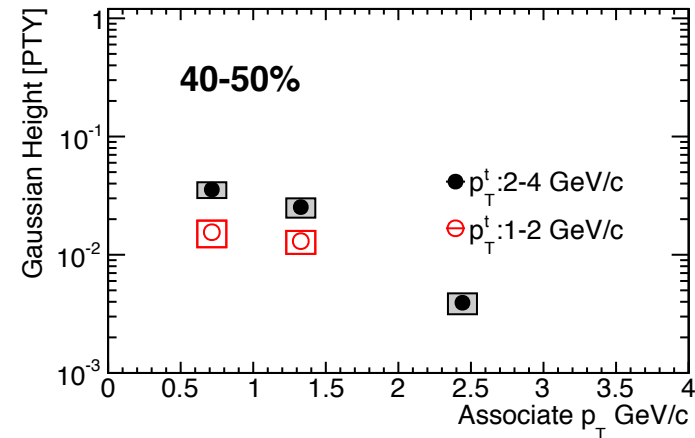
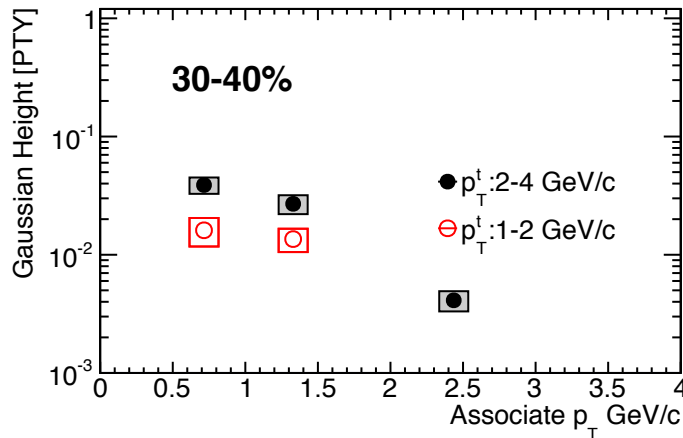
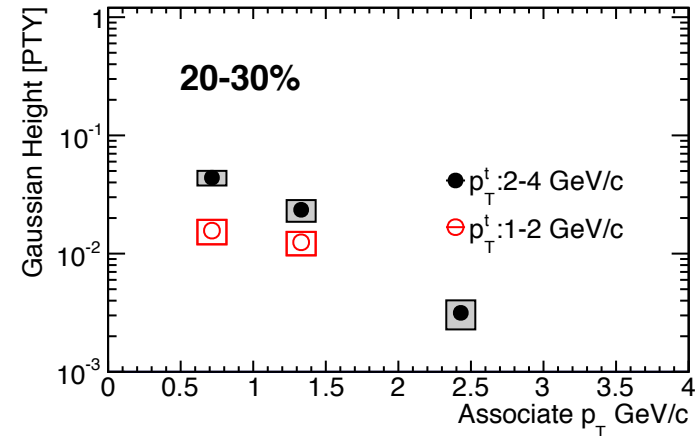
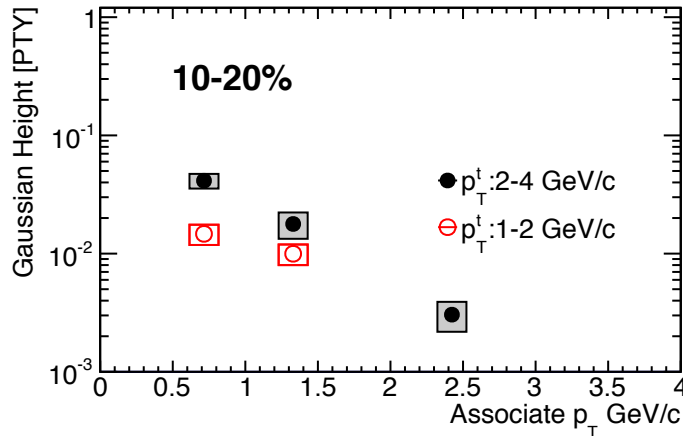
# Extraction of Double-Hump Position



- ◇ Extraction of double-hump position via two-Gaussian fitting to away-side ( $|\Delta\phi - \pi| < \pi$ ) at centrality 10%, where double-humps seen

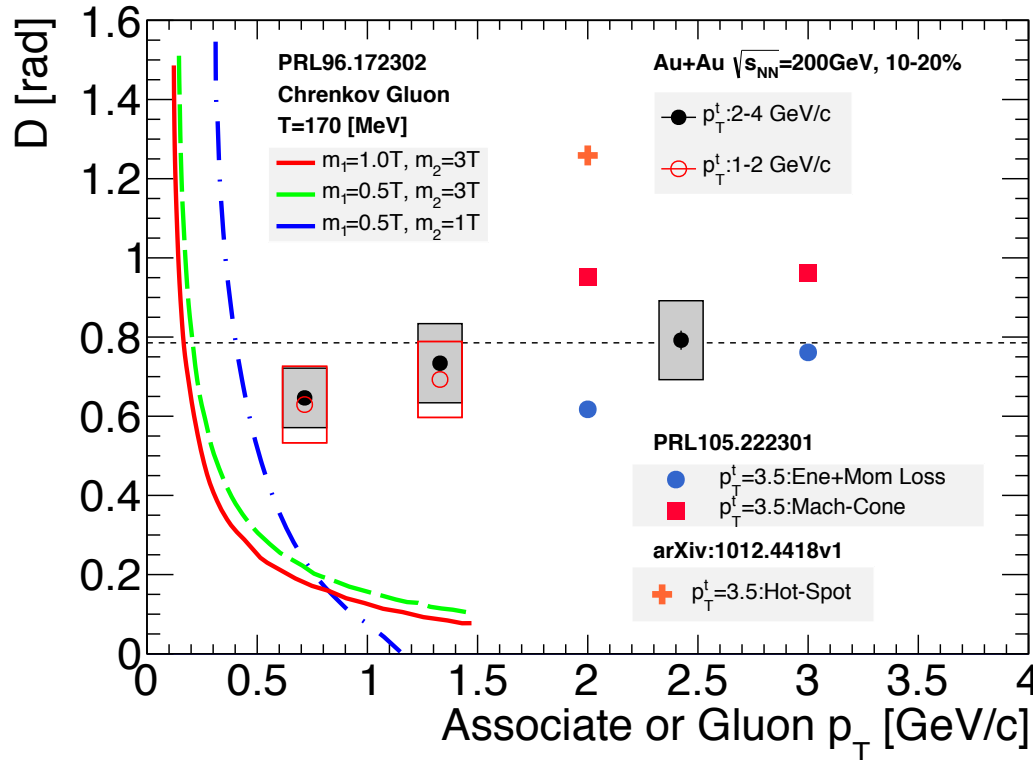
$$F(\Delta\phi) = A e^{-\frac{(\Delta\phi - \pi - D)^2}{\sigma^2}} + A e^{-\frac{(\Delta\phi - \pi + D)^2}{\sigma^2}}$$

# Two-Gaussian Height



- ✧ Double-hump height more than one sigma of systematic uncertainties

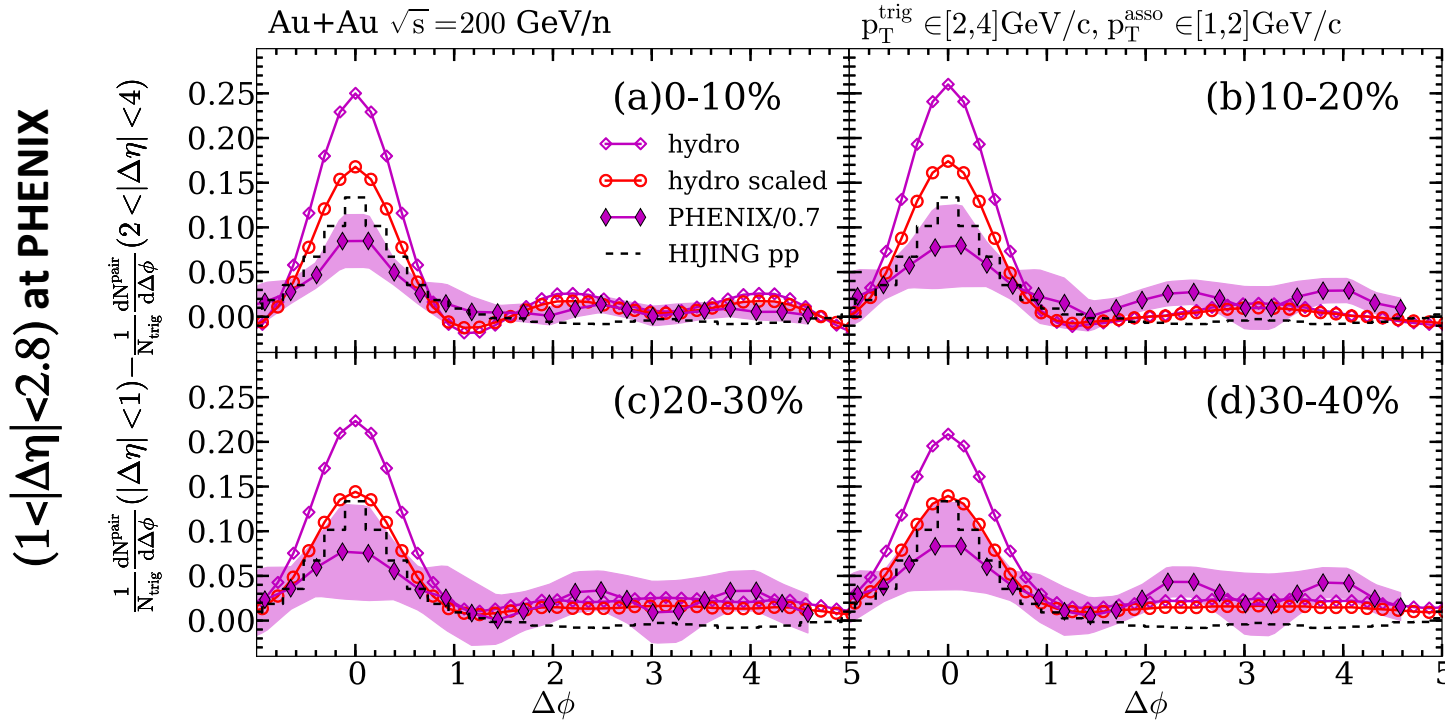
# Comparison with Models



- ✧ Cherenkov gluon : <25 % of experimental data at  $p_T = 1 \text{ GeV}/c$
- ✧ Mach-cone & Energy-momentum loss :
  - Independence of  $p_T$  is similar to the experimental data
  - 20 % larger/smaller than experimental data at  $p_T = 2 \text{ GeV}/c$
- ✧ Hot-spot : 50% larger than experimental data

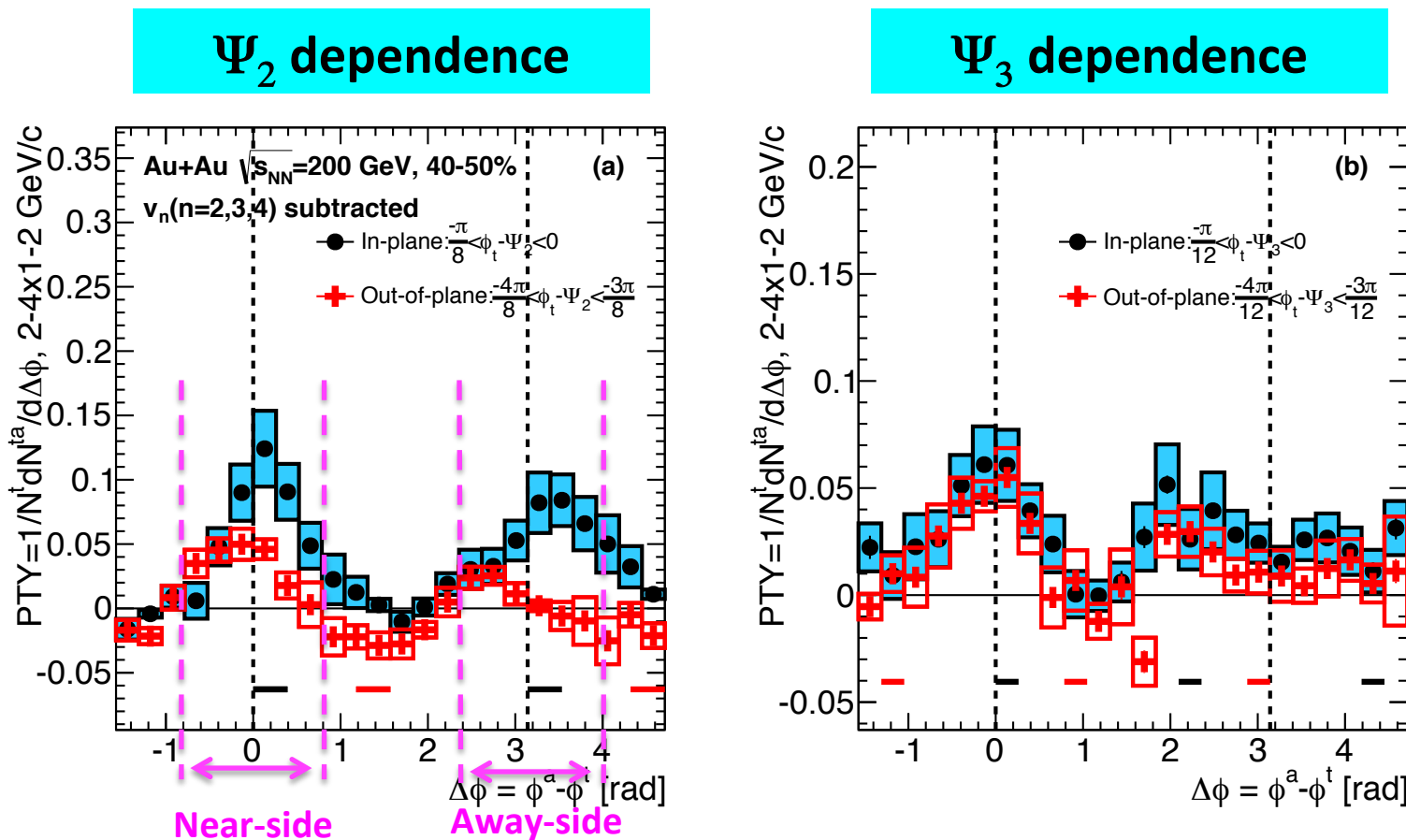
# Realistic Model Calculation

L.Pang & X.N> Wang et al. arXiv:nucl-th/1309.6735v2 (2013)



- ✧ Fluctuations of initial parton energy density
- ✧ Parton cascade
- ✧ Event-by-event (3+1)D hydrodynamics
- ✧ Parton Energy Momentum Loss

# $\Psi_2$ & $\Psi_3$ Dependent Correlations at $p_T$ :2-4x1-2 GeV/c

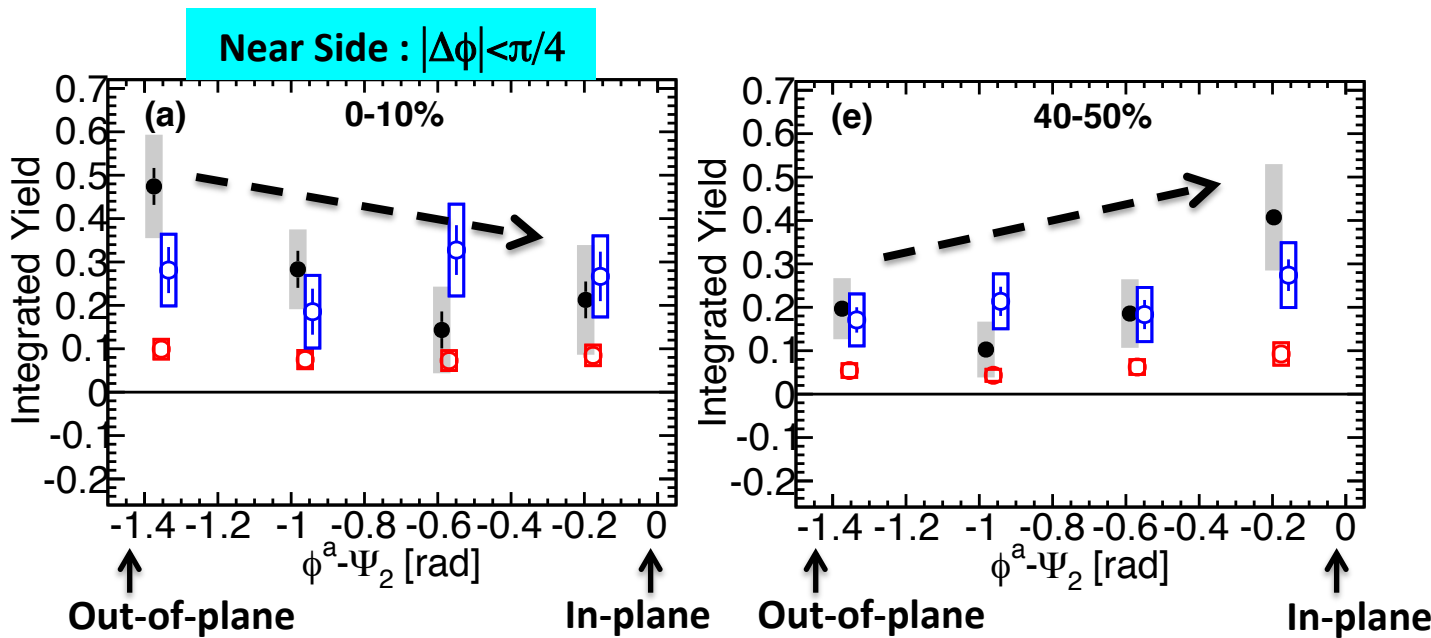


✧  $\Psi_2$  dependence is observed at intermediate- $p_T$  correlations

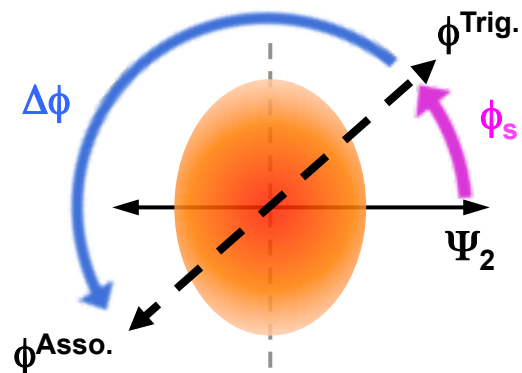
# Near-Side Integrated Yield vs Associate Angle from $\Psi_2$

Au+Au 200GeV  
 $\Psi_2$  dependence  
Near Side :  $|\Delta\phi| < \pi/4$

- 2-4  $\otimes$  1-2 GeV/c
- 2-4  $\otimes$  2-4 GeV/c
- 4-10  $\otimes$  2-4 GeV/c

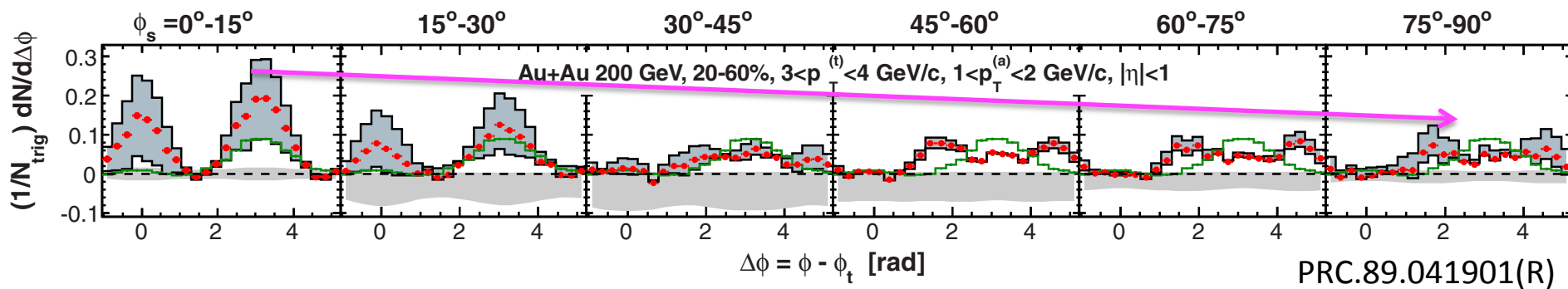


- ✧ Similar near and away-side trends
- ✧  $p_T$  2-4x2-4, 4-10x2-4 GeV/c : **in-plane  $\geq$  out-of-plane**
  - Consistent with the parton energy loss picture
- ✧  $p_T$  2-4x1-2 GeV/c
  - 0-10% : **Out-of-plane  $>$  In-plane**
  - 40-50% : **In-plane  $>$  Out-of-plane**
  - More than  $1\sigma$  significance of total systematics



# STAR Result of $\Psi_2$ Dependent Correlations

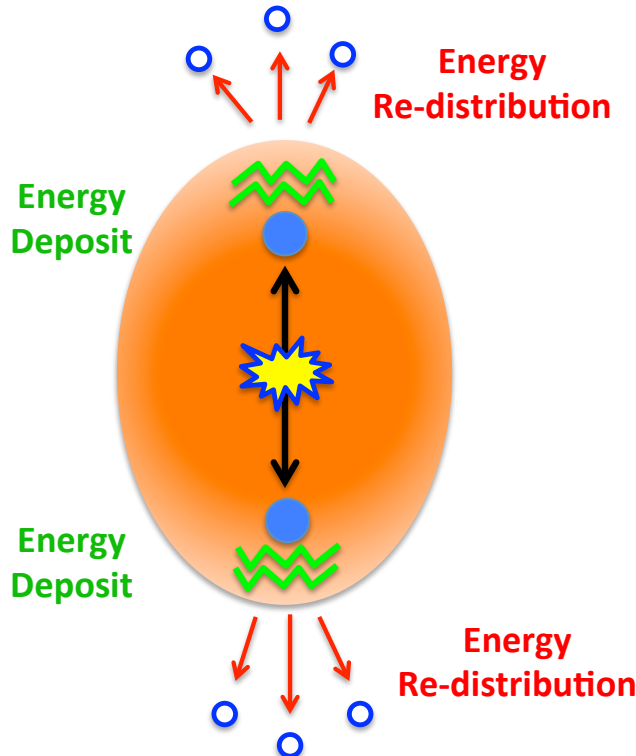
Au+Au 200 GeV, 20-60%,  $3 < p_T^{(t)} < 4 \text{ GeV}/c$ ,  $1 < p_T^{(a)} < 2 \text{ GeV}/c$ ,  $|\eta| < 1$     $v_n(n=2,3,4)$  subtracted



- ✧ Consistent with the results in mid-central collisions by PHENIX

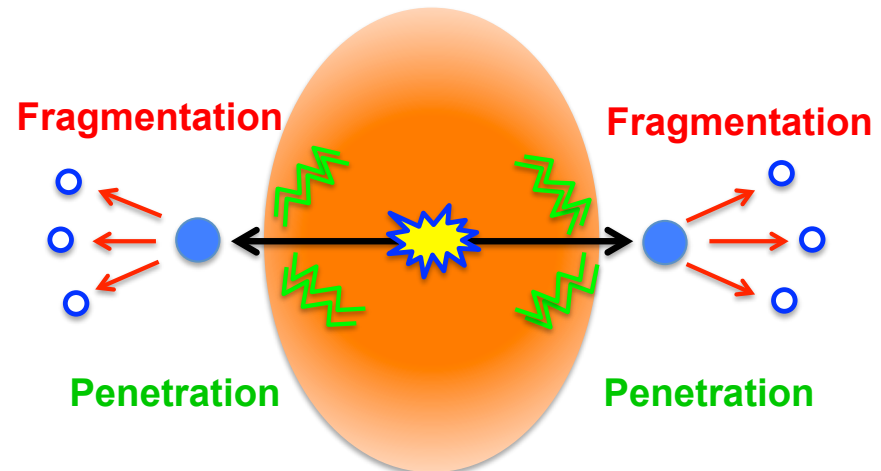
# Interpretation of $\Psi_2$ Dependent Correlations

Central



Re-distribution  
Dominance

Mid-central



Penetration  
Dominance

# Hydro + energy redistribution

## Purposes and Methods

### - Purpose of this study

Study the **collective response** to jet propagation in QGP  
transport of the jet's lost energy

### - Method

Hydrodynamical simulations of di-jet asymmetric events in heavy ion collisions

### - Relativistic hydrodynamic equations with source terms

Hydrodynamic equations with incoming energy and momentum

$$\partial_\mu T^{\mu\nu} = J^\nu$$

$T^{\mu\nu}$ : energy-momentum tensor of the QGP fluid

$J^\nu$  : **source term** (energy-momentum deposit from jets)

QM'14 Y. Tachibana

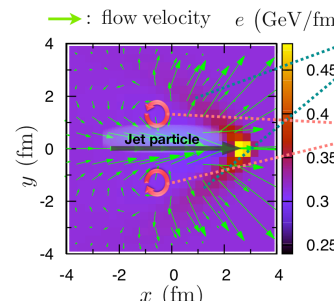
### - Source terms

Assume sudden thermalization of deposited momentum inside a fluid cell

$$J^\mu(x) = - \sum_a \frac{dp_a^\mu}{dt} \delta^{(3)}(\mathbf{x} - \mathbf{x}_a(t)) \quad a: \text{index for each jet particle}$$

### - Collective flow induced by a jet

Test study result in the case of 1-jet traveling through a uniform fluid



#### Mach cone

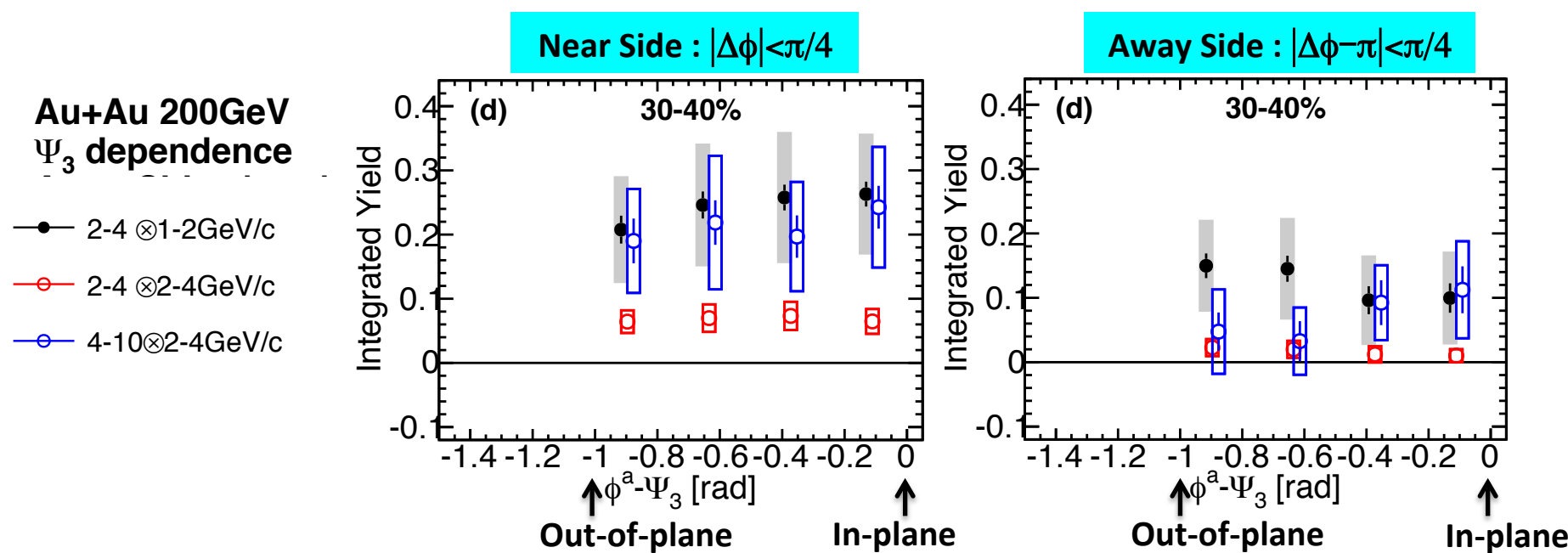
Interference of sound waves induced by a source moving at supersonic speed

#### Vortex

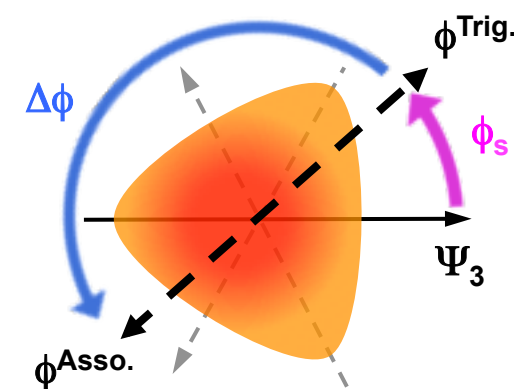
Vortex ring around the jet passage in 3-D space

Mach cone carries information about jet energy loss and properties of QGP

# Integrated Yield vs Associate Angle from $\Psi_3$



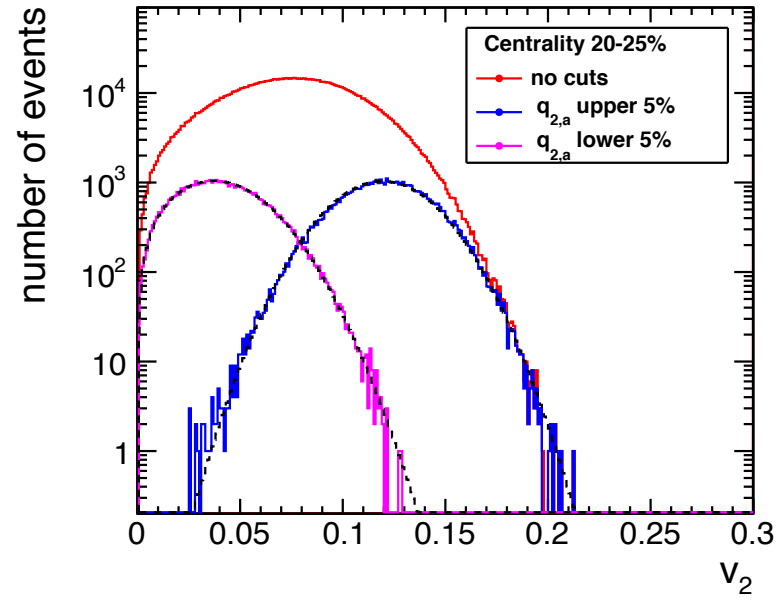
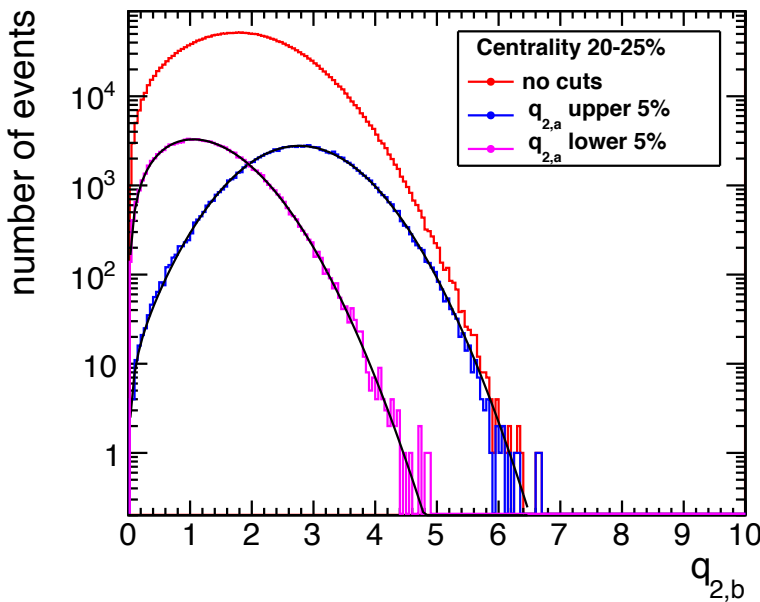
- ❖ Weak centrality dependence
- ❖ Event-plane dependence is not clearly seen
  - Flat within systematic uncertainties



# Out Look : Event-Shape Engineering

✧ Q-vector

$$Q_{n,x} = \sum_i^M \cos(n\phi_i); \quad Q_{n,y} = \sum_i^M \sin(n\phi_i);$$



✧ Selection of flow rich events

✧ Differential analysis of medium response

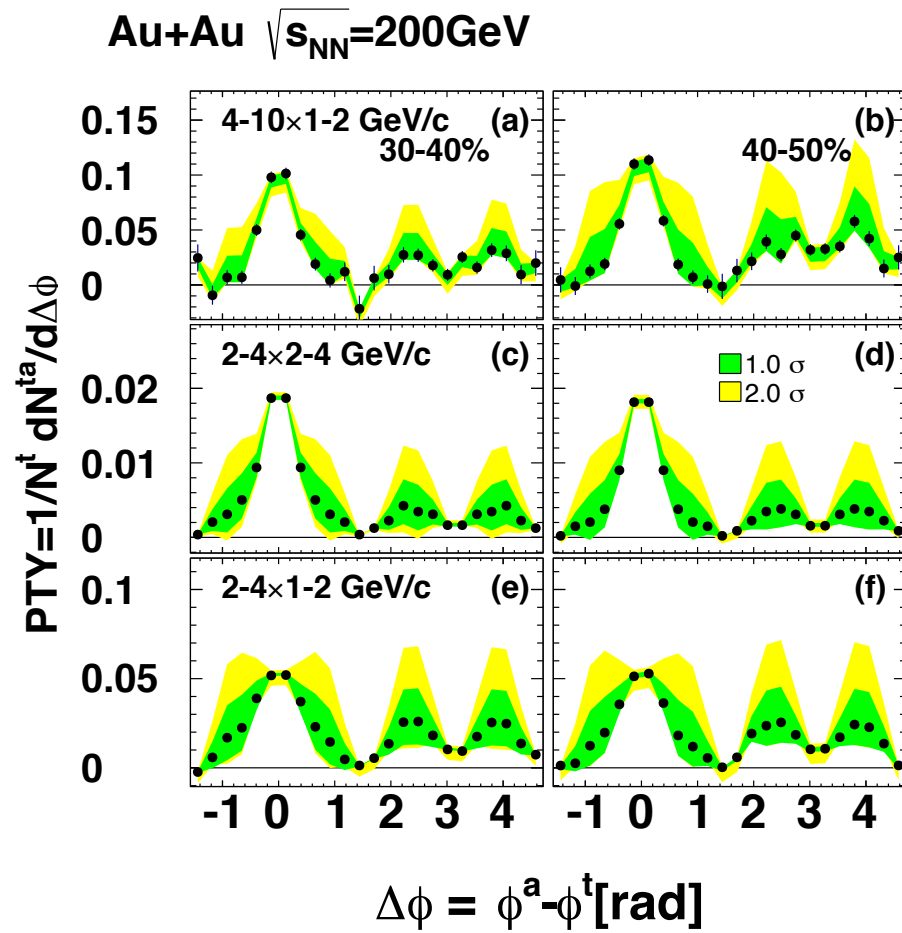
# Summary

- ✧  $v_n$  subtracted correlations are presented
- ✧ Non-monotonic path-length dependence is seen in  $\Psi_2$  dependent correlations at low  $p_T$ 
  - Can be taken as re-distribution of deposited energy?
- ✧ Non- $\Psi_3$  dependence is observed due to large systematics

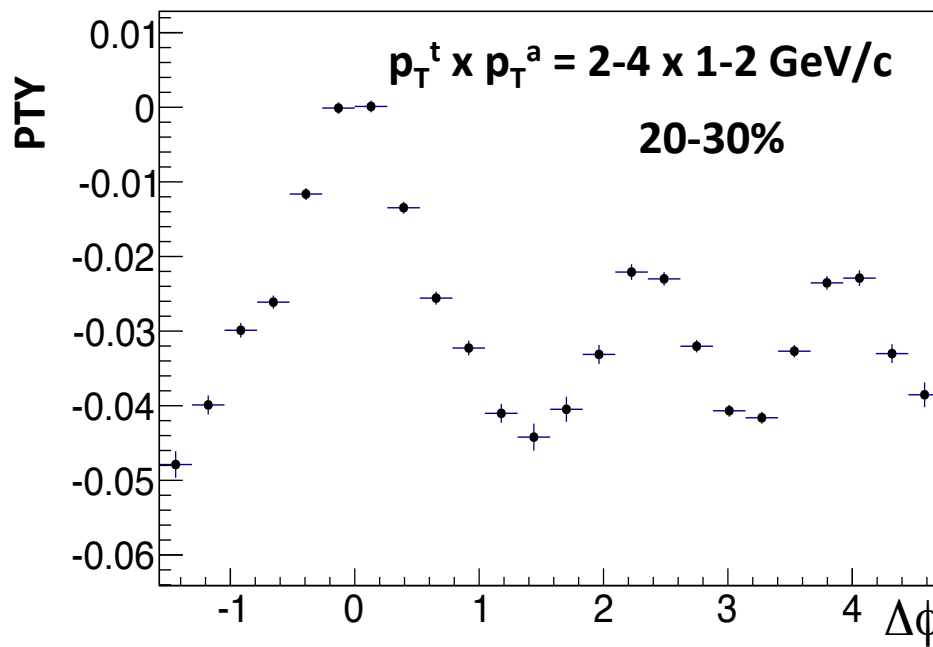
# **BACK UP**

# Significance of Double-Hump

- Examed the significance of Double-Hump in terms of  $v_4$  systematics
- $v_2$  and  $v_3$  are fixed in flow subtractions but  $v_4$  is varied  $\pm 1\sigma$
- Lower boundary of yellow band covers that of green band
- Significance is  $\pm 1\sigma$  level of  $v_4$  systematics



# Zero Yield at Near-Side



- ✧ Correlation and Pure Flow is fitted at  $\Delta\phi=0$
- ✧ Double-hump is not so sensitive to flow subtraction

# Consistency check : high- $p_T$ trigger

- ❖ Three-Centralities
  - 0-20, 20-40, 40-60%

- ❖ Particle Selections
  - Trigger  $p_T$ : **5-10 GeV/c**
  - Associate  $p_T$  : **1-10 GeV/c**

- ❖ Subtracted Backgrounds
  - **Only  $v_2$**

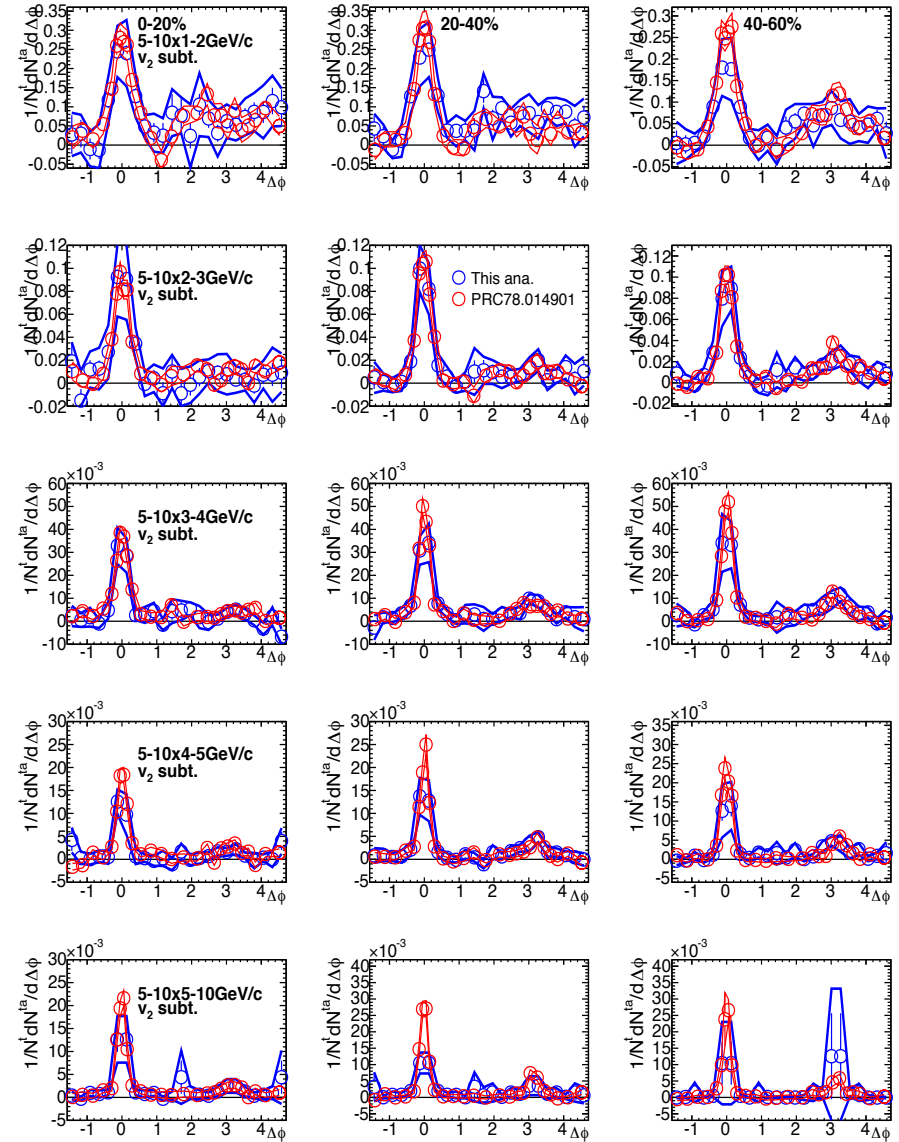
- ❖ Consistent with previous PHENIX results  
**(PRC78.014901)**



: This Analysis



: PRC78.014901



# Consistency check : mid- $p_T$ trigger

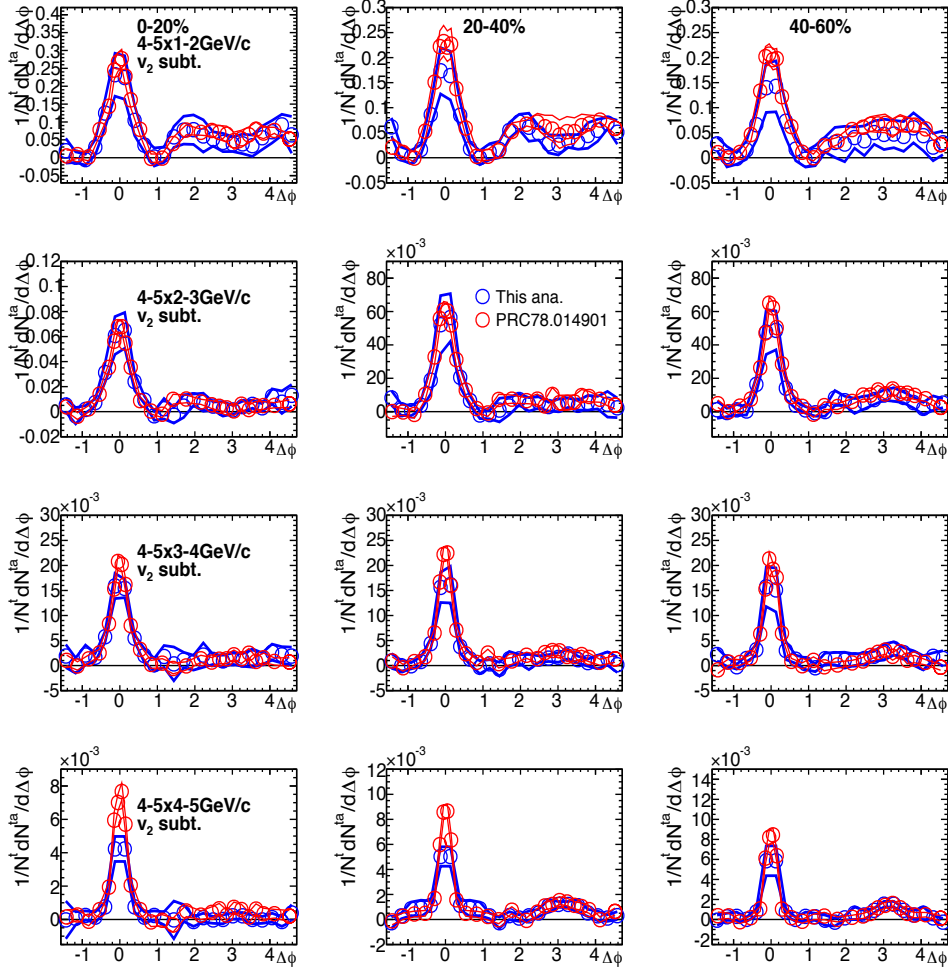
- ❖ Three-Centralities
  - 0-20, 20-40, 40-60%
- ❖ Particle Selections
  - Trigger  $p_T$ : **4-5 GeV/c**
  - Associate  $p_T$  : **1-5 GeV/c**
- ❖ Subtracted Backgrounds
  - Only  **$v_2$**
- ❖ Consistent with previous PHENIX results  
**(PRC78.014901)**



: This Analysis



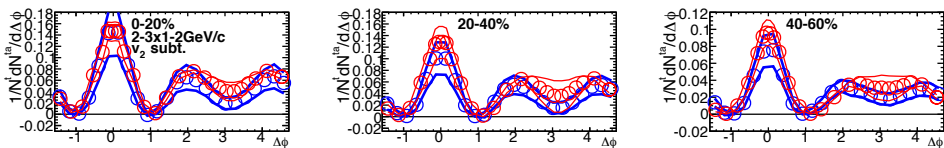
: PRC78.014901



# Consistency check : low- $p_T$ trigger

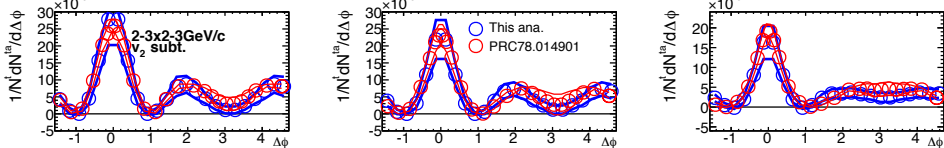
## ✧ Three-Centralities

- 0-20, 20-40, 40-60%

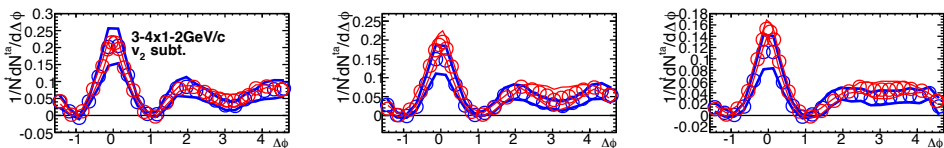


## ✧ Particle Selections

- Trigger  $p_T$ : **2-4 GeV/c**

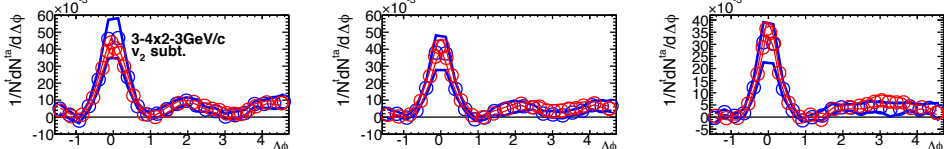


- Associate  $p_T$  : **1-4 GeV/c**

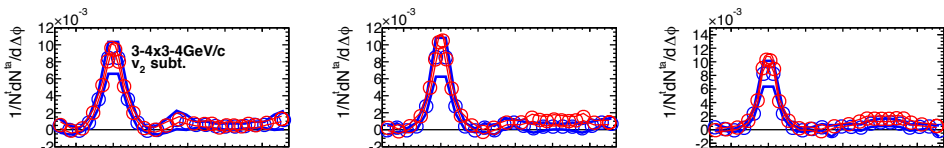


## ✧ Subtracted Backgrounds

- **Only  $v_2$**



## ✧ Consistent with previous PHENIX results (PRC78.014901)

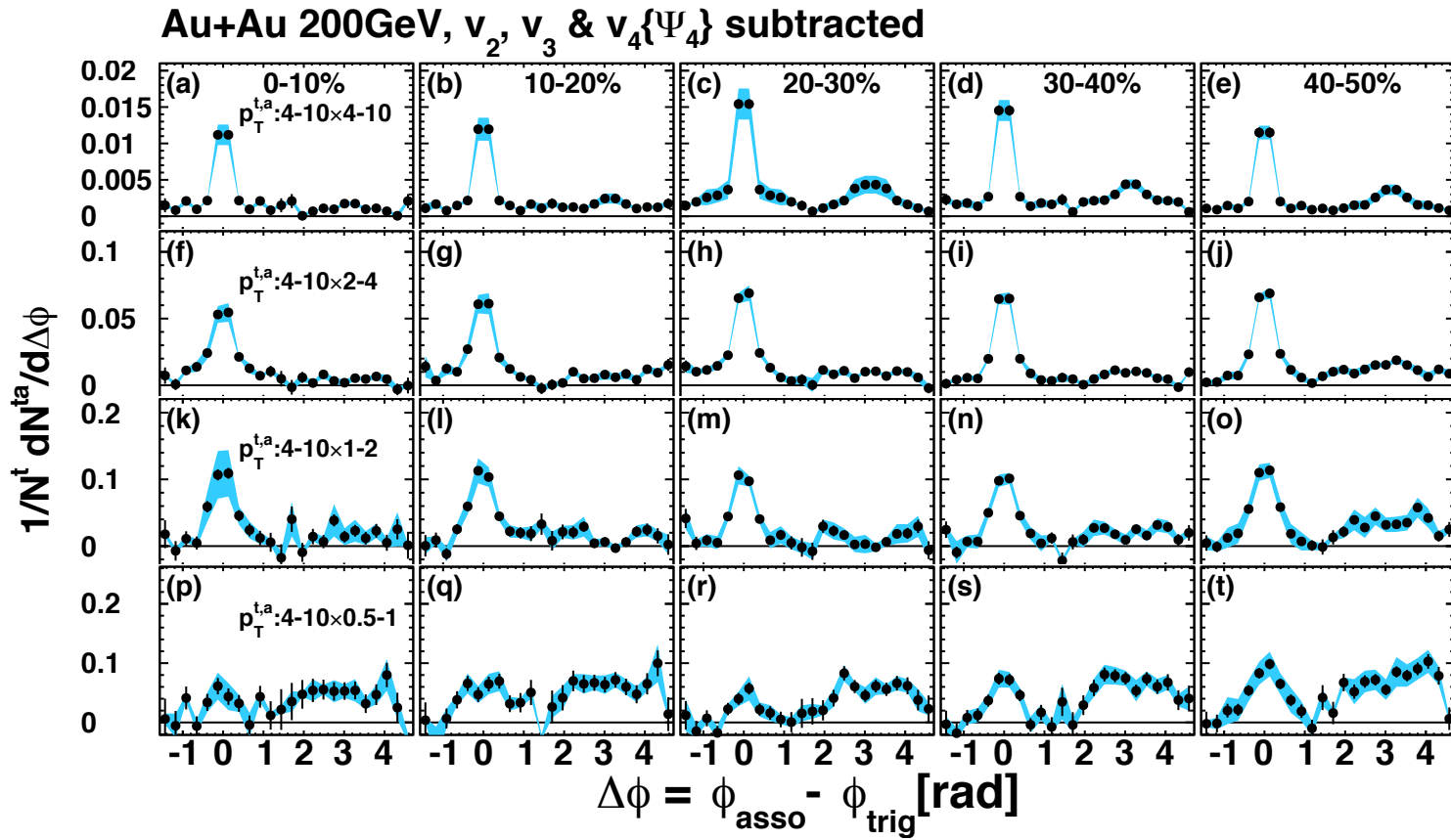


: This Analysis

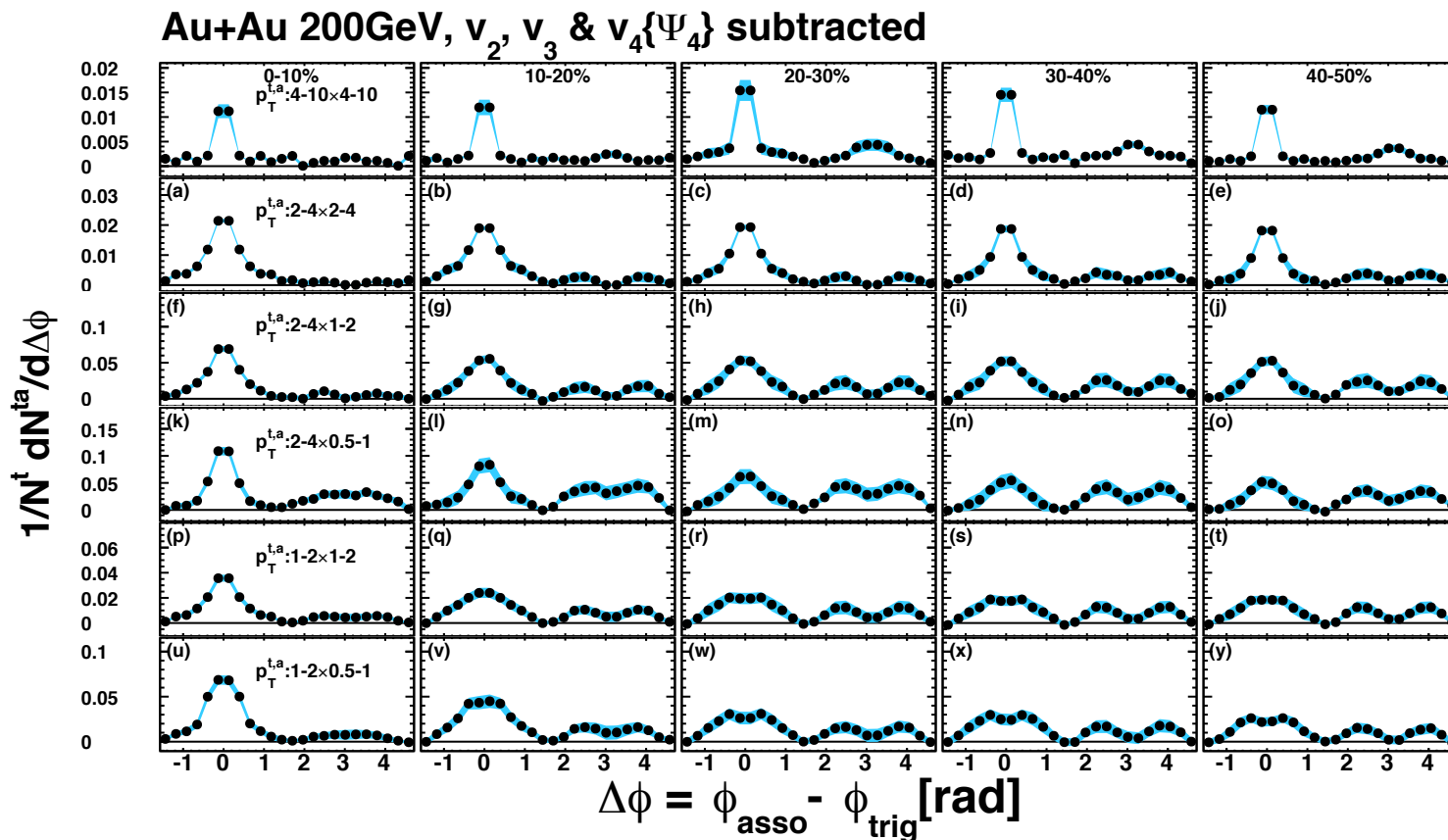


: PRC78.014901

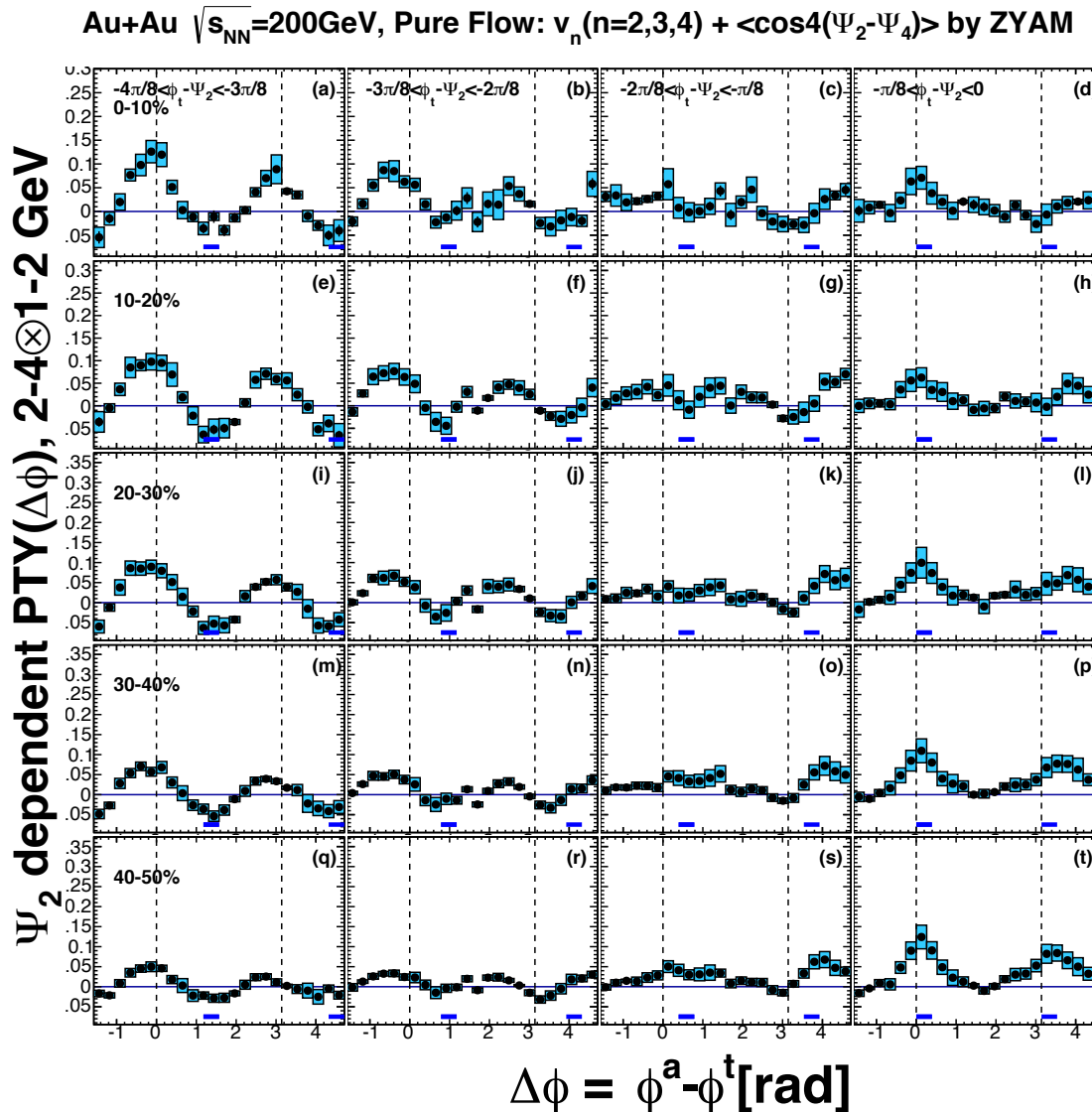
# High $p_T$ Trigger Two-Particle Correlations



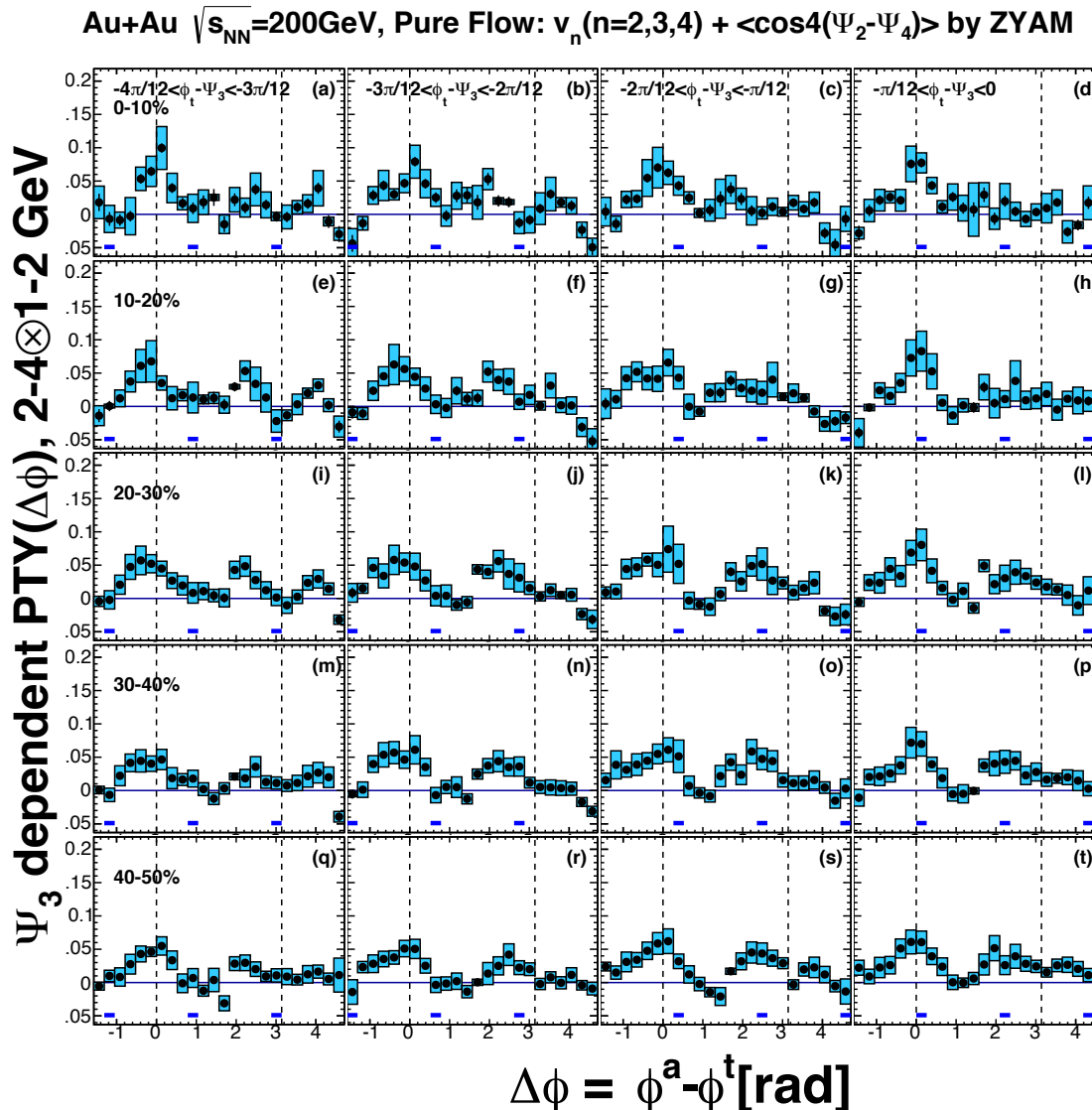
# Intermediate $p_T$ Two-Particle Correlations



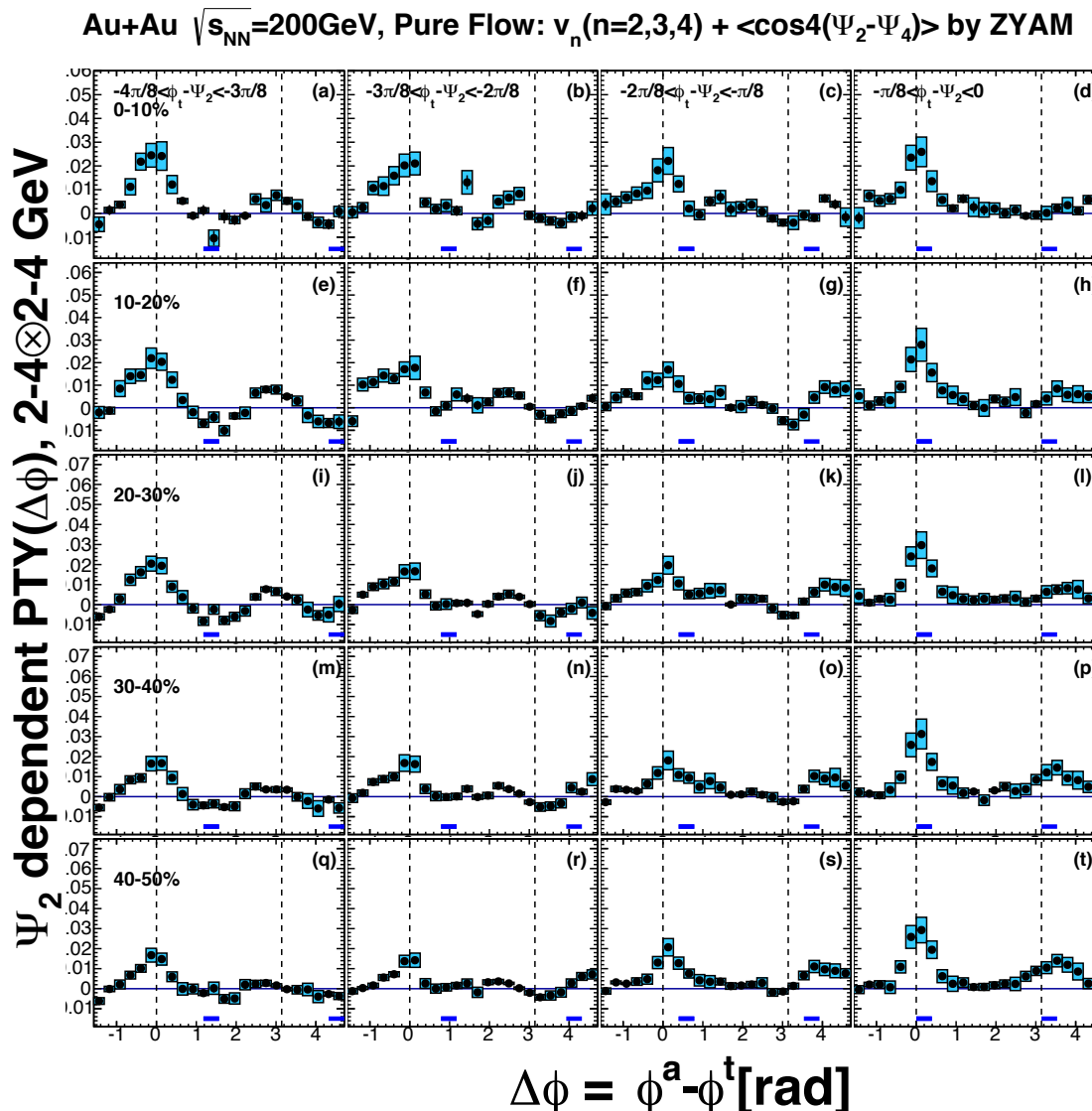
# $\Psi_2$ Dependent Correlations : $p_T$ 2-4x1-2 GeV/c



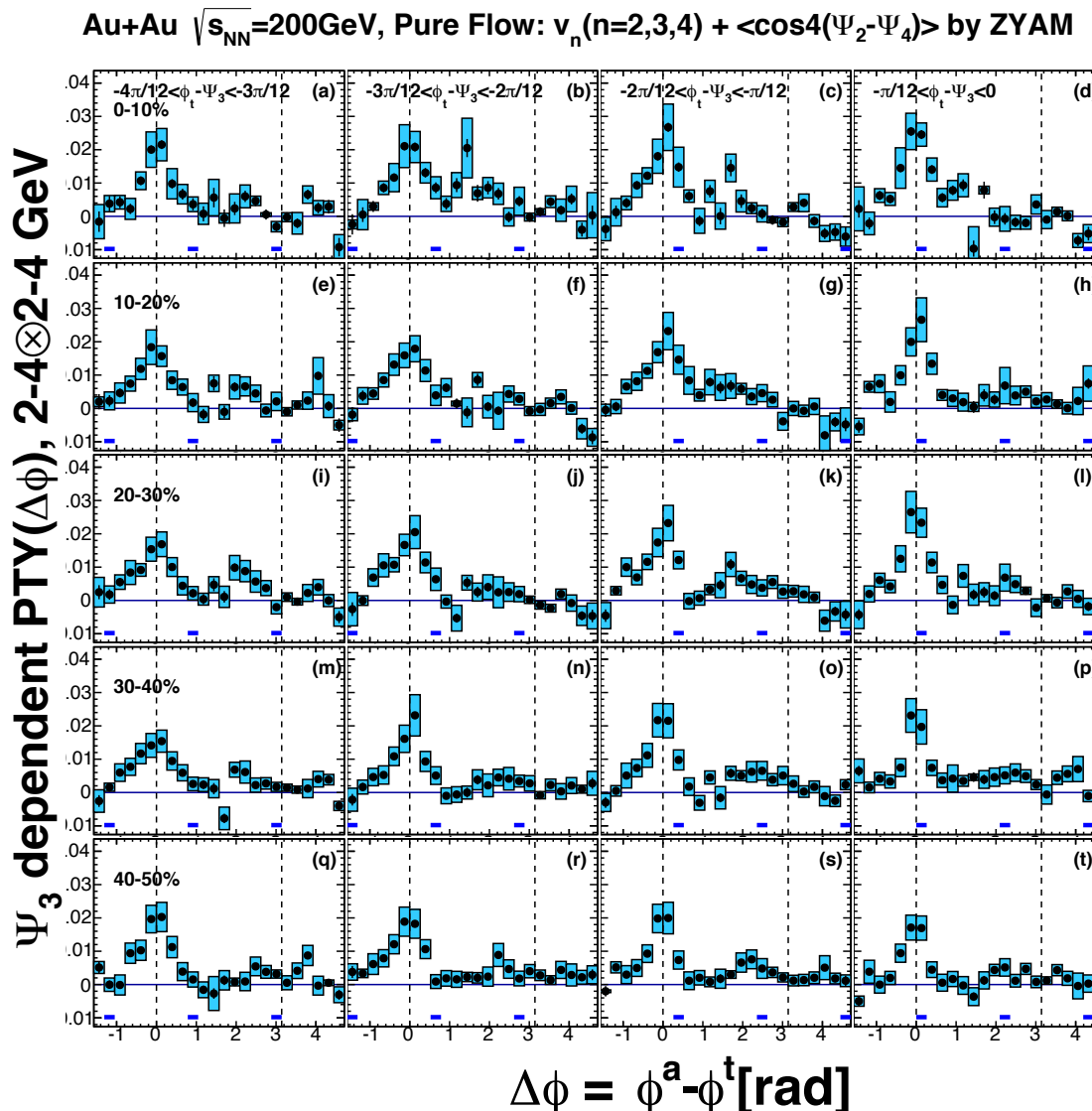
# $\Psi_3$ Dependent Correlations : $p_T$ 2-4x1-2 GeV/c



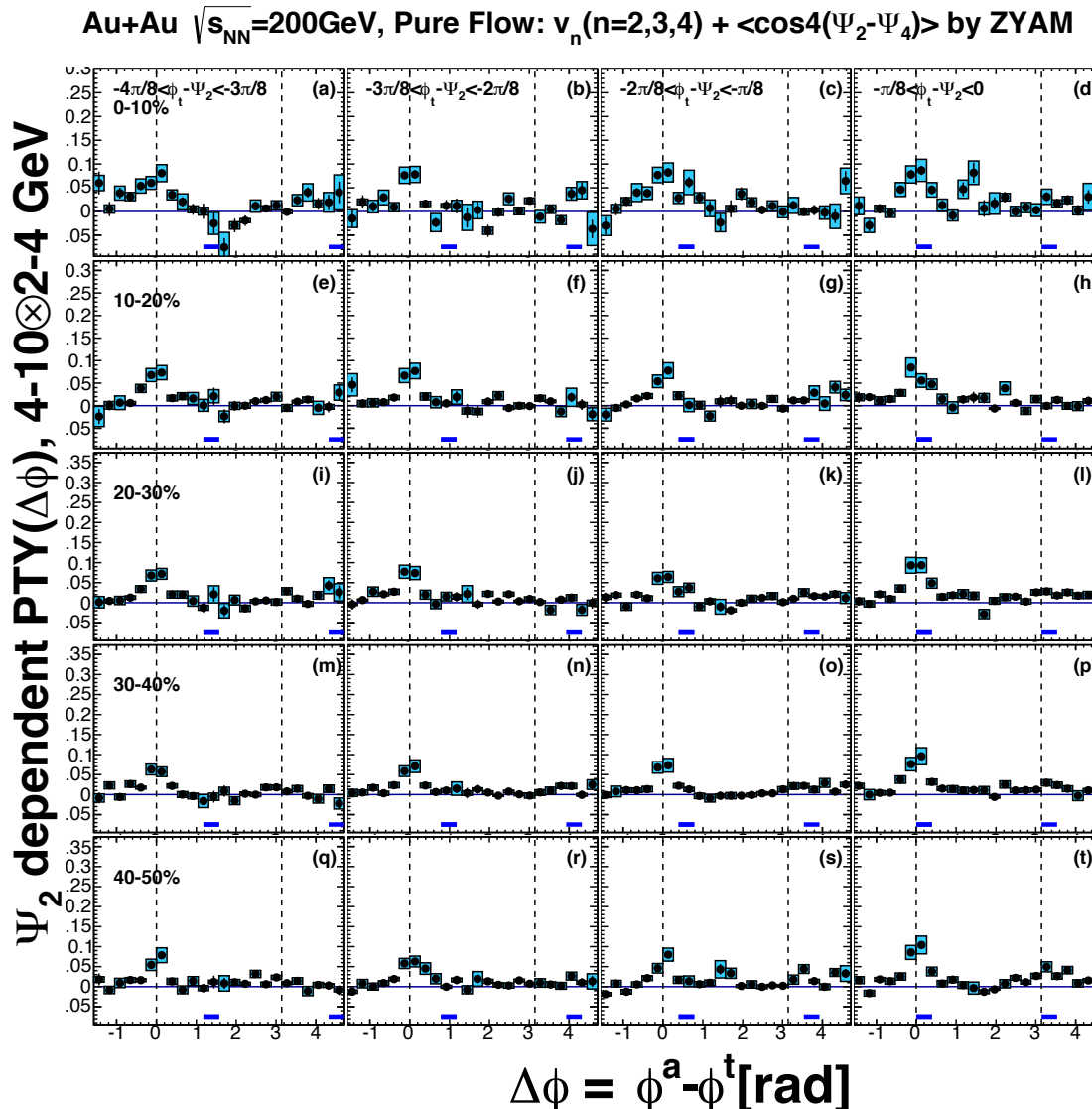
# $\Psi_2$ Dependent Correlations : $p_T$ 2-4x2-4 GeV/c



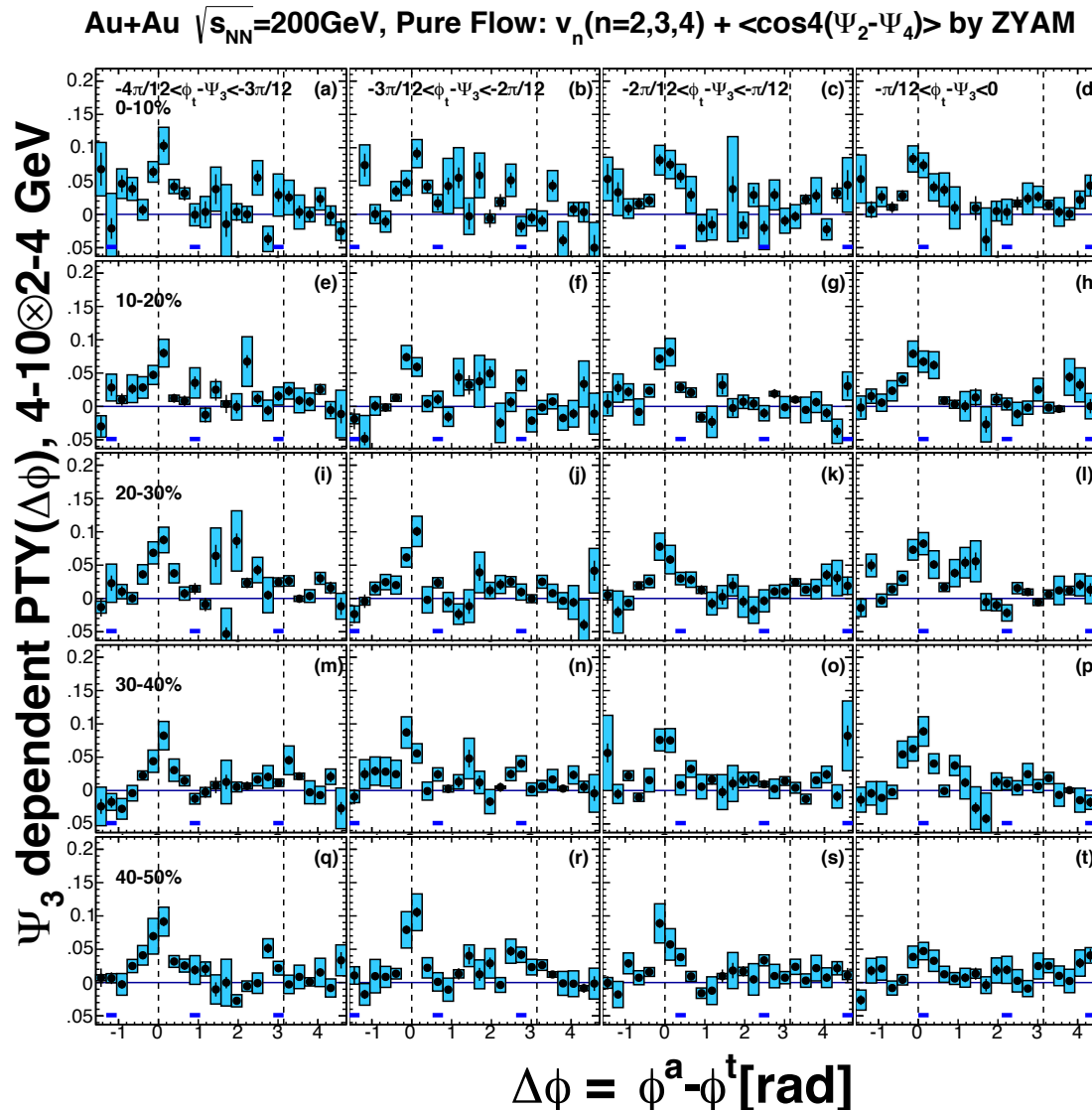
# $\Psi_3$ Dependent Correlations : $p_T$ 2-4x2-4 GeV/c



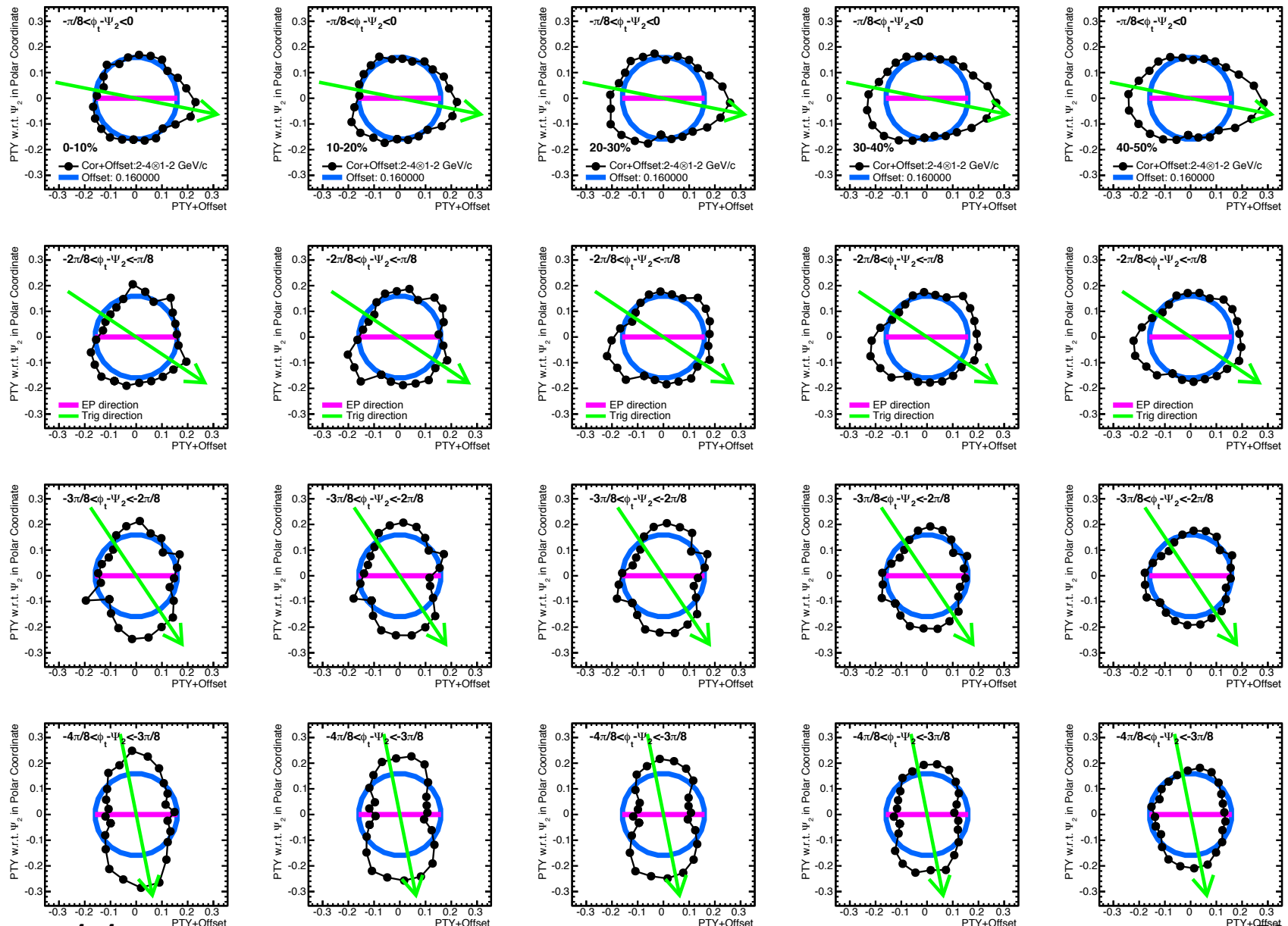
# $\Psi_2$ Dependent Correlations : $p_T$ 4-10x2-4 GeV/c



# $\Psi_3$ Dependent Correlations : $p_T$ 4-10x2-4 GeV/c



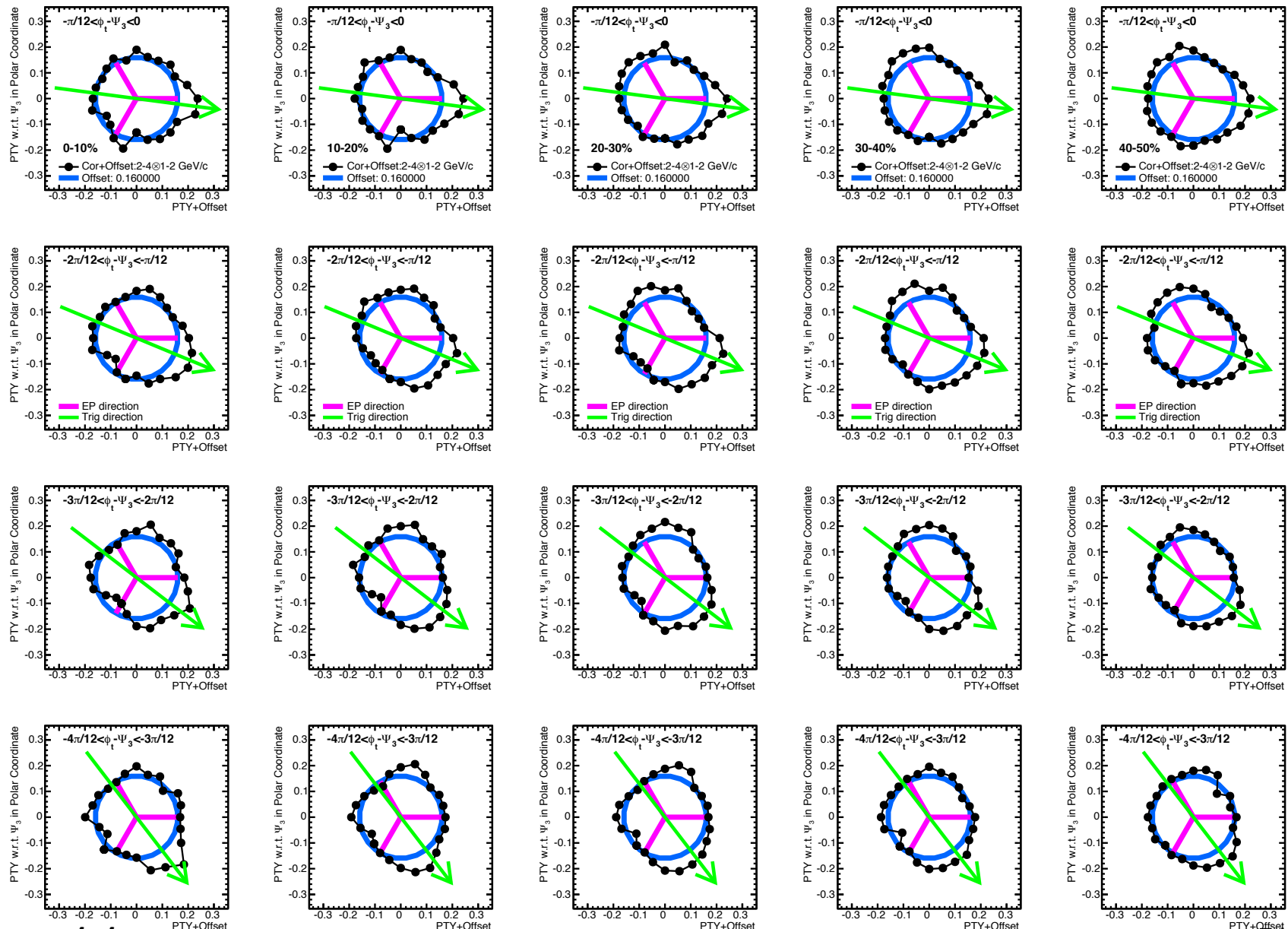
# $\Psi_2$ Dependent Correlations : $p_T$ 2-4x1-2 GeV/c



2014/7/19

HIC

# $\Psi_3$ Dependent Correlations : $p_T$ 2-4x1-2 GeV/c



2014/7/19

HIC

# Gravity Position of Two-Particle Correlations

## Definition

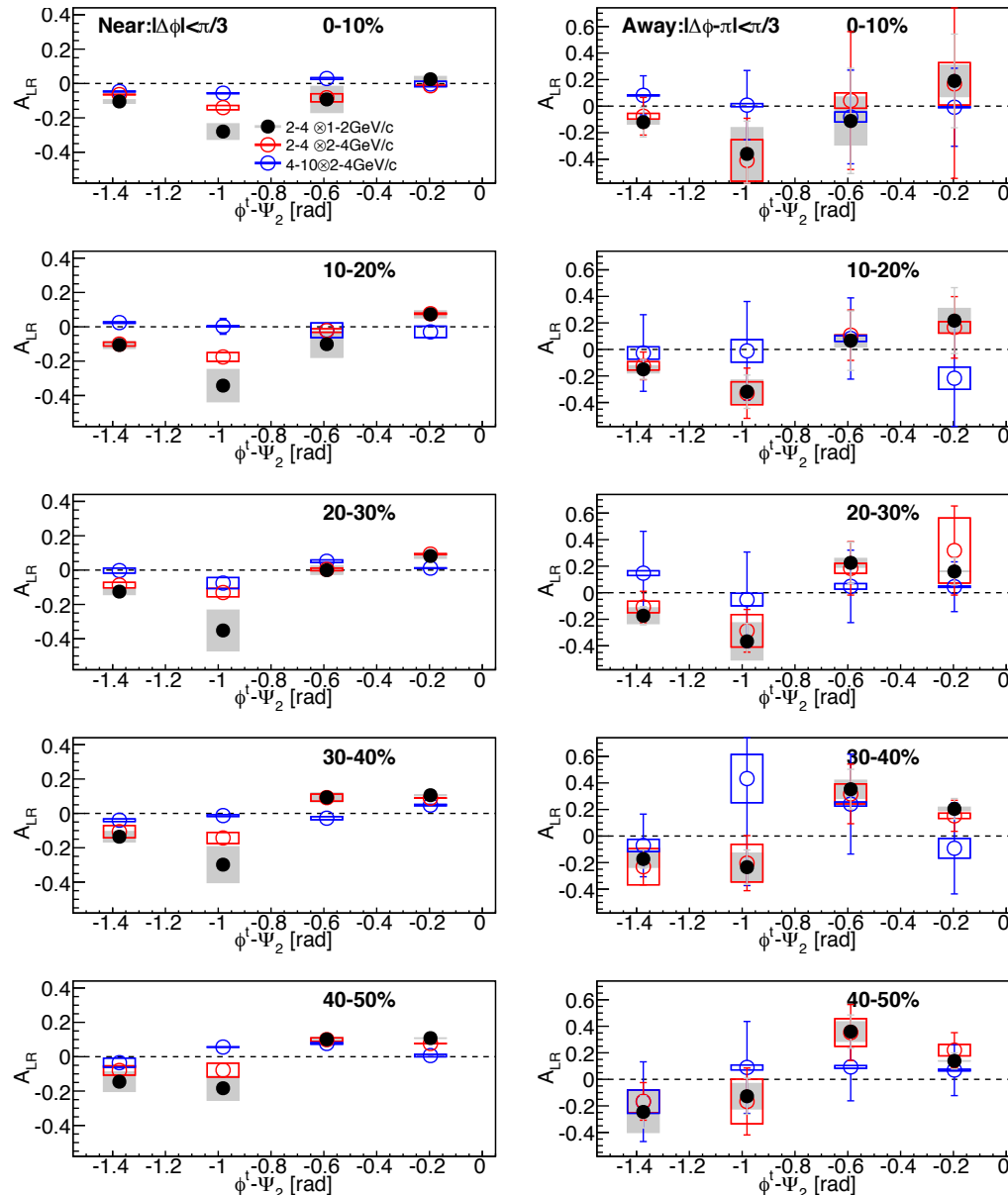
$$A_{LR} = \frac{\int d\Delta\phi \Delta\phi Y(\Delta\phi)}{\int d\Delta\phi Y(\Delta\phi)} - \begin{cases} 0 & \text{if near-side} \\ \pi & \text{if away-side} \end{cases}$$

## Integral Ranges

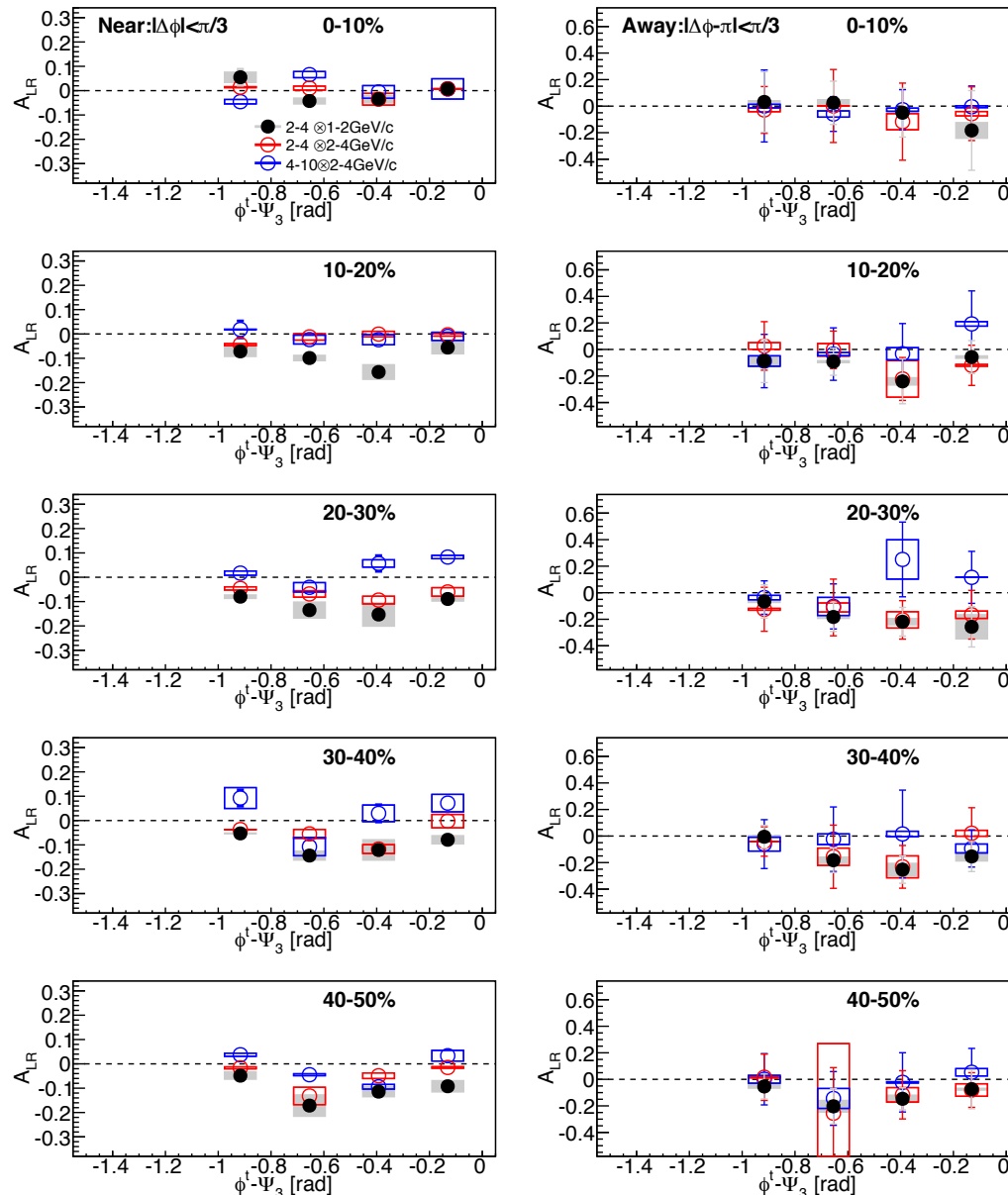
**Near – Side :**  $|\Delta\phi| < \pi/3$

**Away – Side :**  $|\Delta\phi - \pi| < \pi/3$

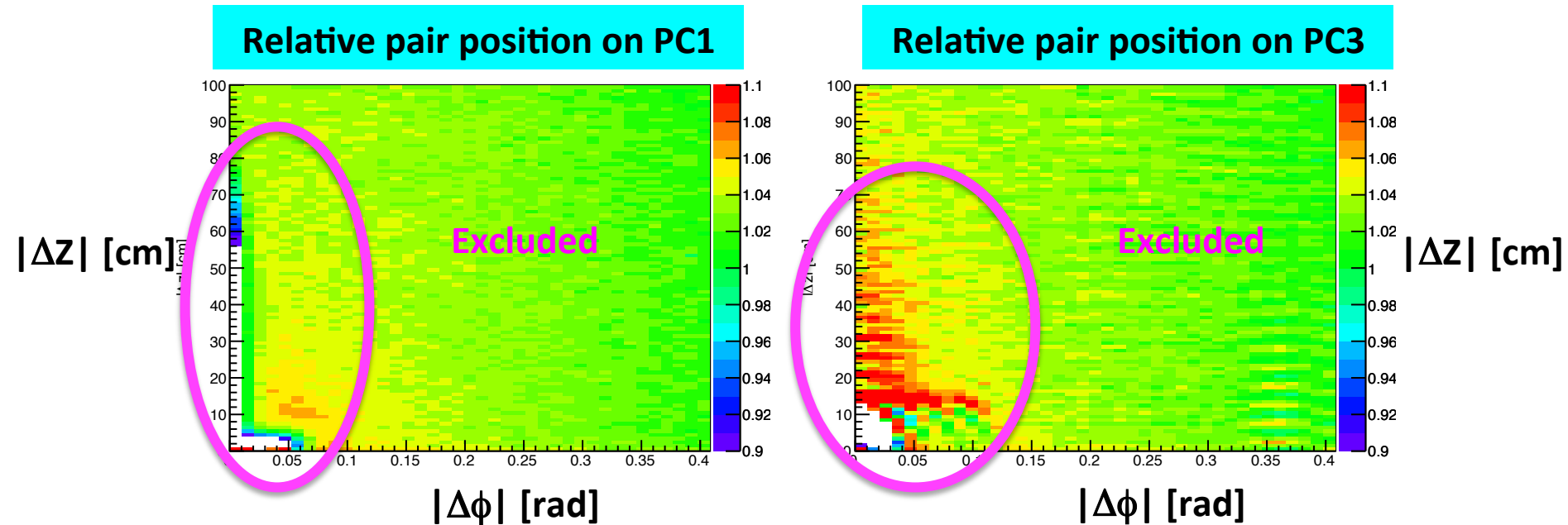
# Gravity position vs trigger angle from $\Psi_2$



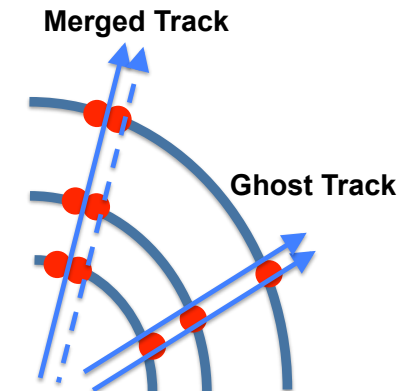
# Gravity position vs trigger angle from $\Psi_3$



# Pair Selection on Tracking Detectors



- ❖ **Ghost track**
  - A **single** particle is counted as **two** tracks
- ❖ **Merged tracks**
  - **Two** particles are counted as **one** track
- ❖ **Real/Mix pair ratio should be 1 if an ideal detector**



# Systematic Uncertainties

## ✧ Flow $v_n$ measurements

- Systematic difference within RXN segments
- Rapidity dependence of EP : RXN-BBC difference
- Matching cut of CNT particles

## ✧ Two-particle correlations

- Systematics from  $v_n$
- Matching cut of CNT particles

## ✧ Unfolding of event plane dependent correlations

- Difference of two methods : Fit & Iteration Methods
- Parameter in the iteration method

# Azimuthal Anisotropy of PTY

- ✧ Integrated yield vs associate angle from EP is translated into azimuthal anisotropy  $v_n^{\text{PTY}}$
- ✧  $v_n^{\text{PTY}}$  can be compared with single particle  $v_n$  because the dimension of PTY is “# of particles”
- ✧  $v_n^{\text{PTY}}$  is extracted via Fourier fitting

**$\Psi_2$  dependence**

$$F(\phi^a - \Psi_2) = a\{1 + 2v_2^{\text{PTY}} \cos 2(\phi^a - \Psi_2) + 2v_4^{\text{PTY}} \cos 4(\phi^a - \Psi_2)\}$$

**$\Psi_3$  dependence**

$$F(\phi^a - \Psi_3) = a\{1 + 2v_3^{\text{PTY}} \cos 3(\phi^a - \Psi_3)\},$$

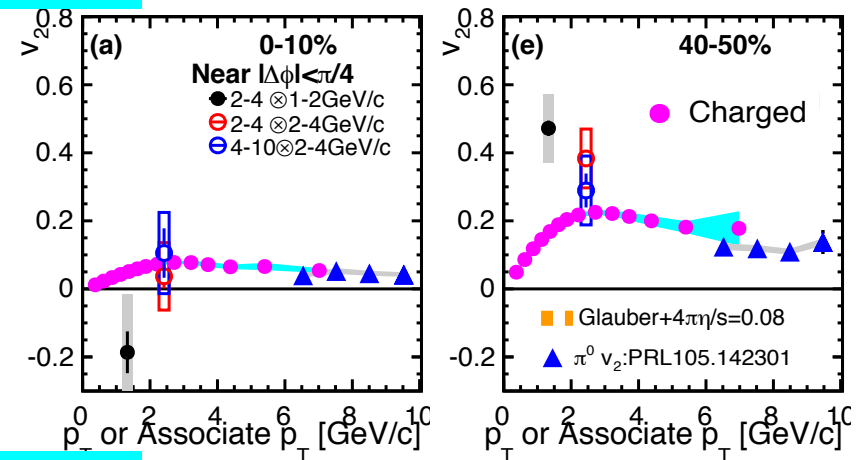
- ✧ Anisotropy of associate particles per a trigger → Anisotropy of associate particles per a event

$$v_n^{\text{PTY},\text{cor}} = v_n^{\text{PTY}} + v_n^{\text{trig}} \cos n(\phi^t - \phi^a)$$

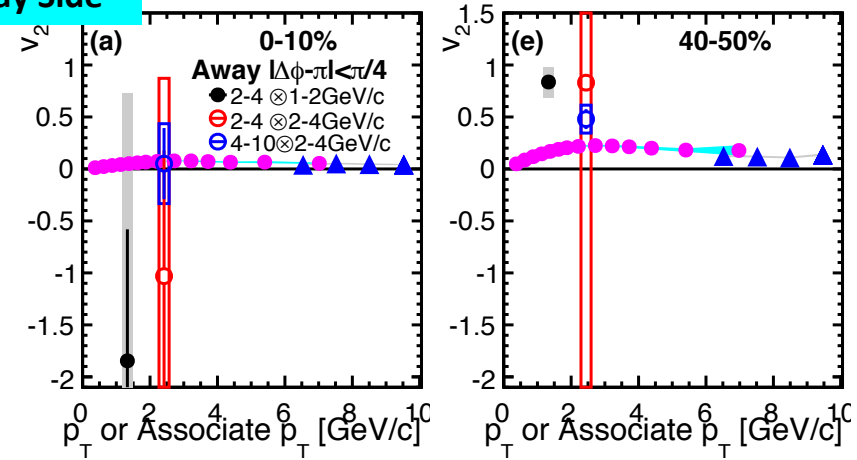
# $v_2^{\text{PTY}}$

- ✧ Positive hadron  $v_2$  (Hydrodynamics)
- ✧ Positive  $\pi^0 v_2$  (Parton energy-loss)
  - Superposition of those assemblies  
**only positive  $v_2$**
- ✧ Near & away-side  $v_2^{\text{PTY}}$ 
  - Positive value at 40-50%
  - Near-side **negative value** at 0-10%
- ✧ New effects need to be considered
- ✧ Possible re-distribution of deposited energy in longer path direction

Near Side

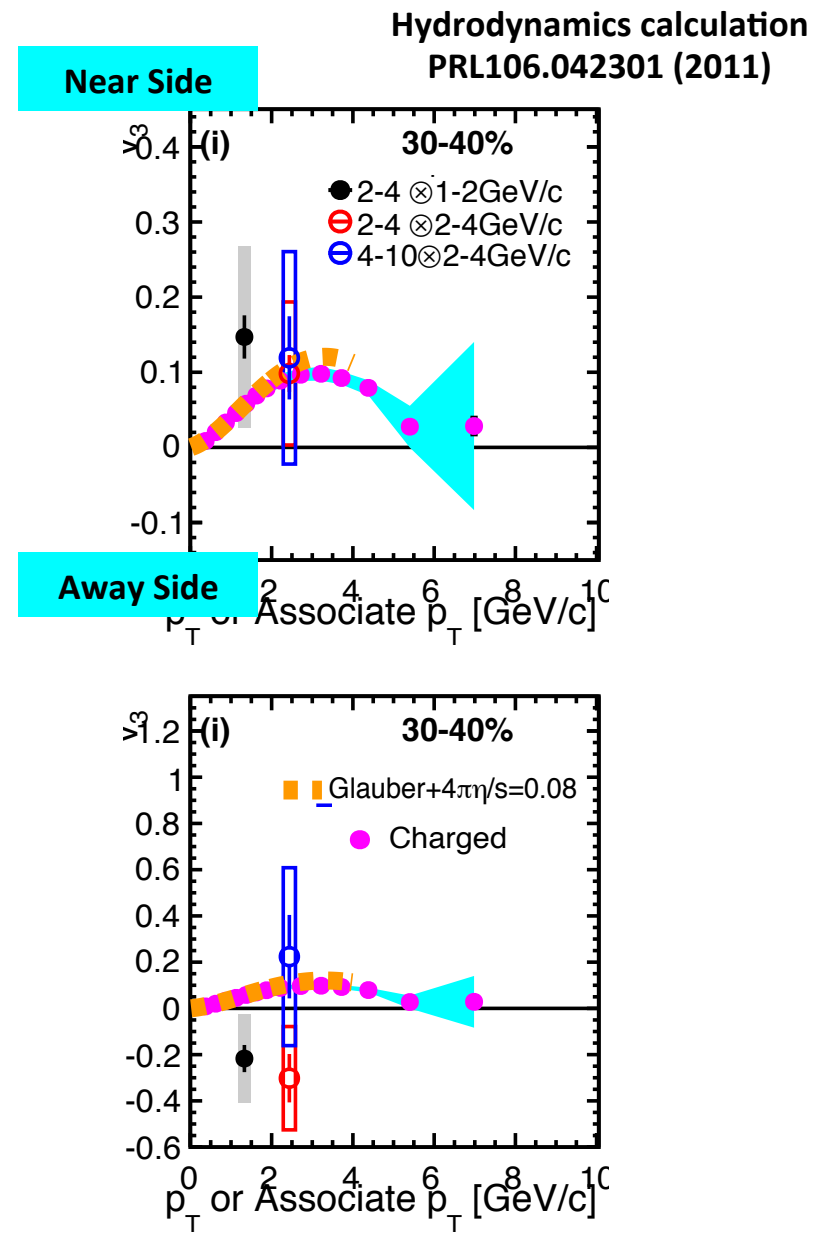


Away Side



# $v_3^{\text{PTY}}$

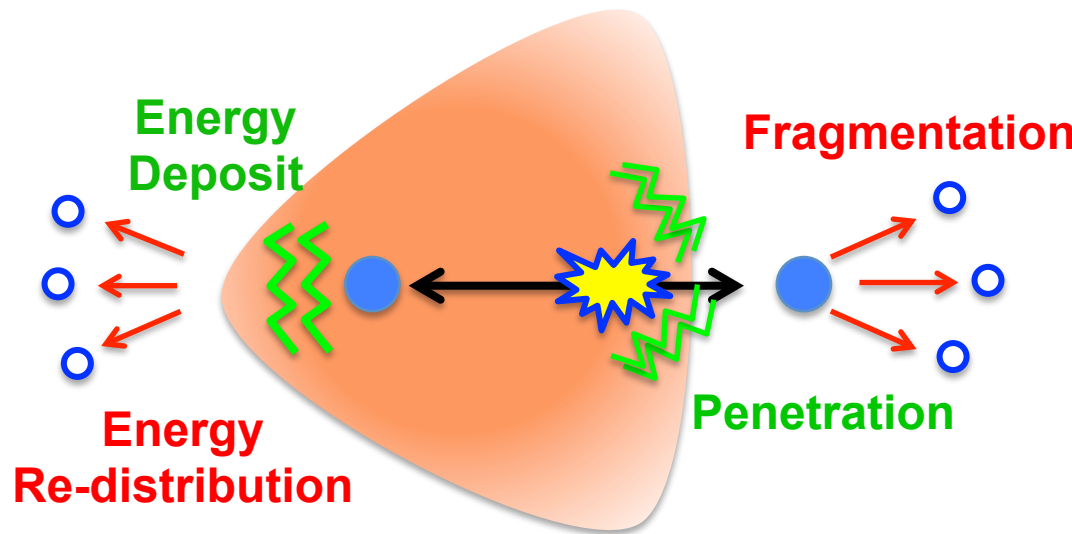
- ✧ Positive hadron  $v_3$  (Hydrodynamics)
- ✧ Near & away-side  $v_3^{\text{PTY}}$  at 30-40%
  - Positive near-side
  - Negative away-side
- ✧ Weak centrality dependence
- ✧ Different near & away-side, as well as centrality dependences from those of  $v_2^{\text{PTY}}$
- ✧ Possible different evolution processes between the 2nd- and 3rd-order geometry planes



# Interpretation of $\Psi_3$ Dependent Correlations

Away-Side

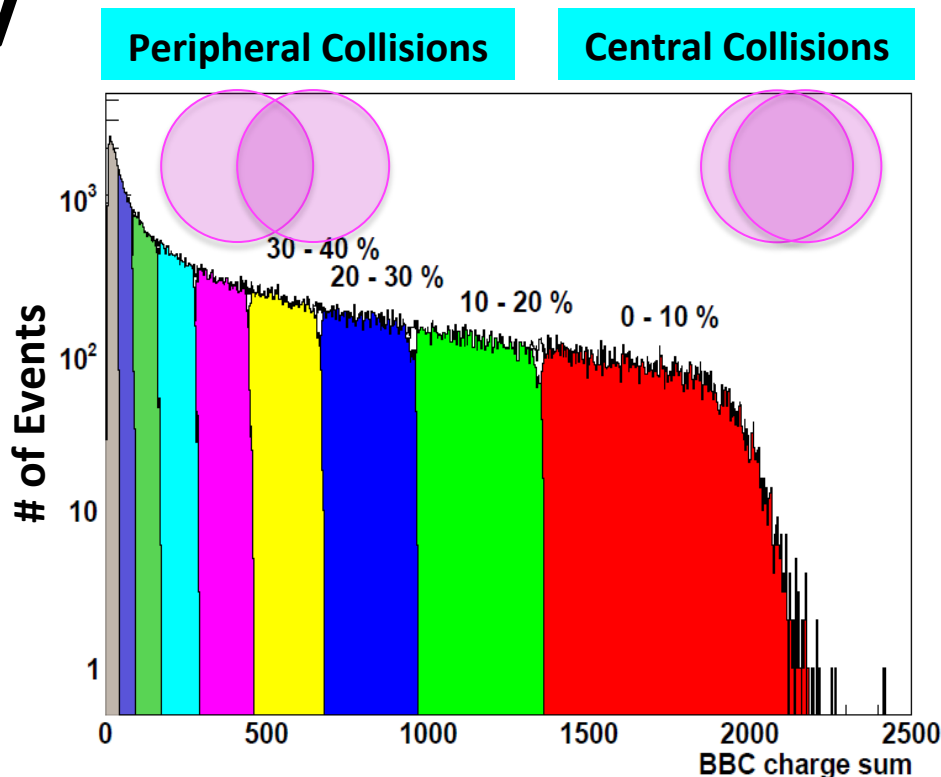
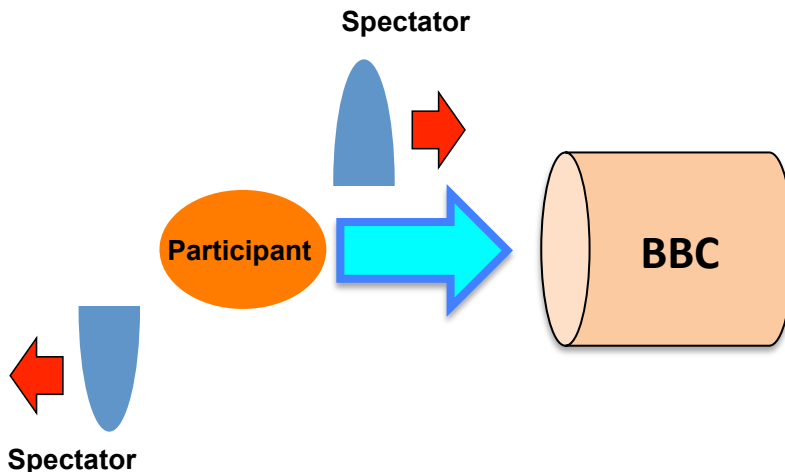
Near-Side



**Re-distribution  
Dominance**

**Penetration  
Dominance**

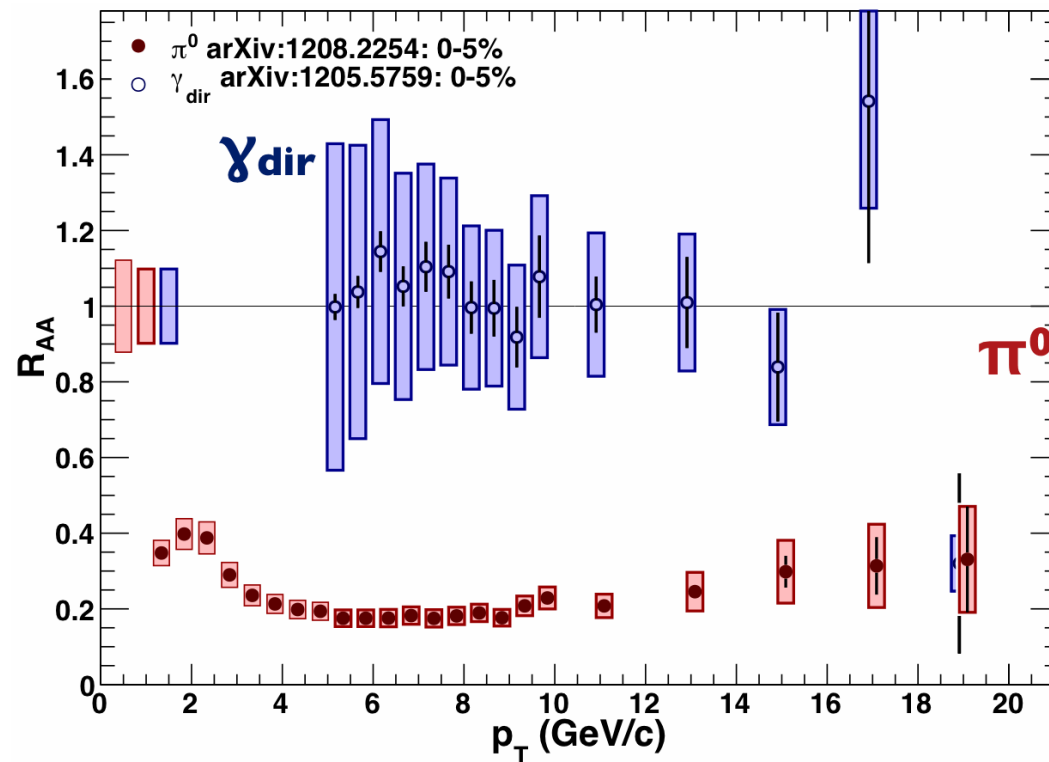
# Collision Centrality



- ✧ A degree of overlap of two colliding nuclei
  - Distance between center of the nuclei → multiplicity → charge deposited in BBC
- ✧ Require each percentile contains same # of events
  - Most-central Collision : 0%
  - Most-peripheral Collision : 100% (PHENIX determines it up to 92%)

# Nuclear Modification Factor $R_{AA}$

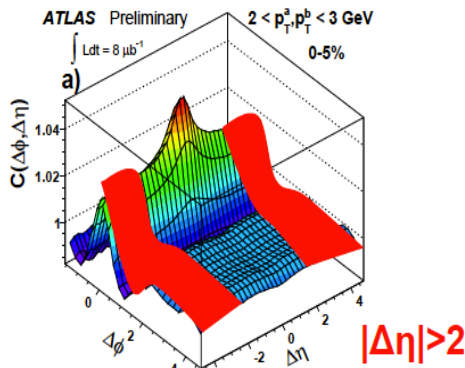
$$R_{AA} = \frac{d^2 N^{AA}/dp_T d\eta}{N_{coll} d^2 N^{pp}/dp_T d\eta}$$



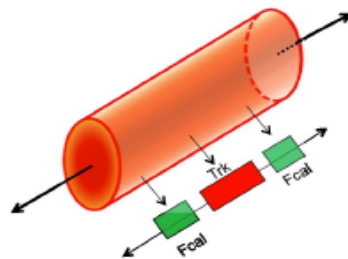
- ✧ Ratio of invariant yield scaled by that in p+p collision with scale
  - $R_{AA} < 1$ (suppression),  $R_{AA} = 1$ (no change),  $R_{AA} > 1$ (enhance)
- ✧ Suppression of hadron production
- ✧ No suppression of direct photon

# Contributions of $v_n$ ( $n>2$ ) in correlations

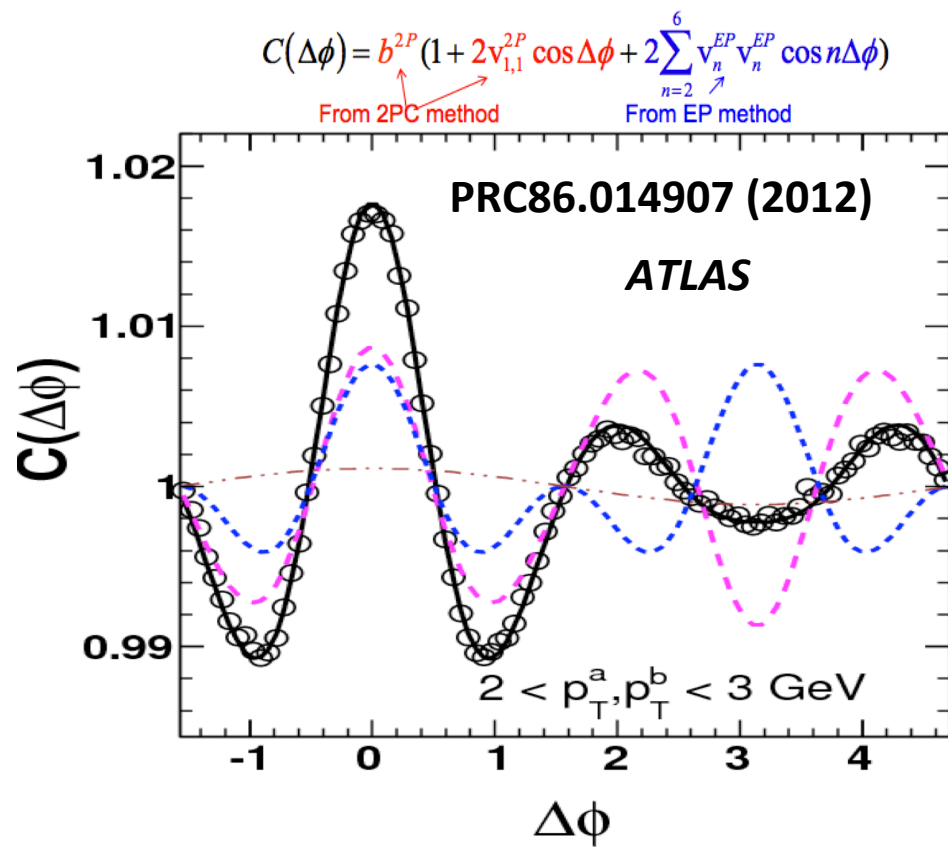
## 2Par. Correlation



## $v_n$ with EP Method



Track at  $|\eta| < 2.5$  with EP  
from full FCAL  
 $3.3 < |\eta| < 4.8$



- ✧ Double-hump & ridge of long-rapidity correlation explained
- ✧ Short-rapidity correlation with  $v_n$  subtraction to discuss parton behavior

# Data Set & Particle Selection

- ✧ PHENIX year 2007 Experiment
- ✧ Au+Au collisions at  $\sqrt{s}_{NN}=200$  GeV
  - Minimum Bias trigger 4.4 billion events
- ✧ Charged hadron selection
  - 2 $\sigma$  cut of track-hit matching
  - Electron veto
  - Energy/momentum cut of high  $p_T$  particles for background rejection
    - $E^{\text{EMC}} < 0.30 + 0.20 * p_T$  rejected for  $p_T > 5.0$  GeV/c
  - Pair cut of miss-reconstructed hadron pairs

# Tracking Efficiency

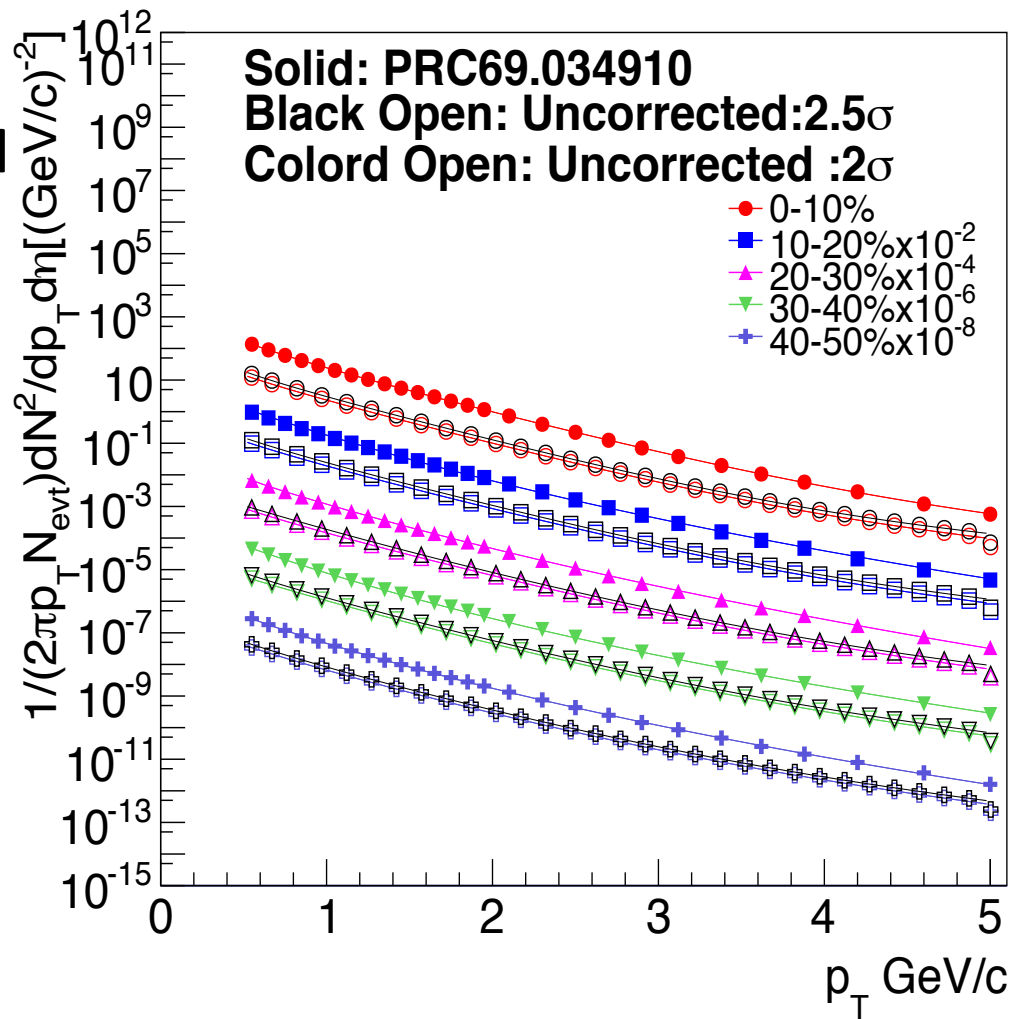
- Efficiency correction by ratio of uncorrected invariant yield over fully corrected ones

$$\varepsilon = \frac{\sigma^{uncor}}{\sigma^{cor}}$$

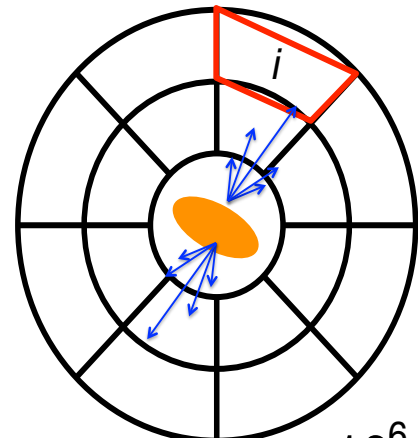
- Ratio calculated by fitting functions to the invariant yields

## Fit Function

$$F(p_T) = p_0 * \left( \frac{p_1}{p_1 + p_T} \right)^{p_2}$$

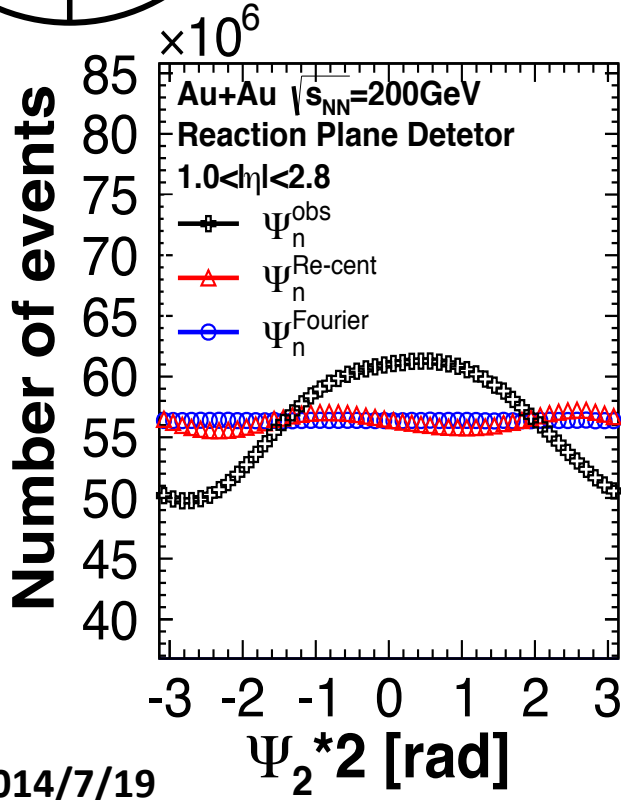


# Event Plane Calibration



$\phi_i$  : Azimuthal angle

$w_i$  : Weight (Charge etc.)



## Raw distribution

$$Q_x = \sum_i w_i \cos(n\phi_i), Q_y = \sum_i w_i \sin(n\phi_i)$$

$$\Psi_n = \frac{1}{n} \tan^{-1} \left( \frac{Q_y}{Q_x} \right)$$

## Re-centering

$$Q_x^{\text{Rec}} = \frac{Q_x - \langle Q_x \rangle}{\sigma_x}, Q_y^{\text{Rec}} = \frac{Q_y - \langle Q_y \rangle}{\sigma_y}$$

$$\Psi_n^{\text{Rec}} = \frac{1}{n} \tan^{-1} (Q_y^{\text{Rec}} / Q_x^{\text{Rec}})$$

## Fourier correction

$$n\Psi_n^{\text{Fourier}} = n\Psi_n^{\text{Rec}} + n\Delta\Psi_n$$

$$n\Delta\Psi_n = \sum_k \{ A_k \cos(kn\Psi_n^{\text{Rec}}) + B_k \sin(kn\Psi_n^{\text{Rec}}) \}$$

$$A_k = -\frac{2}{k} \langle \cos(kn\Psi_n^{\text{Rec}}) \rangle, B_k = \frac{2}{k} \langle \sin(kn\Psi_n^{\text{Rec}}) \rangle$$

# Event Plane Resolution

**EP Resolution**

PRC 58.1671 (1998)

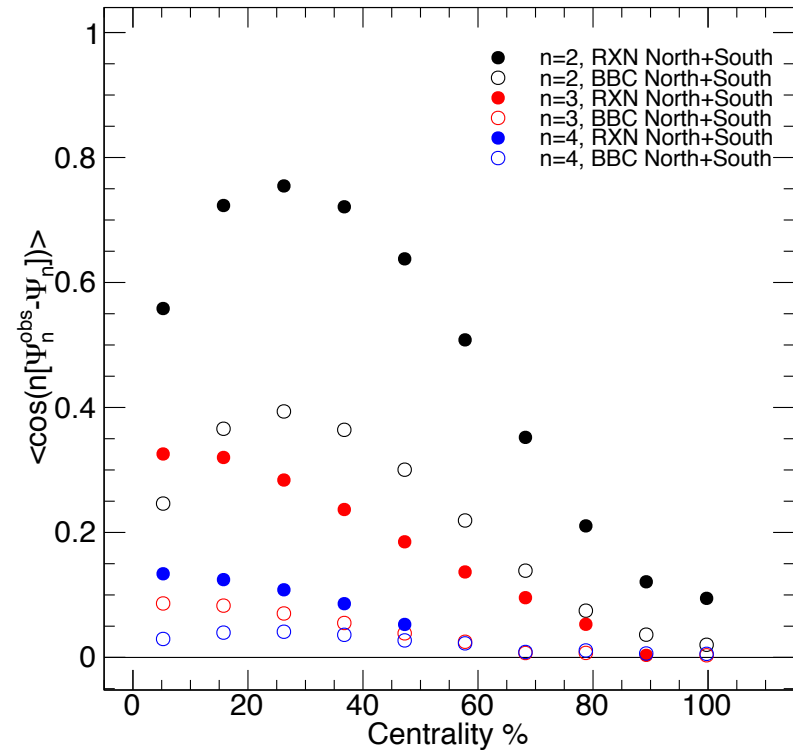
✧ **Resolution +/- $\eta$**

$$\begin{aligned}\sigma_n^{EP} &= \sqrt{\left\langle \cos kn(\Psi_n^{EP(+\eta)} - \Psi_n^{EP(-\eta)}) \right\rangle} \\ &= \left\langle \cos kn(\Psi_n^{EP+/-\eta} - \Psi_n) \right\rangle \\ &= \frac{\pi}{8} \chi_n^2 \left[ I_{(k-1)/2} \left( \frac{\chi_n^2}{4} \right) + I_{(k+1)/2} \left( \frac{\chi_n^2}{4} \right) \right]^2\end{aligned}$$

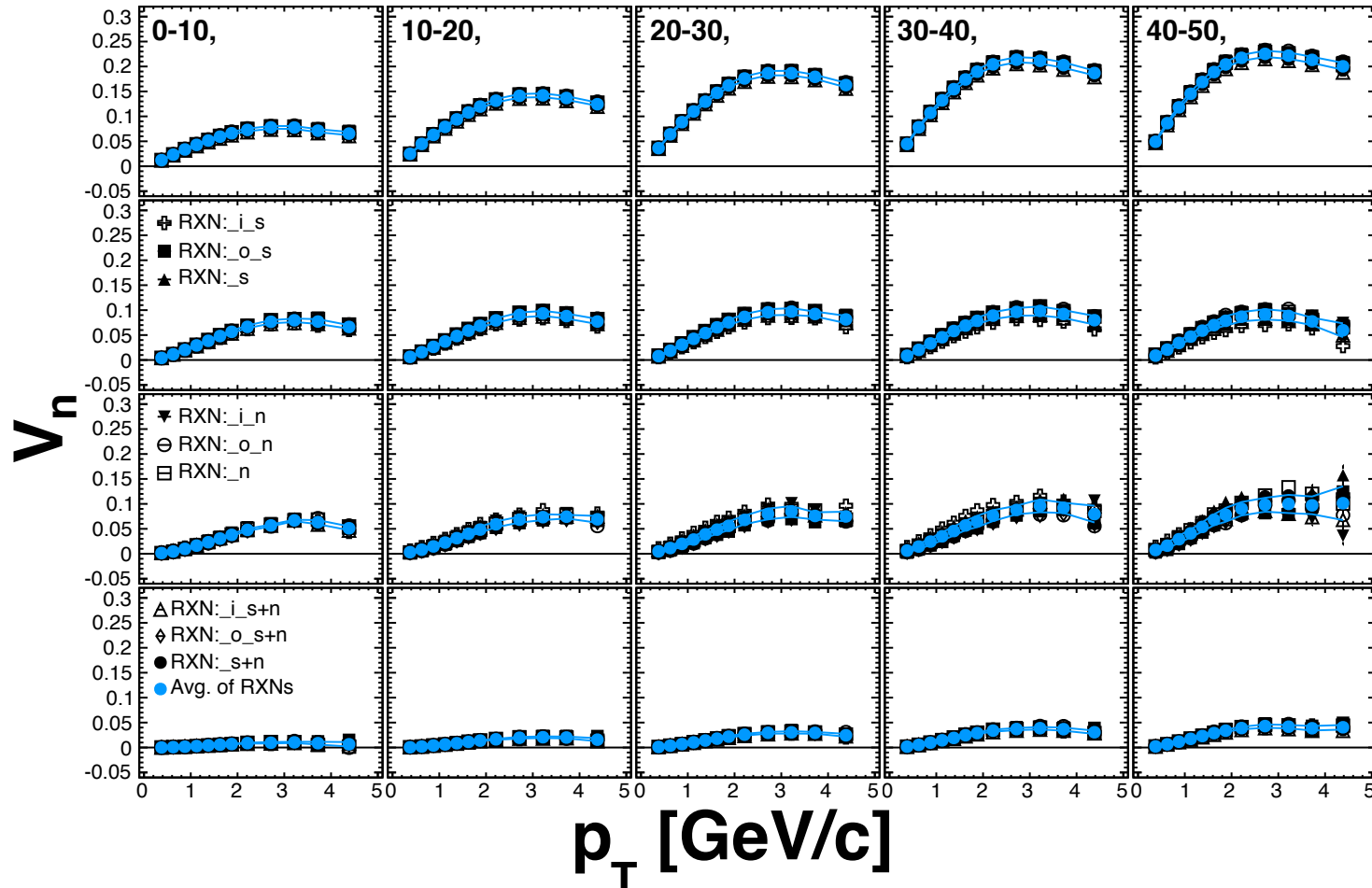
✧ **Resolution +&- $\eta$**

-  $\chi_n \rightarrow \sqrt{2}\chi_n$

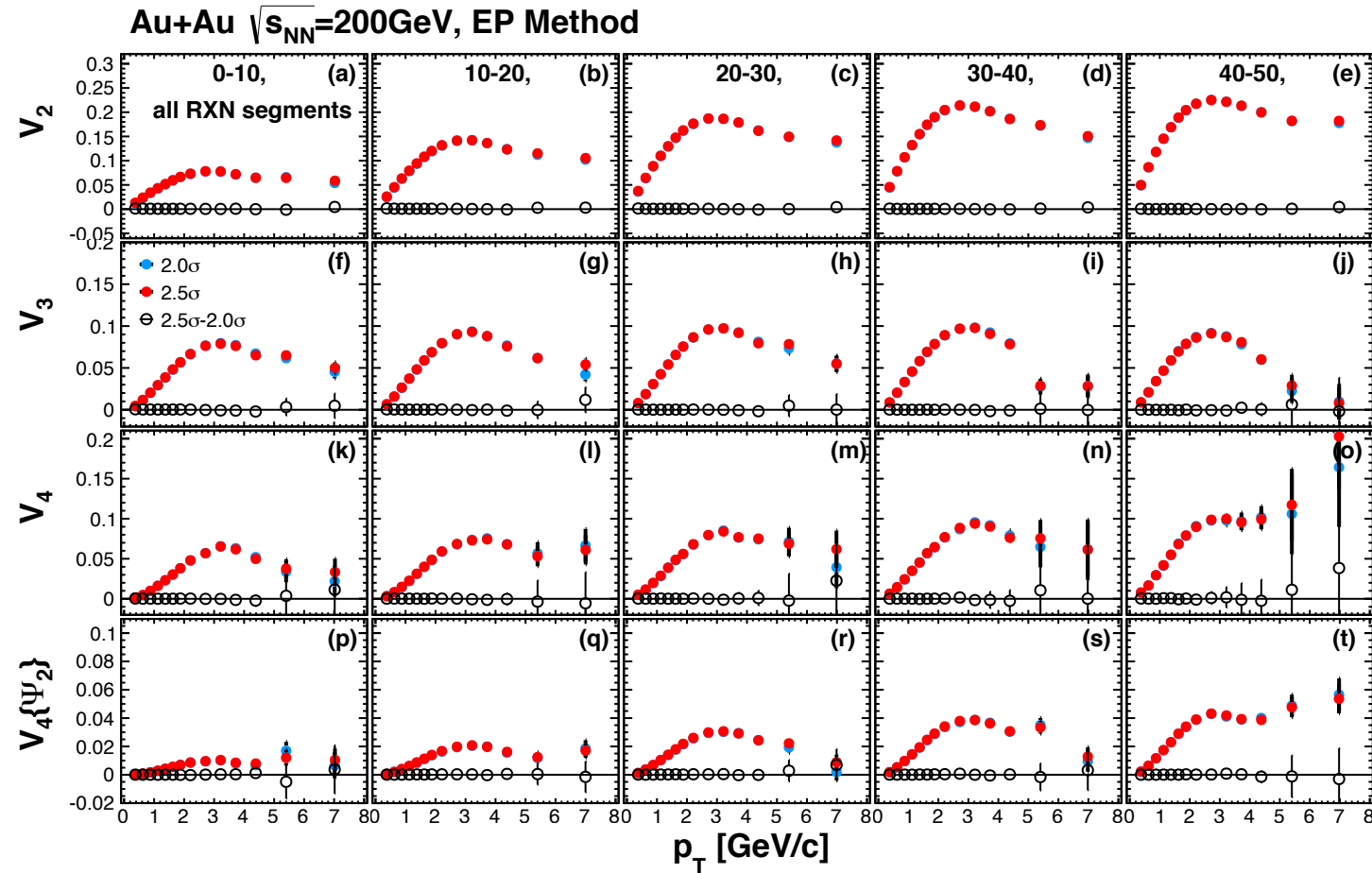
$$\sigma_n^{EP} = \frac{\pi}{8} 2\chi_n^2 \left[ I_{(k-1)/2} \left( \frac{2\chi_n^2}{4} \right) + I_{(k+1)/2} \left( \frac{2\chi_n^2}{4} \right) \right]^2$$



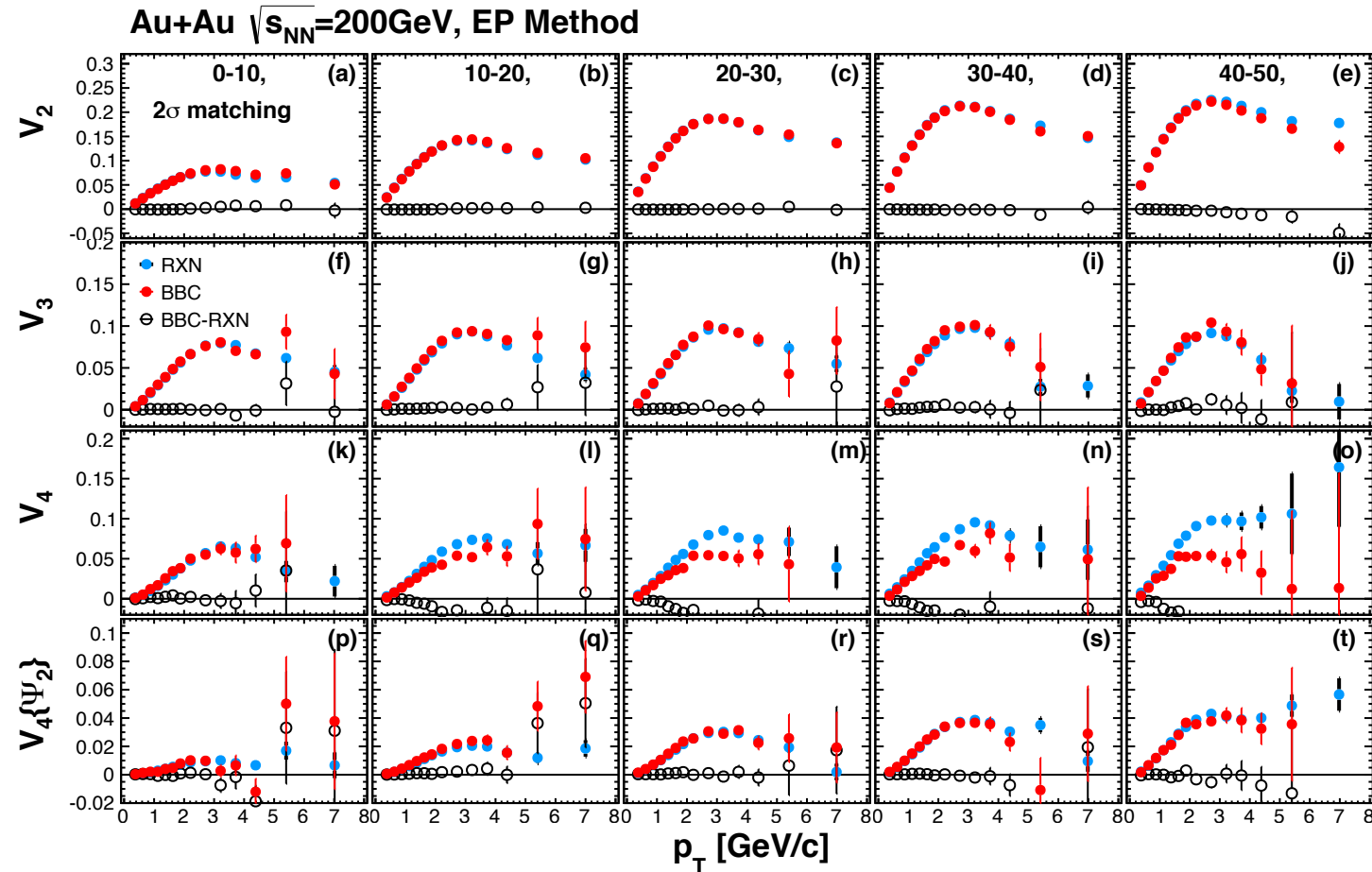
# $v_n$ systematics : RXN segments



# $v_n$ systematics : Matching Cut



# $v_n$ systematics : RXN-BBC Difference



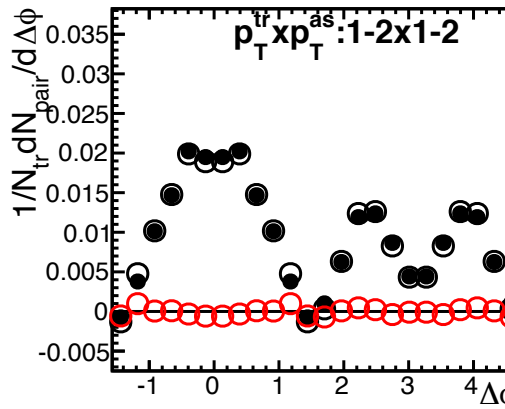
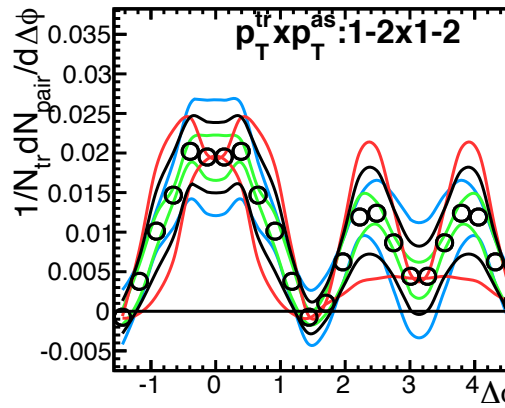
# Table of total $v_n$ systematic uncertainties

Table 3.8: Summary of percentile ratio of  $v_n$  systematic uncertainties

Centrality %	$p_T$ GeV/ $c$	$v_2$ sys. %	$v_3$ sys. %	$v_4$ sys. %	$v_4\{\Psi_2\}$ sys. %
0-10	0.5-1.0	5.449	6.387	24.87	48
	1.0-2.0	4.32	4.911	10.1	14.66
	2.0-4.0	4.536	4.131	4.412	11.39
	4.0-10.0	10.43	6.184	21.67	191.3
10-20	0.5-1.0	3.658	7.992	28.53	12.17
	1.0-2.0	2.891	6.431	20.16	12.27
	2.0-4.0	2.69	6.163	27.64	13.72
	4.0-10.0	3.124	13.62	19.09	32.09
20-30	0.5-1.0	2.811	9.469	35.48	9.633
	1.0-2.0	2.485	7.818	28.85	8.422
	2.0-4.0	2.391	6.822	28.03	6.577
	4.0-10.0	2.98	9.503	32.24	12.21
30-40	0.5-1.0	2.506	12.42	35.81	7.385
	1.0-2.0	2.462	9.695	29.88	6.509
	2.0-4.0	2.556	9.673	36.75	5.913
	4.0-10.0	2.934	14.18	44.32	31.73
40-50	0.5-1.0	2.575	13.8	32.96	6.338
	1.0-2.0	2.688	12.06	34.44	6.479
	2.0-4.0	3.224	11.7	45.4	10.71
	4.0-10.0	7.877	33.53	77.07	29.33

# Systematics of Correlations

- ✧ Systematics propagated from  $v_n$  measurements
  - Varying  $v_n$  value  $\pm 1\sigma$  (# of harmonics  $3 \times \pm 1\sigma = 6$  combinations)
  - Systematics : RMS of above 6 combinations
- ✧ Systematics from matching cut
  - Systematics : Difference between  $2.5\sigma - 2.0\sigma$  (main)
- ✧ Total Systematics
  - Quadrature-sum of above two systematics



# EP Resolution in Monte Carlo

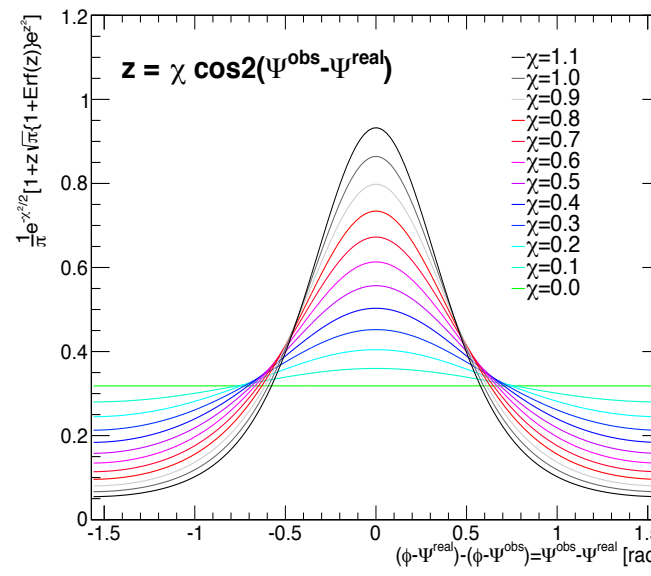
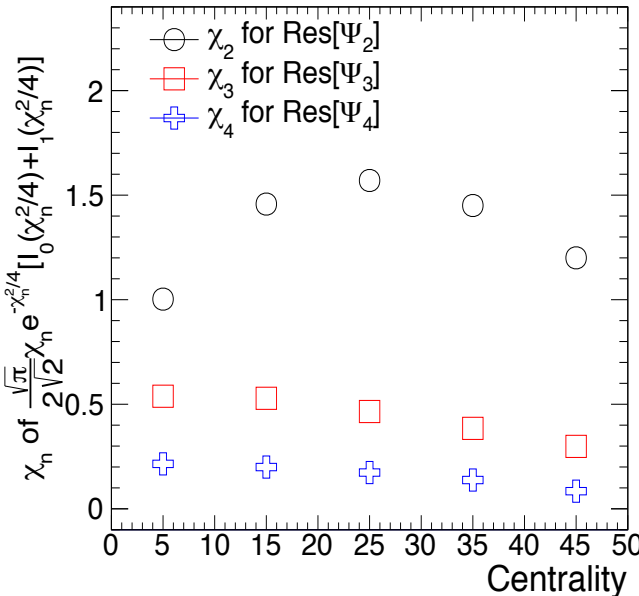
- ✧ Analytical formula of EP Resolution (RXN:S+N) as a function of  $\chi_n$ 
  - Convert Resolution to  $\chi_n$

PRC 58.1671 (1998)

$$\langle \cos [kn(\Psi_n^{obs} - \Psi_n^{real})] \rangle = \frac{\sqrt{\pi}}{2\sqrt{2}} \chi_n e^{-\chi_n^2/4} \left[ I_{(k-1)/2} \left( \frac{\chi_n^2}{4} \right) + I_{(k+1)/2} \left( \frac{\chi_n^2}{4} \right) \right].$$

- ✧ Relative distribution between real and observed EP calculated using  $\chi_n$

$$\frac{dN^{eve}}{d[kn(\Psi_n^{obs} - \Psi_n^{real})]} = \frac{1}{\pi} e^{-\chi_n^2/2} \left[ 1 + z\sqrt{\pi}[1 + \text{erf}(z)]e^{z^2} \right] \quad z = \frac{1}{\sqrt{2}} \chi_n \cos n(\Psi_n^{obs} - \Psi_n^{real})$$



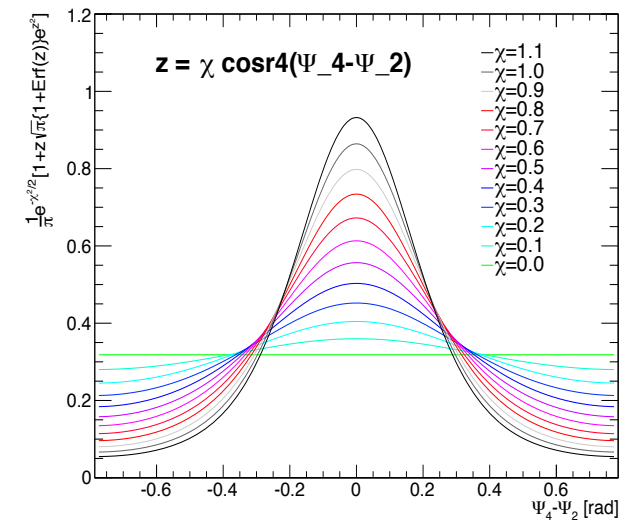
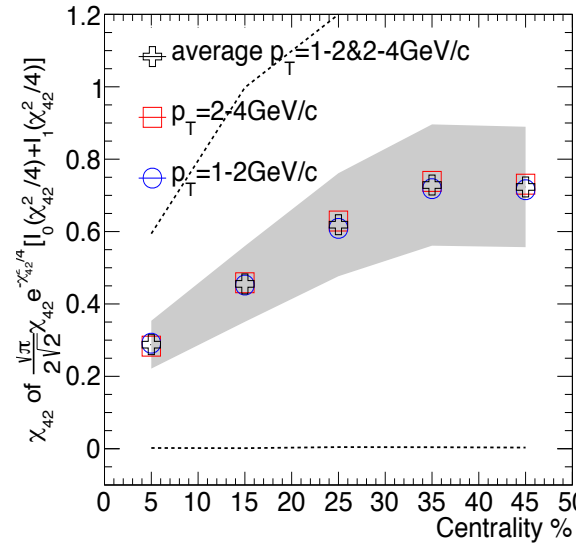
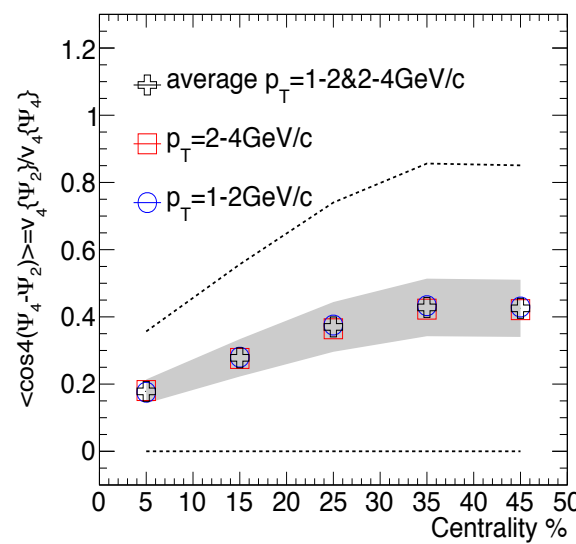
PRD 48.1132 (1993)

# $\Psi_2$ - $\Psi_4$ correlation in Monte Carlo

- ✧  **$\Psi_2$ - $\Psi_4$  correlation at  $p_T$  1-2&2-4GeV :**  $\langle \cos [4(\Psi_2 - \Psi_4)] \rangle = v_4 \{\Psi_2\} / v_4 \{\Psi_4\}$ 
  - To avoid jet contribution to the  $\Psi_2$ - $\Psi_4$  correlation
- ✧ Obtain  $\chi_{42}$  & reconstruct relative distribution between  $\Psi_2$  &  $\Psi_4$

$$\langle \cos [4(\Psi_2 - \Psi_4)] \rangle = \frac{\sqrt{\pi}}{2\sqrt{2}} \chi_{42} e^{-\chi_{42}^2/4} \left[ I_0 \left( \frac{\chi_{42}^2}{4} \right) + I_1 \left( \frac{\chi_{42}^2}{4} \right) \right]$$

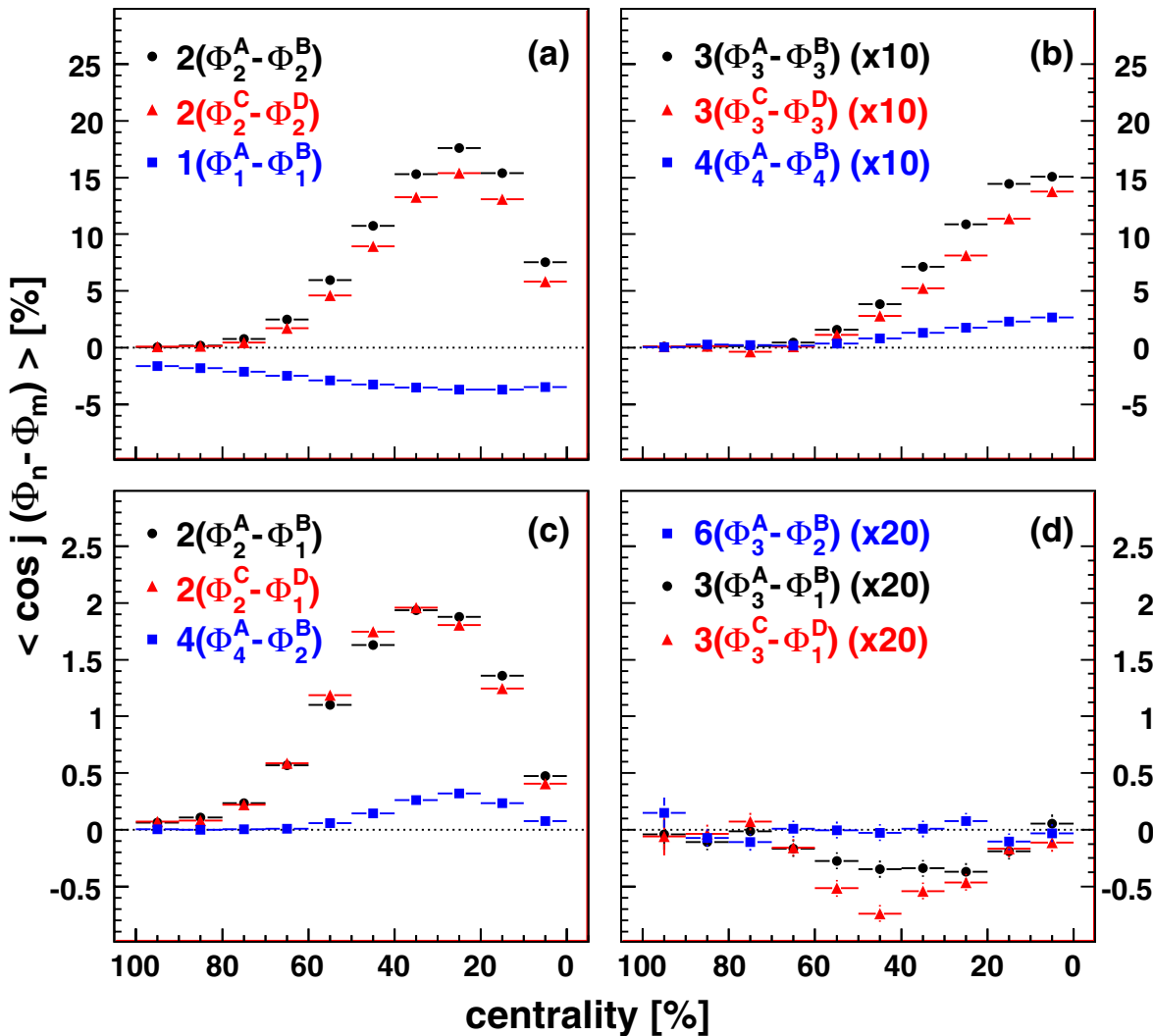
$$\frac{dN^{eve}}{d[kn(\Psi_n^{obs} - \Psi_n^{real})]} = \frac{1}{\pi} e^{-\chi_n^2/2} \left[ 1 + z\sqrt{\pi}[1 + \text{erf}(z)]e^{z^2} \right] \quad z = \frac{1}{\sqrt{2}} \chi_n \cos n(\Psi_n^{obs} - \Psi_n^{real})$$



# $\Psi_2$ - $\Psi_3$ correlation

PRL107.252301 (2011)

- A : RXN North
- B : BBC South
- C : MPC North
- D : MPC South



# EP Resolution Correction : Iteration-1

- Trigger bin is also smeared due to limited EP resolution as  $v_n$ 
  - Add an offset  $\lambda=1.0$  to correlation  $Y$  to avoid possible divisions by zero

## Raw Correlation

$$\mathbf{A}(k) = \begin{pmatrix} 1 - Y(0, k) \\ 1 - Y(1, k) \\ 1 - Y(2, k) \\ 1 - Y(3, k) \\ 1 - Y(4, k) \\ 1 - Y(5, k) \\ 1 - Y(6, k) \\ 1 - Y(7, k) \end{pmatrix}, \quad k = 0, \dots, 23$$

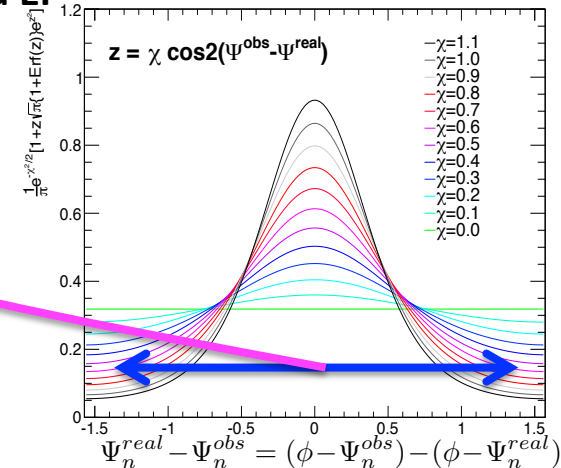
$\Delta\phi$  Bin

## Smearing Effect

### Trigger Bin

$$S = \begin{pmatrix} s_0 & s_1 & s_2 & s_3 & s_4 & s_3 & s_2 & s_1 \\ s_1 & s_0 & s_1 & s_2 & s_3 & s_4 & s_3 & s_2 \\ s_2 & s_1 & s_0 & s_1 & s_2 & s_3 & s_4 & s_3 \\ s_3 & s_2 & s_1 & s_0 & s_1 & s_2 & s_3 & s_4 \\ s_4 & s_3 & s_2 & s_1 & s_0 & s_1 & s_2 & s_3 \\ s_3 & s_4 & s_3 & s_2 & s_1 & s_0 & s_1 & s_2 \\ s_2 & s_3 & s_4 & s_3 & s_2 & s_1 & s_0 & s_1 \\ s_1 & s_2 & s_3 & s_4 & s_3 & s_2 & s_1 & s_0 \end{pmatrix}, \quad \sum_n s_n = 1, \quad s_n : \text{Ratio from } n^{\text{th}} \text{ away-bin}$$

: Calculated by relative distribution between real and observed EP



## Smeared Correlation

## Correction Matrix

## Corrected Correlation

$$\mathbf{C}(\mathbf{k}) = (c_{ij})$$

$$\mathbf{B}(k) = \mathbf{S}\mathbf{A}(k)$$

$$c_{ij} = \begin{cases} \frac{A(i,k)}{B(i,k)} & (i = j) \\ 0 & (i \neq j) \end{cases}$$

$$\mathbf{A}^{\text{cor}}(k) = \mathbf{C}(k)\mathbf{A}(k)$$

# EP Resolution Correction : Iteration-2

- ❖ Start of iteration : experimental results (already smeared once)
  - ❖ Obtained correction is not true
  - ❖ Iteration until convergences of each coefficients
    - 300 Loops

A<sup>(1)</sup>=Offset(1) + PTY,  
Smearing Matrix : S

Smeared PTY  
B<sup>(n)</sup>=SA<sup>(n)</sup>



## Notation in Iteration

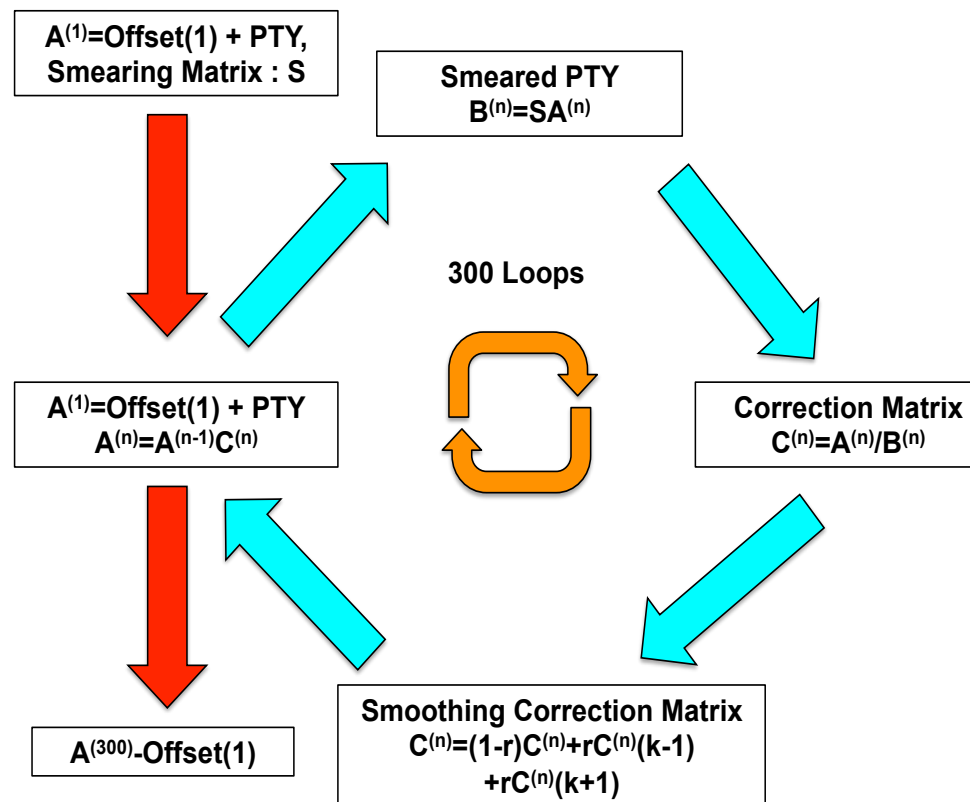
$$A \rightarrow A^{(n)}$$

$$B \rightarrow B^{(n)}$$

$$C \rightarrow C^{(n)}$$

$$A^{cor} \rightarrow A^{(n+1)}$$

# Smoothing

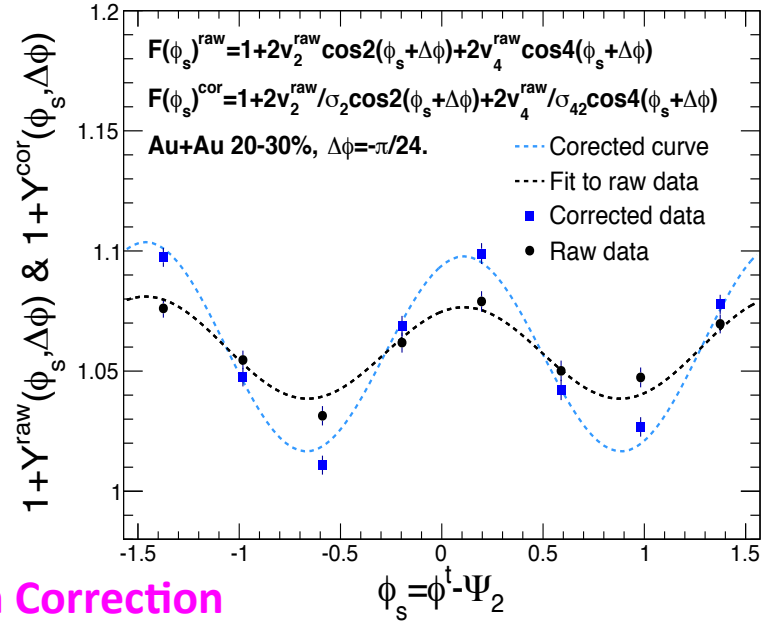


- ❖ Preventing a divergence of statistical fluctuations among  $\Delta\phi$  bins
  - ❖  $2r=0.20 \text{ & } 0.30$

$$c_{ij}^{(n)}(k) = (1 - r)c_{ij}^{(n)}(k) + (r/2)c_{ij}^{(n)}(k-1) + (r/2)c_{ij}^{(n)}(k+1)$$

# EP Resolution Correction : Fitting Method

- Assuming correlation yield has anisotropy with respect to EP
- Correction by EP resolution as done in  $v_n$  measurements
  - Method by PRC.84.024904(2011)
- Offset  $\lambda=1.0$  to avoid possible division by zero



$\Psi_2$  dependent case

EP Resolution Correction

$$\lambda + Y^{cor}(\phi_s, \Delta\phi) = \frac{\lambda + b_0 [1 + 2v_2^Y / \sigma \cos 2(\phi_s + \Delta\phi) + 2v_4^Y / \sigma_{42} \cos 4(\phi_s + \Delta\phi)]}{\lambda + b_0 [1 + 2v_2^Y \cos 2(\phi_s + \Delta\phi) + 2v_4^Y \cos 4(\phi_s + \Delta\phi)]} (\lambda + Y(\phi_s, \Delta\phi))$$

Fitting

$\Psi_3$  dependent case

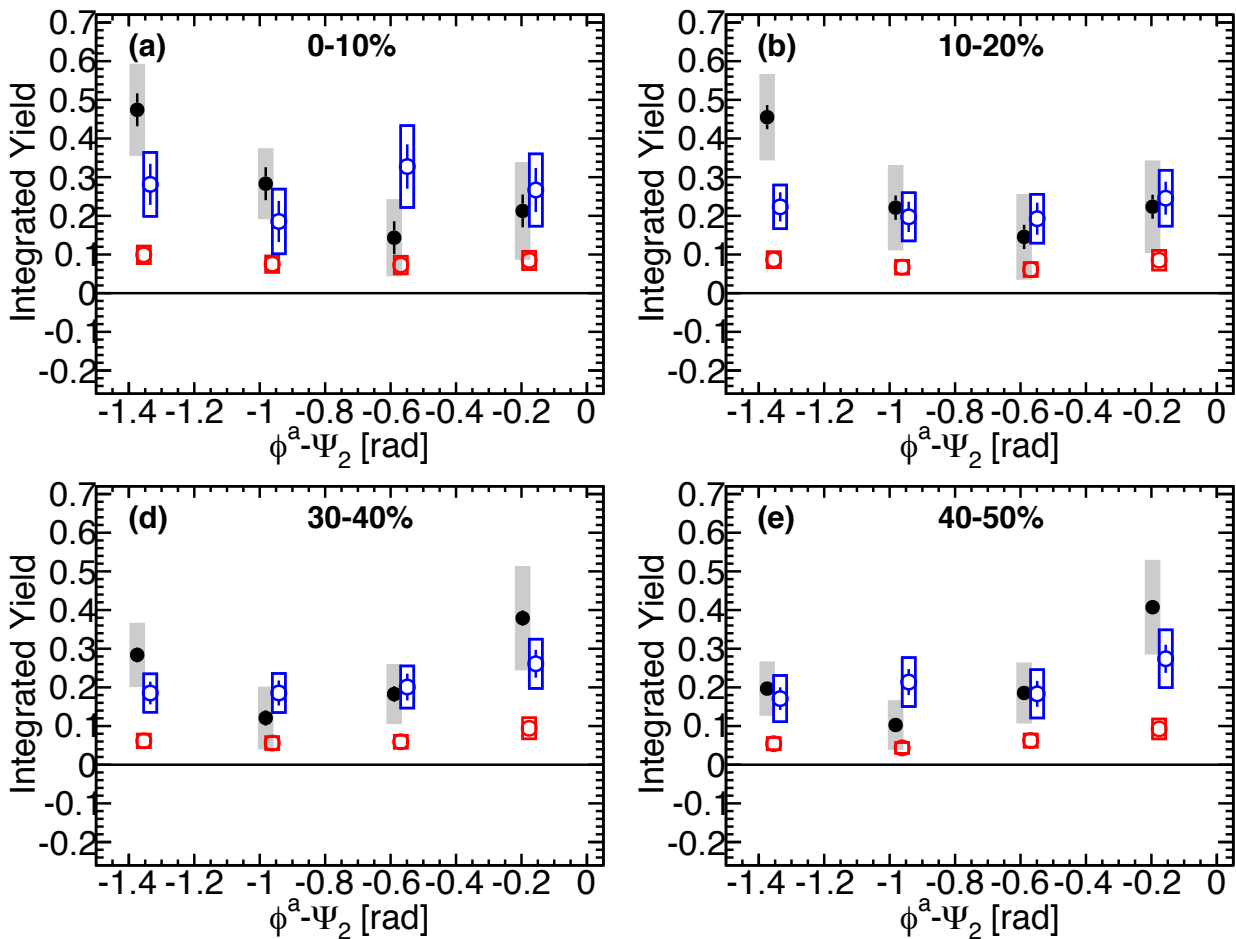
$$\lambda + Y^{cor}(\phi_s, \Delta\phi) = \frac{\lambda + b_0 [1 + 2v_3^Y / \sigma_3 \cos 3(\phi_s + \Delta\phi)]}{\lambda + b_0 [1 + 2v_3^Y \cos 3(\phi_s + \Delta\phi)]} (\lambda + Y(\phi_s, \Delta\phi))$$

Fitting

# Near-Side Integrated Yield vs Associate Angle from $\Psi_2$

**Au+Au 200GeV**  
 $\Psi_2$  dependence  
 Near Side :  $|\Delta\phi| < \pi/4$

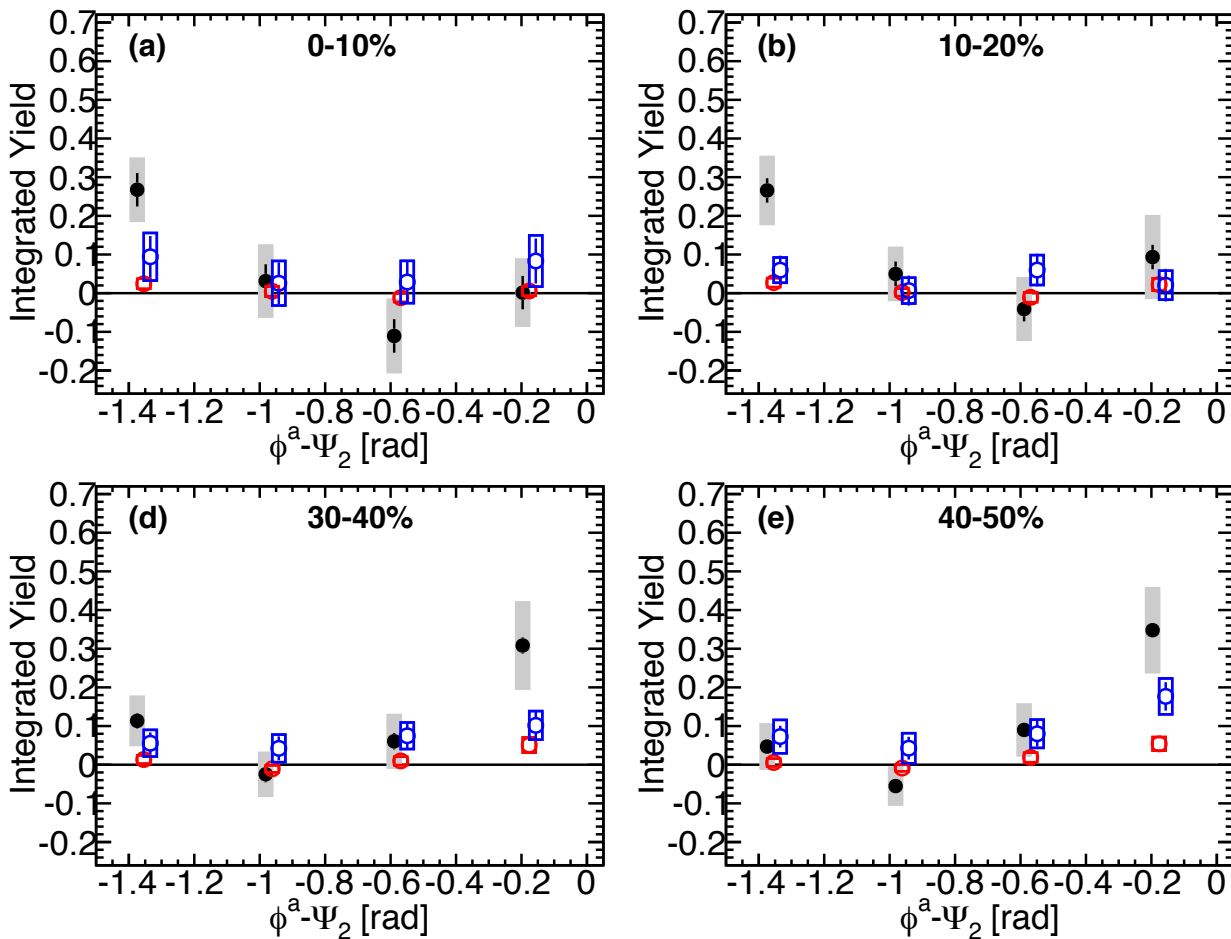
- 2-4  $\otimes$  1-2GeV/c
- 2-4  $\otimes$  2-4GeV/c
- 4-10  $\otimes$  2-4GeV/c



# Away-Side Integrated Yield vs Associate Angle from $\Psi_2$

**Au+Au 200GeV**  
 $\Psi_2$  dependence  
 Away Side :  $|\Delta\phi - \pi| < \pi/4$

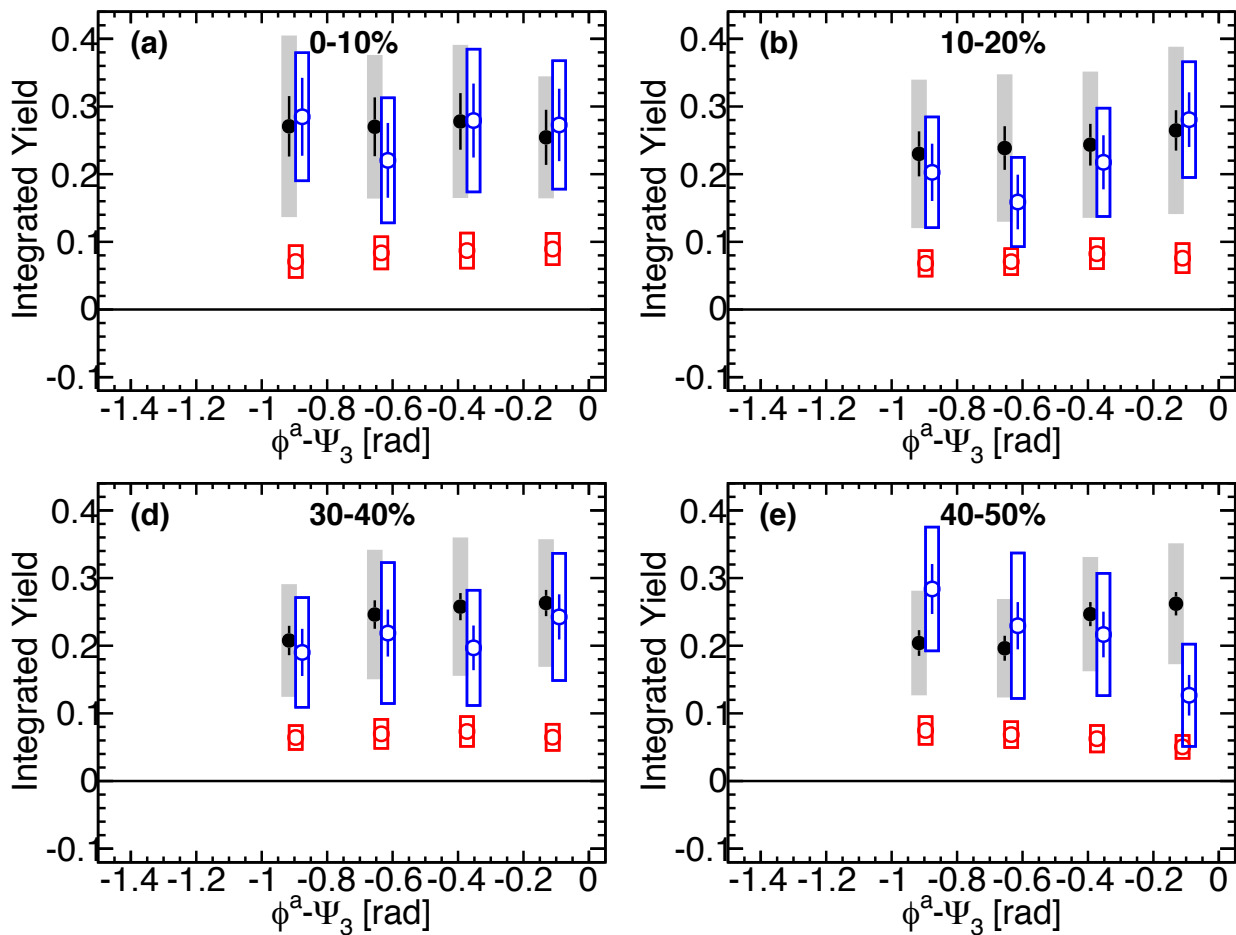
- 2-4  $\otimes$  1-2 GeV/c
- 2-4  $\otimes$  2-4 GeV/c
- 4-10  $\otimes$  2-4 GeV/c



# Near-Side Integrated Yield vs Associate Angle from $\Psi_3$

**Au+Au 200GeV**  
 $\Psi_3$  dependence  
 Near Side :  $|\Delta\phi| < \pi/4$

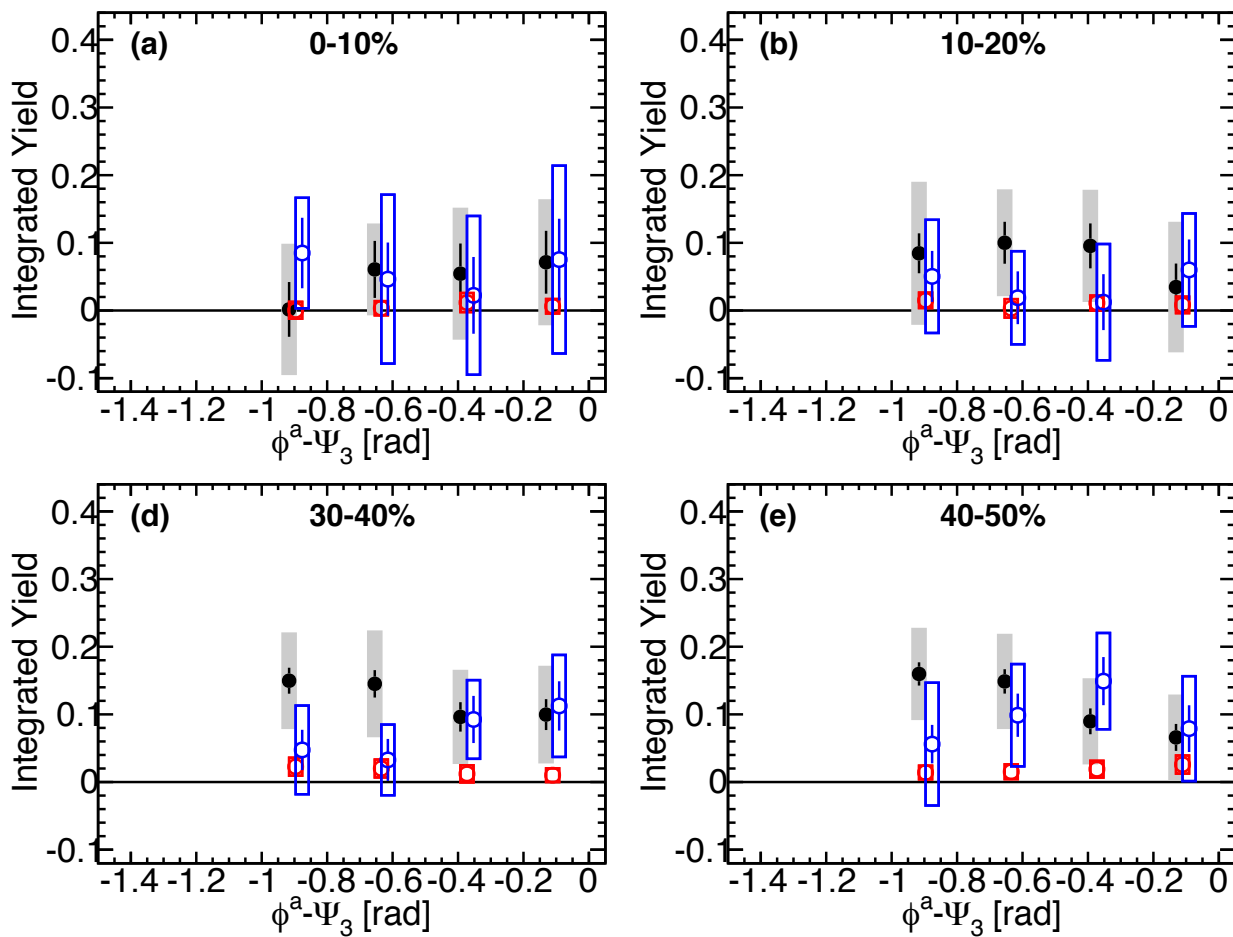
- 2-4  $\otimes$  1-2GeV/c
- 2-4  $\otimes$  2-4GeV/c
- 4-10  $\otimes$  2-4GeV/c



# Away-Side Integrated Yield vs Associate Angle from $\Psi_3$

**Au+Au 200GeV**  
 $\Psi_3$  dependence  
 Away Side :  $|\Delta\phi - \pi| < \pi/4$

- 2-4  $\otimes$  1-2 GeV/c
- 2-4  $\otimes$  2-4 GeV/c
- 4-10  $\otimes$  2-4 GeV/c



# Anisotropy of particles per a jet →

# Anisotropy of particles per a event

$$\begin{aligned} & \{1 + 2v_n^{PTY} \cos n(\phi^a - \Psi_n)\} \times \{1 + 2v_n^t \cos n(\phi^t - \Psi_n)\} \\ &= \{1 + 2v_n^{PTY} \cos n(\phi^a - \Psi_n)\} \times \{1 + 2v_n^t \cos n(\phi^a - \phi^t) \cos n(\phi^a - \Psi_n)\} \\ &\simeq 1 + 2v_n^{PTY} \cos n(\phi^a - \Psi_n) + 2v_n^t \cos n(\phi^a - \phi^t) \cos n(\phi^a - \Psi_n) \end{aligned}$$

$$v_n^{PTY,cor} = v_n^{PTY} + v_n^{trig} \cos n(\phi^t - \phi^a)$$

